

博士論文

Characterization of
Light Reflection of
Fish Guanine Crystals by
Diamagnetic Micromanipulation

反磁性マイクロ
マニピュレーションによる
魚類グアニン結晶の
光反射の特性評価

水川 友里

広島大学大学院先端物質科学研究科

2016年3月

目次

1. 主論文

Characterization of Light Reflection of Fish Guanine Crystals by Diamagnetic Micromanipulation

(反磁性マイクロマニピュレーションによる魚類グアニン結晶の光反射の特性評価)

水川 友里

2. 公表論文

(1) Light Reflection Control in Biogenic Micro-Mirror by Diamagnetic Orientation

M. Iwasaka and Y. Mizukawa

Langmuir, **29**, 4328–4334 (2013).

(2) Synchrotron Microscopic Fourier Transform Infrared Spectroscopy Analyses of Biogenic Guanine Crystals Along Axes of Easy Magnetization

Y. Mizukawa, Y. Ikemoto, T. Moriwaki, T. Kinoshita, F. Kimura, T. Kimura and M. Iwasaka

IEEE Transactions on Magnetics, **50**, 5001804(1–4) (2014).

(3) Rapid magnetic wiper featuring biogenic guanine particles: Magnetic non-contact switching of opto-fluidic mirrors featuring biogenic guanine crystals

M. Iwasaka, Y. Mizukawa and Y. Miyashita

Applied Physics Letters, **104**, 024108(1–4) (2014).

(4) Biaxial Alignment Control of Guanine Crystals by Diamagnetic Orientation

M. Iwasaka, Y. Miyashita, Y. Mizukawa, K. Suzuki, T. Toyota and T. Sugawara

Applied Physics Express, **6**, 037002(1–4) (2013).

(5) Magnetic Manipulation of Nucleic Acid Base Microcrystals for DNA Sensing

Y. Mizukawa, K. Suzuki, S. Yamamura, Y. Sugawara, T. Sugawara and M. Iwasaka

IEEE Transactions on Magnetics, **50**, 5001904(1–4) (2014).

(6) Magnetic control of the inclination of biogenic guanine crystals fixed on a substrate
Y. Mizukawa and M. Iwasaka
Journal of Applied Physics, **117**, 17B730(1–4) (2015).

(7) Magnetic Control of the Light Reflection Anisotropy in a Biogenic Guanine Microcrystal Platelet
M. Iwasaka, Y. Mizukawa and N. W. Roberts
Langmuir, **32**,180–187 (2016).

3. 参考論文

(1) Magnetic field effects on mitochondrion-activity-related optical properties in slime mold and bone forming cells
Y. Mizukawa and M. Iwasaka
35th Annual International Conference of the IEEE Engineering in Medicine and Biology Society (EMBC2013), Proceedings of the Annual International Conference of the IEEE Engineering in Medicine and Biology Society 2013, 1442–1445, Osaka, Japan, July 3-7 (2013).

(2) Magnetic orientational tweezers for cell manipulation
Y. Mizukawa and M. Iwasaka
Transactions of Japanese Society for Medical and Biological Engineering, **51**(Supplement), M–127 (2013).

(3) Electromagnetic Viability Control of Aquatics by the Combination of Weak Electric Currents and 10 T Magnetic Fields
Y. Mizukawa and M. Iwasaka
IEEE Transactions on Magnetics, **49**, 3480–3483 (2013).

(4) Novel Magnetic Responses of Uric Acid Crystals under Light Irradiations
Y. Mizukawa and M. Iwasaka
IEEJ Transactions on Fundamentals and Materials, **133**, 383–384 (2013).

主論文

Table of Contents

1. Introduction

1.1 Magnetism	1
1.2 Light Reflection Systems of Organisms and Biogenic Guanine Crystals	6
1.3 References	11

2. Physical Property Analysis of Biogenic Guanine Crystal

2.1 SEM Imaging and X-ray Powder Diffraction	17
2.1.1 Introduction	17
2.1.2 Methods and Materials.....	17
2.1.3 Results and Discussion	22
2.1.4 Summary	27
2.1.5 References.....	28
2.2 Microscopic Synchrotron FTIR Measurements on Biogenic Guanine Crystals along Two Axes	29
2.2.1 Introduction	29
2.2.2 Methods and Materials.....	30
2.2.3 Results and Discussion	33
2.2.4 Summary	39
2.2.5 References.....	39

3. Magnetic Non-Contact Switching of Light Scattering from Floating Guanine Crystals

3.1 Introduction	40
3.2 Methods and Materials	40
3.3 Results and Discussion	45
3.4 Summary	53
3.5 References	54

4. Light Reflection Changes Caused by Magnetic Orientation

4.1 Optical Behavior of Guanine Crystals on a Substrate

under Magnetic Fields	55
4.1.1 Introduction	55
4.1.2 Methods and Materials	56
4.1.3 Results and Discussion.....	60
4.1.4 Summary	67
4.1.5 References	68

4.2 Two Magnetic Orientations of Biogenic Guanine Crystals.....

4.2.1 Introduction	70
4.2.2 Methods and Materials	70
4.2.3 Results and Discussion.....	75
4.2.4 Summary	84
4.2.5 References	84

5. Reflection Angle Specificity of Biogenic Guanine Crystals

5.1 Introduction	85
5.2 Methods and Materials.....	86
5.3 Results and Discussion.....	89
5.4 Summary.....	105

6. Conclusion

6.1 Conclusions	106
6.2 Future development and applications.....	110

Acknowledgments.....	111
-----------------------------	------------

1. Introduction

1.1 Magnetism

When we hear the word “magnetism”, we associate it with the behavior of a magnet, which has the property of attracting other magnetic substances. Most laypeople might think that it is magnetism that materials are attracted by a magnet. Actually, all substances have magnetism, but they are classified according to two types, disordered magnetism and ordered magnetism. A further partitioning occurs; disordered magnetism is divided into diamagnetism and paramagnetism and ordered magnetism divides into three categories: ferromagnetism, anti-ferromagnetism, and ferrimagnetism. The main concern of this study is diamagnetism and is very important.

Diamagnetism indicates that the substances are magnetized opposite to the direction of the external magnetic field. The levitation of a frog under strong magnetic field is a famous demonstration of the effect of diamagnetism [1]. The levitation of waterdrops and Moses effects which provides the water wall when the strong static magnetic fields are applied to water is also the diamagnetic effect.

In particular, the major diamagnetic effect is “a diamagnetic orientation”. It is known that diamagnetic orientation occurs when diamagnetic energy of a material is larger than the thermal energy kT . Also, the diamagnetic orientation arising from the diamagnetic susceptibility of aromatic molecules [2] (with five- or six-membered rings such as benzophenone [3], naphthalene [4], and a carbon nanotube [5], [6]) is caused by eddy currents associated with π electrons, as shown in Figure 1.1.

- Diamagnetism of biological materials

In the field of magnetic science, previous studies show that organic materials and inorganic materials have a magnetic orientation under an applied magnetic field of order of Teslas [T] [3]-[20]. In the 1980s, when applying the external magnetic fields to biological materials in the field of tissue engineering, many studies reported that biological materials were orientable under strong static magnetic fields.

Two examples in point are fibrin [7]-[12], which is a kind of protein related to the formation of blood clots, and a collagen [13]-[14], which supports the formation of the tissues; under strong magnetic fields, both are magnetically oriented. Also, it was reported that magnetic behavior of DNA was measured by magnetically induced birefringence [18]. Under strong magnetic fields of order of a Tesla, the diamagnetic behavior of substances can be remarkably observable because diamagnetic materials need sufficiently strong fields to produce diamagnetic energies that overcome the thermal energy at room temperature (about 300 K). Also, it is believed that the anisotropy diamagnetic susceptibility is the key to diamagnetic orientation. The diamagnetic susceptibility is related to the orbital magnetic moment and the amount of diamagnetic substances.

- ‘Easy’ and ‘difficult’ axes of magnetization in diamagnetic materials

When discussing magnetism, it is important to clarify that certain magnetic materials have a preferred magnetization axis, resulting in magnetic anisotropy. ‘Magnetic anisotropy’ means that magnetic stability is dependent on the crystallographic orientation of the material. Table 1.1 lists the magnetic anisotropy in the susceptibility of diamagnetic aromatic compounds containing six-membered rings.

As can be seen from this Table, aromatic compounds have a strong magnetic susceptibility about the z-axis. For example, the magnetic susceptibility about the z-axis of benzene is about 2.7 times stronger than that about the other principal axes. The more aromatic six-membered rings there are in a compound, the stronger the magnetic susceptibility associated with that compound becomes. This phenomenon occurs since π electrons in six-membered rings can develop eddy currents under the external magnetic fields. Consequently, crystals that are composed of aromatic compounds may potentially exhibit strong diamagnetic susceptibility. It was previously thought that a particularly strong magnetic field would be needed to move diamagnetic materials, due to their diamagnetic anisotropy. Therefore, most of researchers have not paid sufficient attention to the differences in ‘easy’ and ‘difficult’ axes of magnetization which are present in diamagnetic materials. This is due to the challenge of preparing a setup to investigate these axes experimentally. In this study, we focused on the magnetic properties of the diamagnetic materials, with special reference to the easy and difficult axes of magnetization.

- Crystals derived from biological and organic materials

In the field of biomagnetism, for uncovering the mechanism underpinning the magnetically induced orientation of several biological materials, the magnetic orientation of the crystals derived from organic material has received much attention and is investigated by many researchers. For example, the magnetic behavior of thin-layered crystals of lecithin, which is one of the basic components of membranes, was investigated and their diamagnetic orientation was measured [21]. Also, in the field of polymer science, various studies reported on the magnetic effects of organic polymeric

crystals detected under magnetic fields greater than 1 T [22]–[25]. For example, the magnetic orientation of Lysozyme crystals placed under such magnetic fields was observed for making the crystal of high quality [26],[27]. From these previous studies, most studies reported measuring the magnetic orientation of artificially-produced crystals. But, the light reflection behavior of an individual biogenic crystals derived from organisms was seldom investigated by using the diamagnetic methods. In the next section, we describe these biogenic crystals and their bio-functional role as light reflectors.

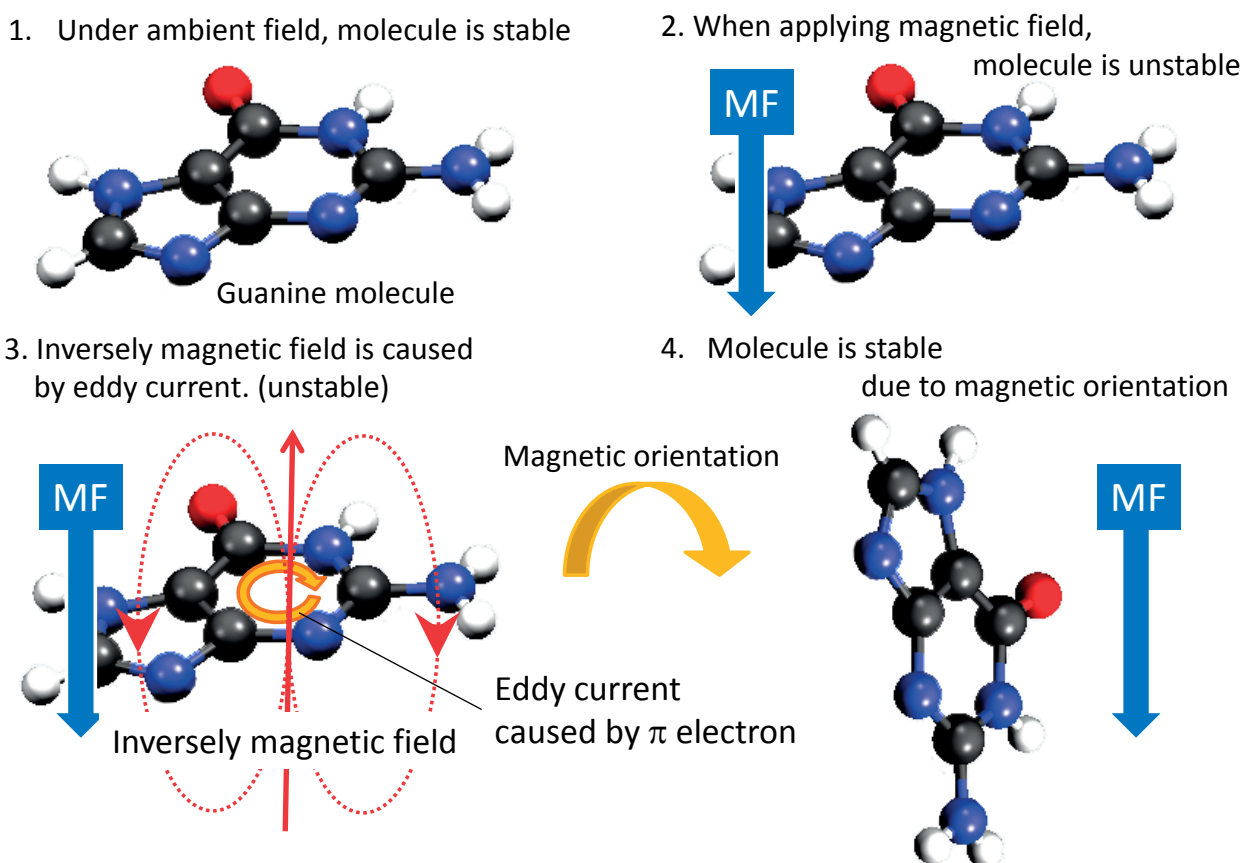
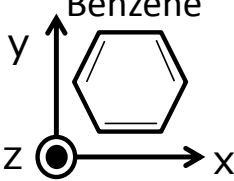
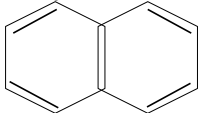
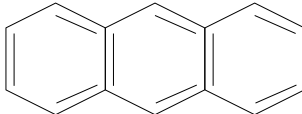


Figure 1.1. Principle of diamagnetic orientation of an organic compound containing an aromatic six-membered ring, (e.g. a guanine molecule), in response to an external magnetic field (MF).

Table 1.1. Magnetic anisotropies in the susceptibility of diamagnetic molecules containing six-membered rings.

Molecule	Magnetic susceptibility (10^{-6} emu.mol $^{-1}$)		
	- χ mol x	- χ mol y	- χ mol z
Benzene 	34.9	34.9	94.6
Naphthalene 	54.7	52.6	173.5
Anthracene 	75.8	62.6	251.6

(cited in Magnetoscience, eds, K.Kitazawa, S. Ozeki, Y.tanimoto, M. Yamaguchi; IPC press, pp.17 (2002).)

1.2 Light Reflection Systems of Organisms and Biogenic Guanine Crystals

The beautiful colors of living organisms displayed in nature, are often produced by periodically patterned microstructures, both in organic tissues and in inorganic matrices. I refer to this subset of natural coloration as structural color. For example, many bird feathers [28]–[30], insects [31]–[32], seashells [33] and others, can exhibit structural color. Structural colors and iridescence like this arise from microstructures which are smaller than optical wavelengths. In the case of chameleons [34], their skins contain biogenic guanine crystals, which produce rapid color changes during male contests or courtship. Additionally, many aquatic organisms have reflective systems based on naturally occurring biogenic guanine crystals, which act as biogenic photonic crystals. In particular, various fish species reflect light and exhibit structural color owing to the presence of such crystals in their skin or ocular fundus. Since the 1930s, the distinctive “light reflection of white-silver color” from the fish body surface has attracted attention and been investigated [35], [36]. In particular, the research reported that the angular distribution of light for the surface of a fish was investigated and this experimental result supported the hypothesis that the light reflection produced by the surface of a fish may behave as a camouflage function to obliterate their shadow [36]. It is also considered that the light reflection may have a role of communication between fishes. But, the aim of the function of their light reflection was not yet revealed clearly. Also, the neon tetra (*Paracheirodon innesi*) [37]–[39] has been studied to gain an insight into iridescent color reflection, which this species can control in a light-sensitive fashion. Their light reflection system operates in a manner analogous to Venetian blinds, generating a structural color change. These light reflection changes and structural color

changes are caused by the biogenic guanine crystals in the chromatophore cells on their scales. Most reports reported the light property from the surface of a fish or the iridophore cells on the fish scales from the point of morphology. Also, most studies reported about the relationship between their light reflection and multi-layered structures by the biogenic guanine crystal and cytoplasm. However, the light reflection property of a single guanine crystal platelet in the chromatophore cells was not yet investigated.

- Guanine crystal structure

In the case of fish, biogenic guanine crystals can exist in the chromatophore cells on their scales on the surface of a fish. Biogenic guanine crystals are formed and stacked in chromatophore cells on the scales of fish (goldfish [40], [41], Japanese koi [42]–[43], neon tetra [37]–[39], fish in the abyssal zone of the ocean [44] and others). These crystals scatter light strongly due to high refraction and optical properties, such as those that confer structural color to photonic crystals. Next, we describe about a guanine molecule and an anhydrous and monohydrated guanine crystal structure.

Guanine molecules consist of a purine ring, which is a kind of aromatic compound containing a fused pyrimidine and imidazole ring. Crystalline guanine displays high anisotropy and diamagnetic orientation under magnetic fields [40], [41]. But, the issue related to the axes of easy and difficult magnetization for diamagnetic guanine crystals has remained.

Solid-state guanine can be found in two forms, either the anhydrous base form or the monohydrated base form. Generally, anhydrous guanine crystals prefer to adopt the 7H-keto-amino tautomer, as shown in Figure 1.2(a) [45], [46]. Anhydrous guanine

crystals can form the monoclinic structure, in space group $P2_1/c$, with unit cell dimensions of $a = 3.55$, $b = 9.69$, $c = 16.35$ Å, ($\beta = 95.8^\circ$) [42], [46]. In contrast, monohydrated guanine crystals adopt the 9H-keto-amino tautomer (Figure 1.2(b)) [45], [47]. Monoclinic crystals of monohydrated guanine have also been reported, in space group $P2_1/n$, with unit cell dimensions of $a = 16.51$, $b = 11.28$, $c = 3.65$ Å, ($\beta = 96.8^\circ$) [42], [47]. In addition, Figure 1.3 shows the water columns in monohydrated guanine crystals [47], [48].

It was reported previously that the biogenic guanine crystals derived from Japanese koi (ornamental carp, *Cyprinus carpio*) are the anhydrous form [42], and that these crystals are located adjacent to an amorphous guanine region, which also includes some monohydrated guanine crystals [49]. In this report, this disordered guanine phase is a precursor of crystalline anhydrous guanine on the scales derived from Japanese koi. Figure 1.4 shows the structure of a biogenic anhydrous guanine crystal from koi [42]. These biogenic guanine crystals have a high refractive index (~ 1.83) and scatter light from the body surface of the fish [42], [43], [50]–[52].

There are several studies reporting the presence of light scattering systems that depend on biogenic guanine crystals on the body surfaces of fish. In spite of this, there have been few studies investigating the magnetic and optical behavior of biogenic guanine crystals.

- **Magnetic behavior of biogenic guanine crystals**

In 2009, our laboratory demonstrated the magnetic behavior of biogenic guanine crystals stacked in the chromatophore cells on goldfish scales. Quenching of light scattering was measured under magnetic fields exceeding 260 mT [40]. In addition,

the suppression of structural colors under magnetic fields was reported [41]. These studies lead to the hypothesis that the quenching of light scattering, from guanine crystals stacked in the chromatophore cells, resulted from diamagnetic orientation. However, this hypothesis remained untested issues and the available data did not permit definitive conclusions related to the directionality of oriented guanine crystals under magnetic fields.

- The aims of this study

In this study, we aimed to reveal the angular specificity of light scattering from an individual biogenic guanine crystal derived from the chromatophore cells of the goldfish scales, and to establish diamagnetic methods to remotely-control the light scattering from an individual biogenic guanine crystal. This was performed to gain the experimental methods for contributing to an insight into the functioning of light-scattering reflectors derived from a fish. In addition, we aimed to reveal the axes of easy and difficult magnetization for biogenic guanine crystals, as this was not completely investigated for the diamagnetic manipulation of a guanine crystal.

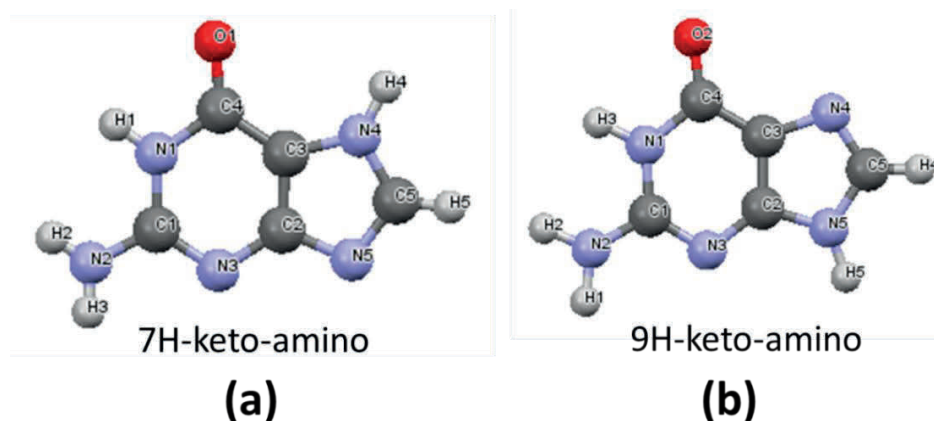


Figure 1.2. Images of a guanine molecule. (a) 7H-keto-amino tautomer (the preferred anhydrous crystal form) and (b) 9H-keto-amino tautomer (the preferred monohydrated crystal form)

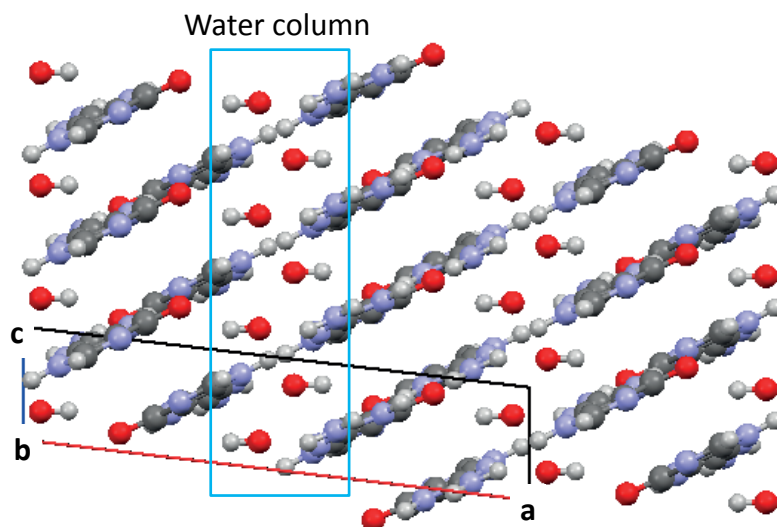
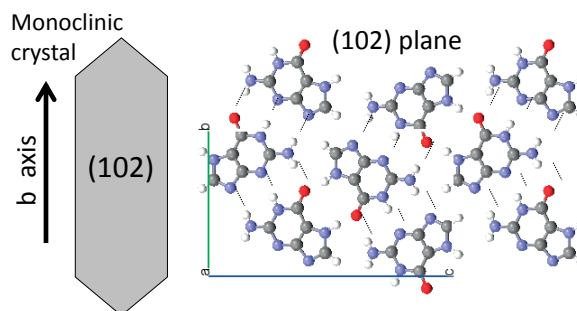
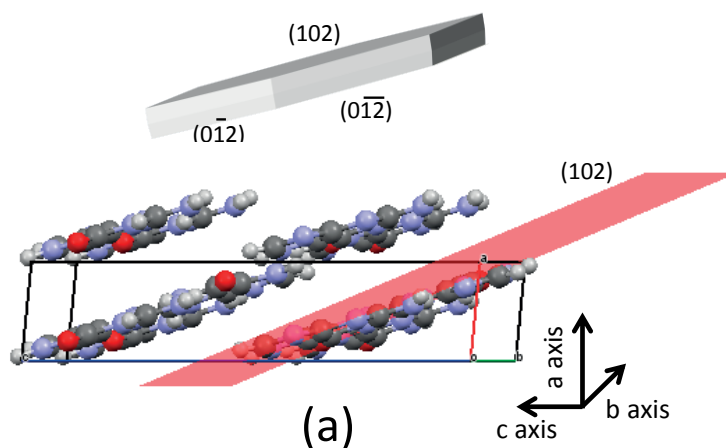


Figure 1.3. Schematics of the monohydrated guanine crystal morphology. This crystal contains water columns. The parallelogram labeled a-c shows the unit cell.



(b)

Figure 1.4. Images of anhydrous guanine crystal morphology. (a) Guanine molecules forming sheets to (102) plane. (b) Schematic image of a biogenic guanine crystal and guanine molecular arrangement on (102) plane of the crystal.

1.3 References

- [1] M. D. Simon, and A. K. Geim, “Diamagnetic levitation: Flying frogs and floating magnets (invited),” *J. Appl. Phys.*, vol. 87, pp. 6200–6204, 2000.
- [2] L. Pauling, “The Diamagnetic Anisotropy of Aromatic Molecules,” *J. Chem. Phys.*, vol. 4, pp. 673–677, 1936.
- [3] M. Fujiwara, M. Fukui, and Y. Tanimoto, “Magnetic Orientation of Benzophenone Crystals in Fields up to 80.0 KOe,” *J. Phys. Chem. B*, vol. 103, pp. 2627–2630, 1999.
- [4] M. Fujiwara, T. Chidiwa, and Y. Tanimoto, “Magnetic Orientation under Gravity: Biphenyl and Naphthalene Crystals,” *J. Phys. Chem. B*, vol. 104, pp. 8075–8079, 2000.
- [5] M. Fujiwara, E. Oki, M. Hamada, and Y. Tanimoto, “Magnetic Orientation and Magnetic Properties of a Single Carbon Nanotube,” *J. Phys. Chem. A*, vol. 105, pp. 4383–4386, 2001.
- [6] H. Yokomichi, H. Sakima, M. Ichihara, F. Sakai, K. Itoh, and N. Kishimoto, “Effects of high magnetic field on the morphology of carbon nanotubes and selective synthesis of fullerenes,” *Appl. Phys. Lett.*, vol. 74, pp. 1827–1829, 1999.
- [7] J. Torbet, J. M. Freyssinet, and G. Hudry-Clergeon, “Oriented fibrin gels formed by polymerization in strong magnetic fields,” *Nature*, vol. 289, pp. 91–93, 1981.
- [8] J. M. Freyssinet, J. Torbet, G. Hudry-Clergeon, and G. Maret, “Fibrinogen and fibrin structure and fibrin formation measured by using magnetic orientation,” *Proc Natl Acad Sci U S A.*, vol. 80, pp. 1616–1620, 1983.
- [9] J. Torbet, “Fibrin assembly in human plasma and fibrinogen/albumin mixtures,” *Biochemistry*, vol. 25, pp. 5309–5314, 1986.
- [10] A. Yamagishi, T. Takeuchi, T. Higashi, and M. Date, “Magnetic field effect on the

- polymerization of fibrin fibers,” *Physica B*, vol. 164, pp. 222–228, 1990.
- [11] A. Yamagishi, T. Takeuchi, T. Higashi, and M. Date, “Polymerization of biological molecules under high magnetic fields,” *Physica B*, vol. 155, pp. 433–436, 1989.
- [12] M. Iwasaka, S. Ueno, and H. Tsuda, “Effects of magnetic fields on fibrinolysis,” *J. Appl. Phys.*, vol. 75, pp. 7162–7164, 1994.
- [13] J. Torbet and M. C. Ronziere, “Magnetic alignment of collagen during self-assembly,” *Biochem. J.*, vol. 219, pp. 1057–1059, 1984.
- [14] J. Torbet, M. Malbouyres, N. Builles, V. Justin, M. Roulet, O. Damour, A. Oldberg, F. Ruggiero, and D. J. S. Hulmes, “Orthogonal scaffold of magnetically aligned collagen lamellae for corneal stroma reconstruction,” *Biomaterials*, vol. 28, pp. 4268–4276, 2007.
- [15] T. Higashi, A. Yamagishi, T. Takeuchi, N. Kawaguchi, S. Sagawa, S. Onishi, and M. Date, “Orientation of erythrocytes in a strong static magnetic field,” *Blood*, vol. 82, pp. 1328–1334, 1993.
- [16] T. Takeuchi, T. Mizuno, T. Higashi, A. Yamagishi, and M. Date, “High field magnetic orientation of red blood cells,” *Physica B*, vol. 201, pp. 601–605, 1994.
- [17] M. Chabre, “Diamagnetic anisotropy and orientation of α helix in frog rhodopsin and meta II intermediate,” *Proc. Natl. Acad. Sci. U.S.A.*, vol. 75, pp. 5471–5474, 1978.
- [18] J. Torbet, “Solution behavior of DNA studied with magnetically induced birefringence,” *Methods Enzymol.*, vol. 211, pp. 518–532, 1992.
- [19] N. Morii, and H. Morii, “DNA as functional material with one-dimensionally oriented molecular chains,” *J. Biol. Macromol.*, vol. 9, pp. 3–12, 2009.
- [20] K. Suzuki, T. Toyota, K. Sato, M. Iwasaka, S. Ueno, and T. Sugawara,

- “Characteristic curved structure derived from collagen-containing tubular giant vesicles under static magnetic field,” *Chem. Phys. Lett.*, vol. 440, pp. 286–290, 2007.
- [21] I. Sakurai, Y. Kawamura, A. Ikegami, and S. Iwayanagi, “Magneto-orientation of lecithin crystals,” *Proc. Natl. Acad. Sci. U.S.A.*, vol. 77, pp. 7232–7236, 1980.
- [22] T. Kimura, “Study on the Effect of Magnetic Fields on Polymeric Materials and Its Application,” *Polym. J.*, vol. 35, 823–843, 2003.
- [23] F. Kimura, T. Kimura, K. Matsumoto, and N. Metoki, “Single-Crystal X-ray Diffraction Study of a Magnetically Oriented Microcrystal Array of Lysozyme,” *Cryst. Growth Des.*, vol. 11, pp. 12–15, 2011.
- [24] G. Sazaki, E. Yoshida, H. Komatsu, T. Nakada, S. Miyashita, and K. Watanabe, “Effects of a magnetic field on the nucleation and growth of protein crystals,” *J. Cryst. Growth*, vol. 173, pp. 231–234, 1997.
- [25] N. I. Wakayama, M. Ataka, and H. Abe, “Effect of a magnetic gradient on the crystallization of hen lysozyme,” *J. Cryst. Growth*, vol. 178, pp. 653–656, 1997.
- [26] S. Sakurazawa, T. Kubota, and M. Ataka, “Orientation of protein crystals grown in a magnetic field,” *J. Cryst. Growth*, vol. 196, pp. 325–331, 1999.
- [27] T. Sato, Y. Yamada, S. Saijo, T. Hori, R. Hirose, N. Tanaka, G. Sazaki, K. Nakajima, N. Igarashi, M. Tanaka, and Y. Matsuura, “Enhancement in the perfection of orthorhombic lysozyme crystals grown in a high magnetic field (10 T),” *Acta Crystallogr. Sect. D*, vol. 56, pp. 1079–1083, 2000.
- [28] S. Yoshioka, E. Nakamura, and S. Kinoshita, “Origin of Two-Color Iridescence in Rock Dove's Feather,” *J. Phys. Soc. Jpn.*, vol. 76, Art. no. 013801, 2007.
- [29] E. Nakamura, S. Yoshioka, and S. Kinoshita, “Structural color of rock dove's neck

- feather,” *J. Phys. Soc. Jpn.*, vol. 77, Art. no. 124801, 2008.
- [30] S. Yoshioka, and S. Kinoshita, “Effect of Macroscopic Structure in Iridescent Color of the Peacock Feathers,” *Forma*, vol. 17, pp. 169–181, 2002.
- [31] C. W. Mason, “Structural colors in insects. II,” *J. Phys. Chem.*, vol. 31, pp. 321–354, 1927.
- [32] H. Ghiradella, “Structure of iridescent lepidopteran scales: variations on several themes,” *Ann. Entomol. Soc. Am.*, vol. 77, pp. 637–645, 1984.
- [33] K. Takahashi, H. Yamamoto, A. Onoda, M. Doi, T. Inaba, M. Chiba, A. Kobayashi, T. Taguchi, T. Okamura, and N. Ueyama, “Highly oriented aragonite nanocrystal-biopolymer composites in an aragonite brick of the nacreous layer of *Pinctada fucata*,” *Chem. Commun.*, no. 8, pp. 996–997, 2004.
- [34] J. Teyssier, S. V. Saenko, D. van der Marel, and M. C. Milinkovitch, “Photonic crystals cause active colour change in chameleons,” *Nat. Commun.*, vol. 6, Art. no. 6368, 2015.
- [35] K. W. Foster, “Color Changes in *Fundulus* with Special Reference to the Color Changes of the Iridosomes,” *Proc. natn. Acad. Sci. U.S.A.*, vol. 19, pp. 535–540, 1933.
- [36] E. J. Denton, J. B. Gilpin-Brown, and P. G. Wright, “The angular distribution of the light produced by some mesopelagic fish in relation to their camouflage,” *Proc. R. Soc. Lond. B.*, vol. 182, pp. 145–158, 1972.
- [37] S. Yoshioka, B. Matsuhana, S. Tanaka, Y. Inouye, N. Oshima, and S. Kinoshita, “Mechanism of variable structural color in the neon tetra: quantitative evaluation of the Venetian blind model,” *J. R. Soc. Interface*, vol. 8, pp. 56–66, 2011.
- [38] H. Nagaishi, N. Oshima, and R. Fujii, “Light-reflecting properties of the iridophores

- of the neon tetra *Paracheirodon innesi*,” *Comp. Biochem. Physiol.*, vol. 95A, pp. 337–341, 1990.
- [39] J. N. Lyngsum, and J. Shand, “Changes in spectral reflexions from the iridophores of the Neon tetra,” *J. Physiol.*, vol. 325, pp. 23–34, 1982.
- [40] M. Iwasaka, “Effects of static magnetic fields on light scattering in red chromatophore of goldfish scale,” *J. Appl. Phys.*, vol. 107, Art. no. 09B314, 2010.
- [41] M. Iwasaka, Y. Miyashita, M. Kudo, S. Kurita, and N. Owada, “Effect of 10-T magnetic fields on structural colors in guanine crystals of fish scales,” *J. Appl. Phys.*, vol. 111, Art. no. 07B316, 2012.
- [42] A. Levy-Lior, B. Pokroy, B. Levavi-Sivan, L. Leiserowitz, S. Weiner, and L. Addadi, “Biogenic Guanine Crystals from the Skin of Fish May Be Designed to Enhance Light Reflectance,” *Cryst. Growth Des.*, vol. 8, pp. 507–511, 2008.
- [43] A. Levy-Lior, E. Shimoni, O. Schwartz, E. Gavish-Regev, D. Oron, G. Oxford, S. Weiner, and L. Addadi, “Guanine-Based Biogenic Photonic-Crystal Arrays in Fish and Spiders,” *Adv. Funct. Mater.*, vol. 20, pp. 320–329, 2010.
- [44] M. Kreysing, R. Pusch, D. Haverkate, M. Landsberger, J. Engelmann, J. Ruiter, C. M.-Ferrer, E. Ulbricht, J. Grosche, K. Franze, S. Streif, S. Schumacher, F. Makarov, J. Kacza, J. Guck, H. Wolburg, J. K. Bowmaker, G. von der Emde, S. Schuster, H.-J. Wagner, A. Reichenbach, and M. Francke, “Photonic Crystal Light Collectors in Fish Retina Improve Vision in Turbid Water,” *Science*, vol. 336, pp. 1700–1703, 2012.
- [45] R. P. Lopes, M. P. M. Marques, R. Valero, J. Tomkinson, and Luís A. E. Batista de Carvalho, “Guanine: A Combined Study Using Vibrational Spectroscopy and Theoretical Methods,” *Spectroscopy: An International Journal*, vol. 27, pp. 273–292,

2012.

- [46] K. Guille, and W. Clegg, “Anhydrous guanine: a synchrotron study,” *Acta Crystallogr., Sect. C*, vol. 62, pp. O515–517, 2006.
- [47] U. Thewalt, C. E. Bugg, and R. E. Marsh, “The crystal structure of guanine monohydrate,” *Acta Crystallogr. Sect. B*, vol. B27, pp. 2358–2363, 1971.
- [48] F. Ortman, K. Hannewald, and F. Bechstedt, “Guanine Crystals: A First Principles Study,” *J. Phys. Chem. B*, vol. 112, pp. 1540–1548, 2008.
- [49] D. Gur, Y. Politi, B. Sivan, P. Fratzl, S. Weiner, and L. Addadi, “Guanine-based photonic crystals in fish scales form from an amorphous precursor,” *Angew. Chem., Int. Ed.*, vol. 52, pp. 388–391, 2013.
- [50] P. J. Herring, “Reflective systems in aquatic animals,” *Comp. Biochem. Physiol.*, vol. 109A, pp. 513–546, 1994.
- [51] E. J. Denton, “Review Lecture: On the organization of reflecting surfaces in some marine animals,” *Philos. Trans. R. Soc. London, Ser. B*, vol. 258, pp. 285–313, 1970.
- [52] T. M. Jordan, J. C. Partridge, and N. W. Roberts, “Non-polarizing broadband multilayer reflectors in fish,” *Nat. Photonics*, vol. 260, pp. 759–763, 2012.

2. Physical Property Analysis of Biogenic Guanine Crystal

2.1 SEM Imaging and X-ray Powder Diffraction

2.1.1 Introduction

In this chapter, we physically investigated biogenic guanine crystals obtained from goldfish. We used scanning electron microscopy for micro- to nano- scale observations of this micro-material. Further physical analysis was carried out by X-ray powder diffraction. Motivating our physical analyses were the needs to determine the structure of our guanine crystals [1], [2], and to characterize the easy and difficult axes of magnetization. Previous analyses, on structure of guanine crystals isolated from chromatophore cells which are present on goldfish scales, were not carried out on the micro-scale (μm – nm).

2.1.2 Methods and Materials

- Sample preparation

Figure 2.1.1 schematically depicts the process whereby a biogenic guanine crystal suspension was prepared from the scales of a Japanese goldfish (*Carassius auratus*). We collected the fish scales from the living goldfish using plastic tweezers. The collected scales were added to distilled water and placed in a centrifuge tube (capacity: 15 mL, polypropylene, Corning 430052) and were washed by pipetting. Further, we removed both the supernatant and all undesired substances from the centrifuge tube. After replacing with fresh water, we poked the washed scales with a plastic stick, which isolated and dispersed the biogenic guanine crystals from the chromatophore cells into the distilled water. After centrifuging to precipitate the scales,

we collected the supernatant liquid, which contained the guanine crystals, and placed it into a new centrifuge tube. Undesired substances, including lipids and cellular debris, were removed from the guanine crystal suspension by centrifugation (1500–2000 rpm) for 5–10 sec. Centrifugal treatment was repeated to remove undesired substances until undesired substances could not be seen. We obtained a high purity, homogeneous suspension of biogenic guanine crystals in distilled water via this method.

- Scanning Electron Microscopy (SEM)

We used an SEM system (JSM-6510LA / Chiba Univ. Center for Analytical Instrumentation) to observe single platelet of a biogenic guanine crystal at the micro-scale (μm – nm). The biogenic guanine crystal suspension obtained from goldfish was pipetted onto the glass piece. Next, the guanine crystals on the glass piece were dried in a vacuum apparatus. A measurement sample (Figure 2.1.2) contained dried guanine crystals on the glass piece (approximately $5\text{ mm} \times 3\text{ mm} \times 1\text{ mm}$) fixed to the horizontal sample stage, which was made of aluminum ($\Phi 10\text{ mm} \times 1\text{ mm}$), using an electrically-conductive carbon tape. By using an ion-sputtering apparatus (JFC-1100 / Chiba Univ. Center for Analytical Instrumentation), gold evaporation was carried out, to coat the measurement sample. The schematics of the sample preparation process are shown in Figure 2.1.3. This prepared sample was fixed on the stage and observed by SEM.

- X-ray powder diffraction

A dried powder of biogenic guanine crystals was used for X-ray diffraction experiments. The crystal suspension was placed in a 15 mL centrifuge tube and condensed by centrifugation at 2000 rpm for 5 min. After removing the supernatant (mostly distilled water), we added acetone, about 300 mL, to the sediments containing biogenic guanine crystals in the centrifuge tube. By exploiting the evaporation of acetone, this liquid containing biogenic guanine crystals was dried with a heater and kept in a desiccator for more than three hours. The dried flakes were crushed in a mortar, and we obtained a powder of biogenic guanine crystals. This powder was used for X-ray powder diffraction (D8 ADVANCE, Bruker). Detailed parameters of diffraction data collection were follows: The exposure time was 4 seconds. The capture step was 0.02° . The range of 2θ was from 5° to 55° . The divergence slit was 0.3° . The generator voltage was 40 kV.

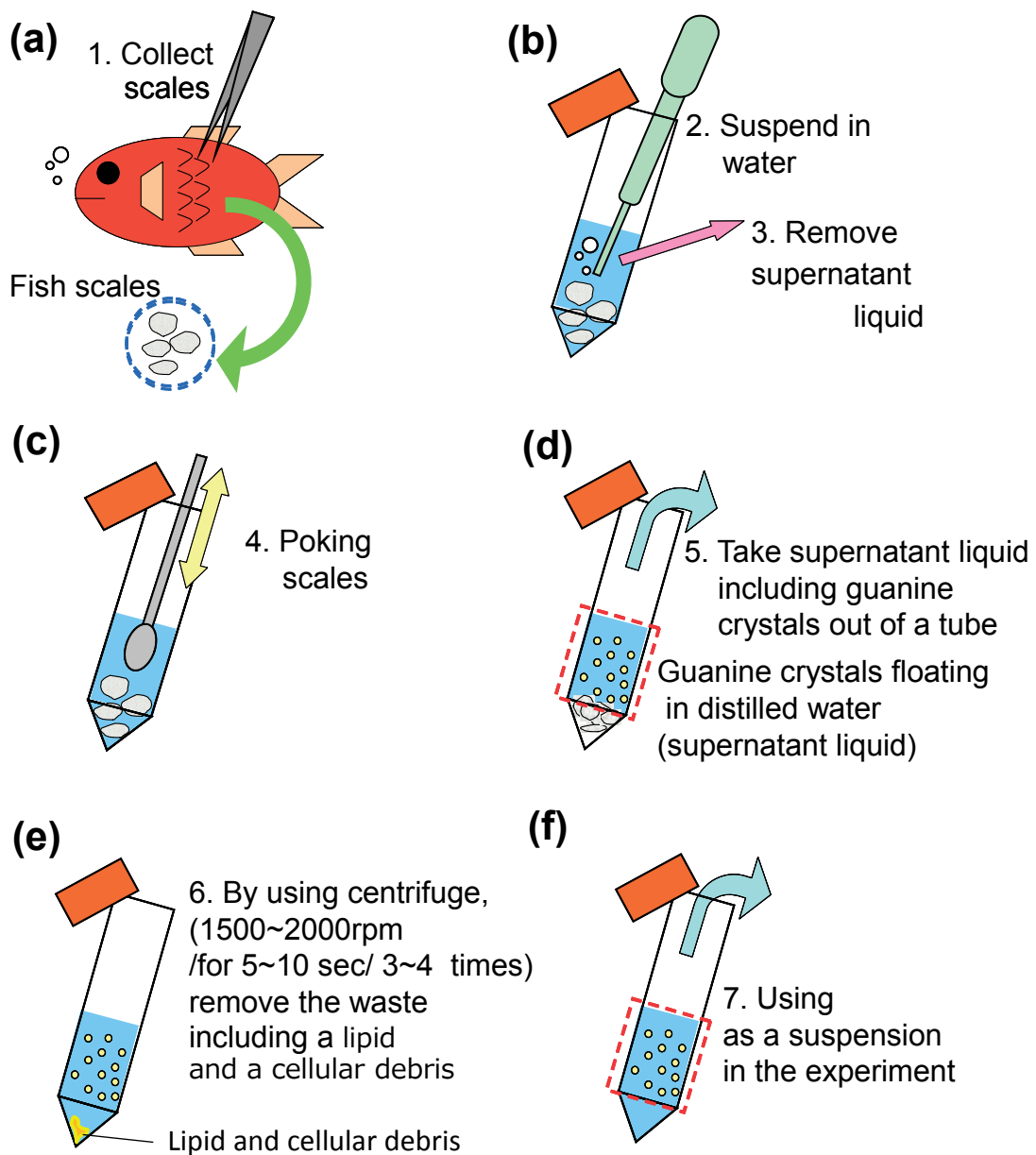


Figure 2.1.1. Preparation process for obtaining a suspension of biogenic guanine crystals from goldfish scales. (a) Collecting the goldfish scales. (b) Washing the collected scales into the centrifuge tube with the distilled water and removing the supernatant. (c) Poking scales with a plastic stick. (d) Extracting the supernatant liquid containing guanine crystals. (e) Removing the undesired substances, including lipids and cellular debris, 3–4 times by using centrifuge for 5–10 sec. (f) Using as the obtained suspension in the experiment.

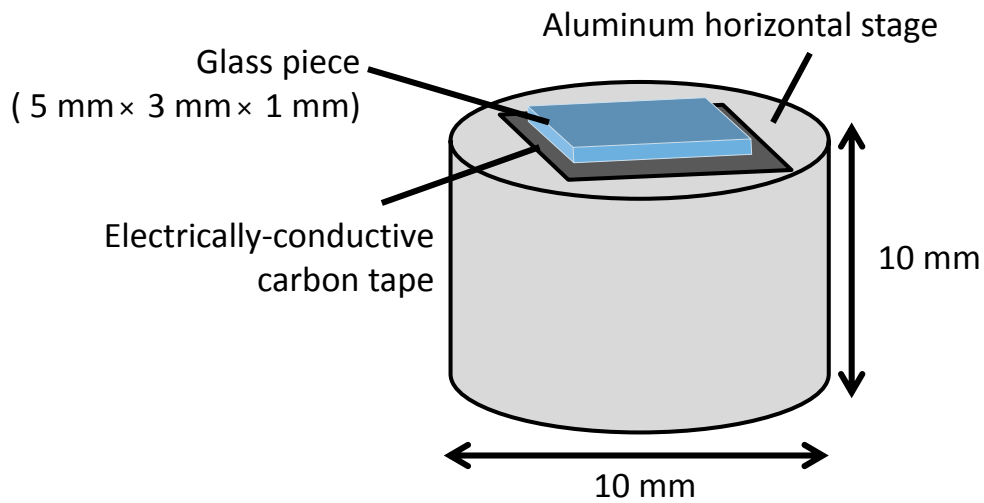


Figure 2.1.2. Illustration of the measurement sample setup used for SEM.

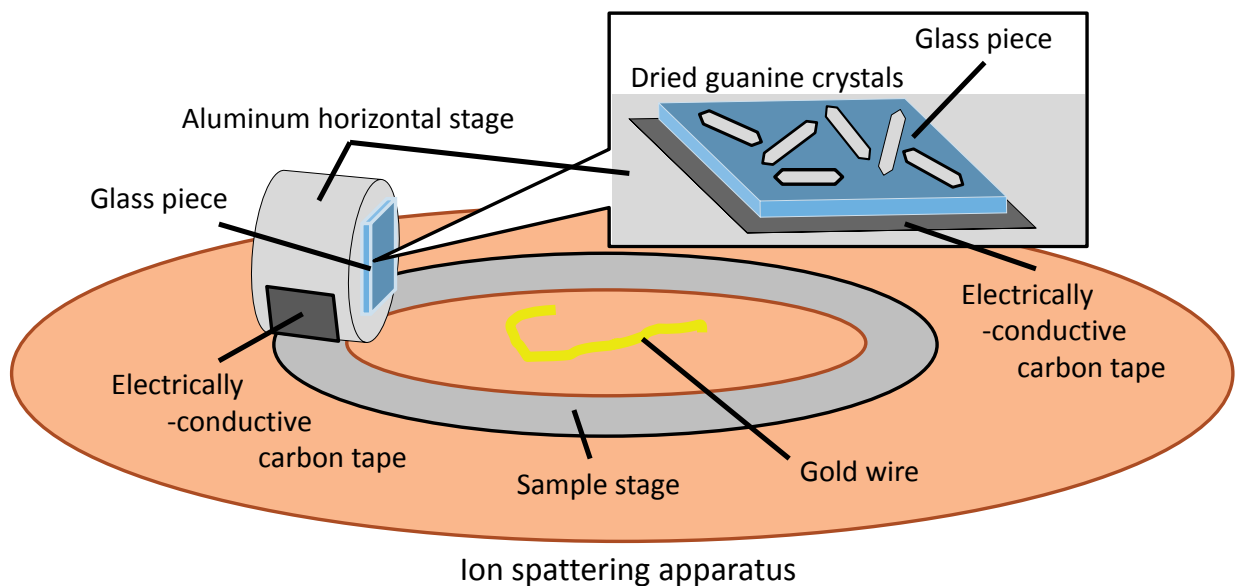


Figure 2.1.3. Schematics of the preparation of guanine crystals for observation using an SEM system. By using an ion-sputtering apparatus, the measurement samples (guanine crystals dried with a vacuum apparatus) were coated in gold in preparation for imaging.

2.1.3 Results and Discussion

- **Scanning Electron Microscopy (SEM)**

We measured biogenic guanine crystals using an SEM system, and analyzed the SEM images obtained. Figures 2.1.4 and 2.1.5 show that the SEM images of biogenic guanine crystals had various properties. The guanine crystals in both Figure 2.1.4 and 2.1.5 had been dried in a vacuum apparatus.

The SEM image in Figure 2.1.4 shows that biogenic guanine crystals possess a lamellar structure and smooth planes. Figure 2.1.4 indicates that the crystals exhibit the elongated hexagonal platelet morphology, and had an average size of approximately $20\ \mu\text{m} \times 5\ \mu\text{m} \times \sim 100\ \text{nm}$ (length \times width \times thickness). Individual guanine crystals in Figure 2.1.4 (b) and (c), had very thin layers. For electron beam exposures, these thin crystals could be seen through. Figure 2.1.5 shows SEM images of guanine crystals containing defects. The edge formed by the overlap of multiple guanine crystals resembled a jagged blade, and the overlapping of multiple guanine crystals produced a platelet with a rough surface (Figure 2.1.5(a)). The surface of a single guanine crystal in Figure 2.1.5(b), (c) contained holes and other defects.

These results revealed that biogenic guanine crystals are very thin and have smooth planes. Some guanine crystals contain deforming holes and other defects. We discovered that biogenic guanine crystalline platelets have an elongated hexagonal morphology and an average size of $20\ \mu\text{m} \times 5\ \mu\text{m} \times \sim 100\ \text{nm}$.

- X-ray powder diffraction

X-ray powder diffraction measurements were performed on the condensed crystalline guanine powder. We compared our experimental results with the results of previous studies on monohydrated [3] and anhydrous guanine crystals [4].

Figure 2.1.6 shows the X-ray powder diffraction patterns obtained from the powder of guanine crystals. The powder of biogenic guanine crystals was prepared by drying the guanine crystal suspension. Our comparisons showed that the diffraction patterns from our goldfish guanine crystals were similar to the diffraction patterns for anhydrous guanine crystals from a Japanese carp [5], [6]. In particular, the same peak from the (012) crystal plane (A (012)) was apparent, and this peak was only present in the dataset from anhydrous guanine crystals [5]. In contrast, the peak from the (110) crystal plane (M (110)), which is a distinctive property of monohydrated guanine crystals, only appeared weakly in the left side of Figure 2.1.6(a).

According to a previous study, the anhydrous guanine crystals from Japanese carp are located adjacent to an amorphous region, which includes monohydrated guanine crystals [7]. We speculated that goldfish guanine crystals have a similar morphology, and are analogously located adjacent to a guanine amorphous region containing monohydrated guanine crystals.

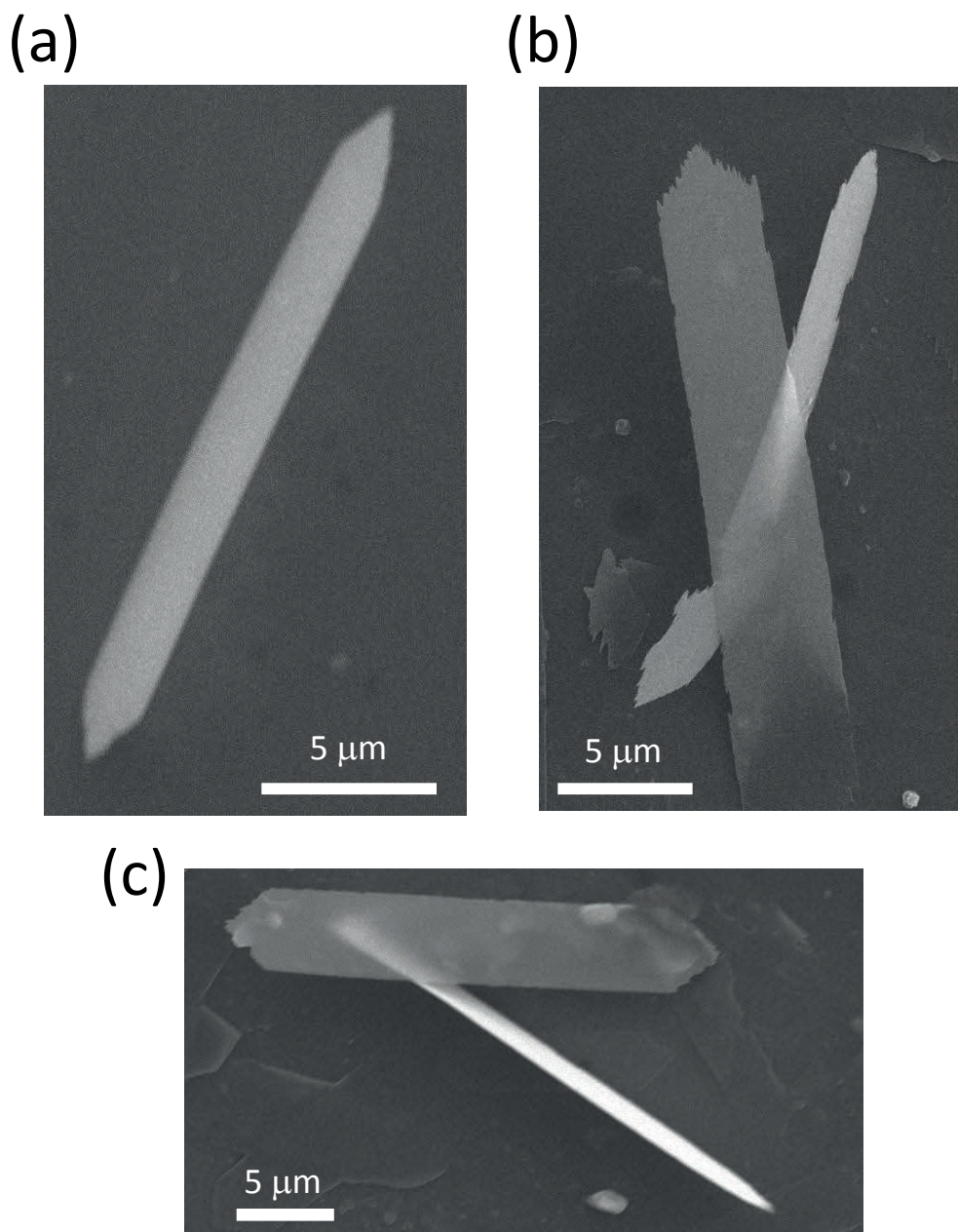


Figure 2.1.4. SEM images of guanine crystals. The crystals had a lamellar structure and smooth planes. (a) Elongated hexagonal plate morphology of a guanine crystal. (Bar: 5 μm). (b), (c) Single guanine crystal with a very thin layer. (Bar: 5 μm). (Reprinted (adapted) with permission from (M. Iwasaka, and Y. Mizukawa, “Light Reflection Control in Biogenic Micro-Mirror by Diamagnetic Orientation,” *Langmuir*, vol. 29, pp.4328–4334, 2013.). Copyright (2013) American Chemical Society.)

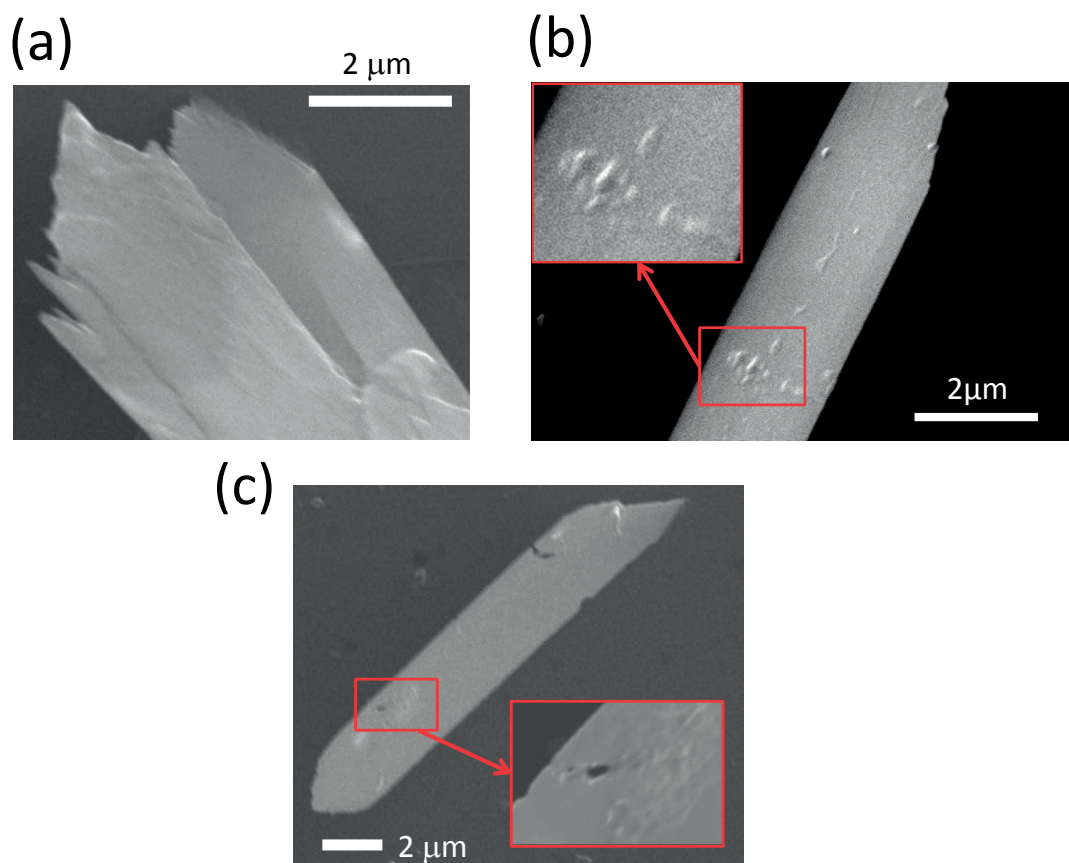


Figure 2.1.5. SEM images of guanine crystals containing defects. (a) Edge of multiple overlapping guanine crystals. (Bar: 2 μm). (b), (c) Surface of a single guanine crystal that contained many holes and other defects. (Bar: 2 μm). (Reprinted (adapted) with permission from (M. Iwasaka, and Y. Mizukawa, “Light Reflection Control in Biogenic Micro-Mirror by Diamagnetic Orientation,” *Langmuir*, vol. 29, pp.4328–4334, 2013.). Copyright (2013) American Chemical Society.)

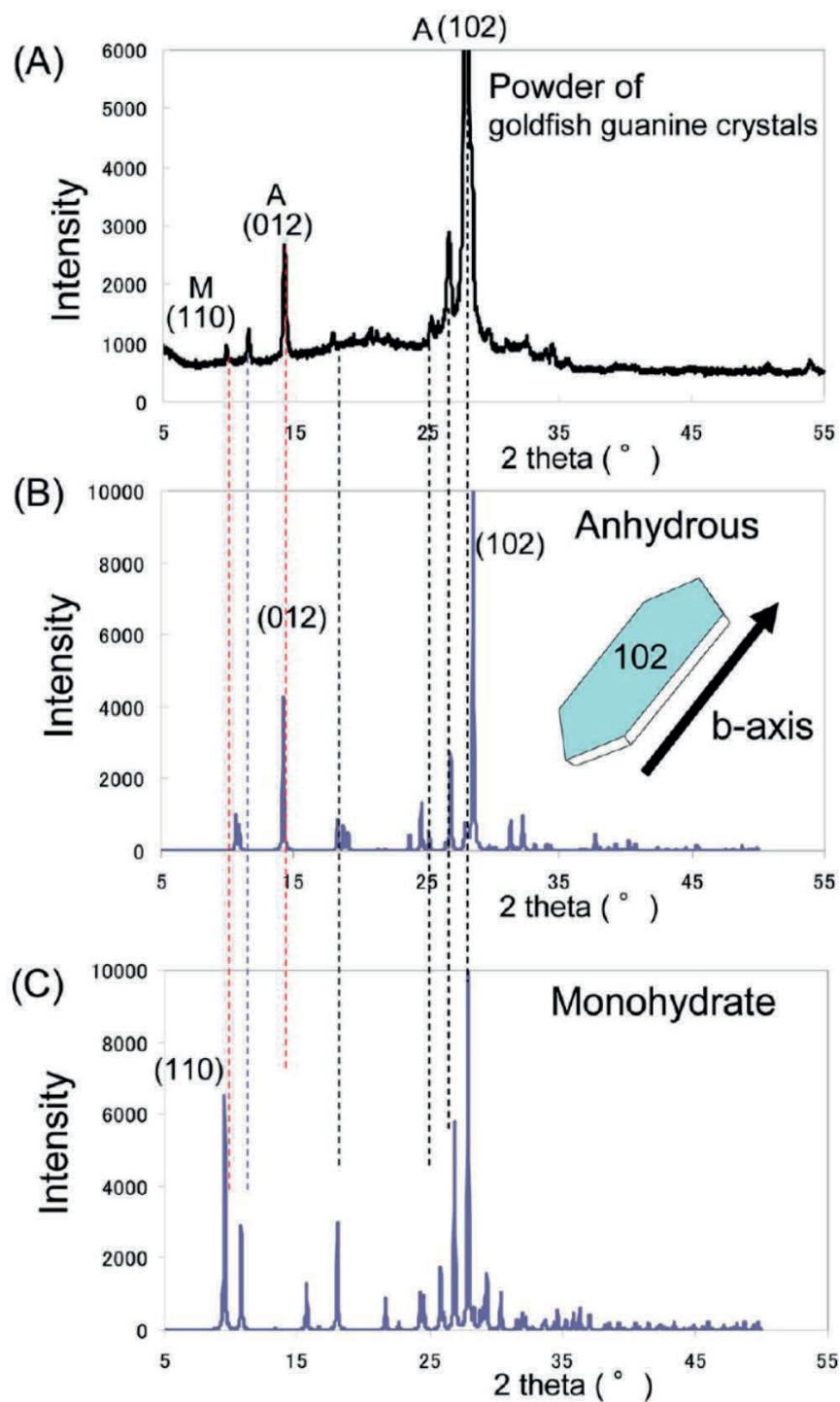


Figure 2.1.6. X-ray powder diffraction analyses on the powders of guanine crystals from goldfish. (A) Experimental result. (B) Diffraction patterns of anhydrous guanine crystals. (C) Diffraction patterns of monohydrated guanine crystals. (M; Monohydrate, A; Anhydrous) (Reprinted (adapted) with permission from (M. Iwasaka, and Y. Mizukawa, "Light Reflection Control in Biogenic Micro-Mirror by Diamagnetic Orientation," *Langmuir*, vol. 29, pp.4328–4334, 2013.). Copyright (2013) American Chemical Society.)

2.1.4 Summary

In this section, SEM imaging clarified that biogenic guanine crystals from goldfish are very thin and gauzy plates with an elongated hexagonal morphology (about $20\ \mu\text{m} \times 5\ \mu\text{m} \times \sim 100\ \text{nm}$). In particular, biogenic guanine crystals had either smooth surfaces, or contained defects such as holes. X-ray powder diffraction results indicated that guanine crystals from goldfish had the features of both of anhydrous crystals and monohydrate crystals. When comparing our results to the latest report [7], we speculate that guanine crystals of goldfish have a structure similar to those found in Japanese carp, which have an amorphous region that includes monohydrated guanine crystals.

2.2.5 References

- [1] M. Iwasaka, “Effects of static magnetic fields on light scattering in red chromatophore of goldfish scale,” *J. Appl. Phys.*, vol. 107, Art. no. 09B314, 2010.
- [2] M. Iwasaka, Y. Miyashita, M. Kudo, S. Kurita, and N. Owada, “Effect of 10-T magnetic fields on structural colors in guanine crystals of fish scales,” *J. Appl. Phys.*, vol. 111, Art. no. 07B316, 2012.
- [3] K. Guille, and W. Clegg, “Anhydrous guanine: a synchrotron study,” *Acta Crystallogr., Sect. C*, vol. 62, pp. O515–517, 2006.
- [4] U. Thewalt, C. E. Bugg, and R. E. Marsh, “The crystal structure of guanine monohydrate,” *Acta Crystallogr., Sect. B*, vol. B27, 2358–2363, 1971.
- [5] A. Levy-Lior, B. Pokroy, B. Levavi-Sivan, L. Leiserowitz, S. Weiner, and L. Addadi, “Biogenic Guanine Crystals from the Skin of Fish May Be Designed to Enhance Light Reflectance,” *Cryst. Growth Des.*, vol. 8, pp. 507–511, 2008.
- [6] A. Levy-Lior, E. Shimoni, O. Schwartz, E. Gavish-Regev, D. Oron, G. Oxford, S. Weiner, and L. Addadi, “Guanine-Based Biogenic Photonic-Crystal Arrays in Fish and Spiders,” *Adv. Funct. Mater.*, vol. 20, pp. 320–329, 2010.
- [7] D. Gur, Y. Politi, B. Sivan, P. Fratzl, S. Weiner, and L. Addadi, “Guanine-based photonic crystals in fish scales form from an amorphous precursor,” *Angew. Chem., Int. Ed.*, vol. 52, pp. 388–391, 2013.

2.2 Microscopic Synchrotron FTIR Measurements on Biogenic Guanine Crystals along Two Axes

2.2.1 Introduction

In section 2.1, the powder X-ray diffraction results indicated the possibility that biogenic guanine crystals have properties of both anhydrous and monohydrated crystals.

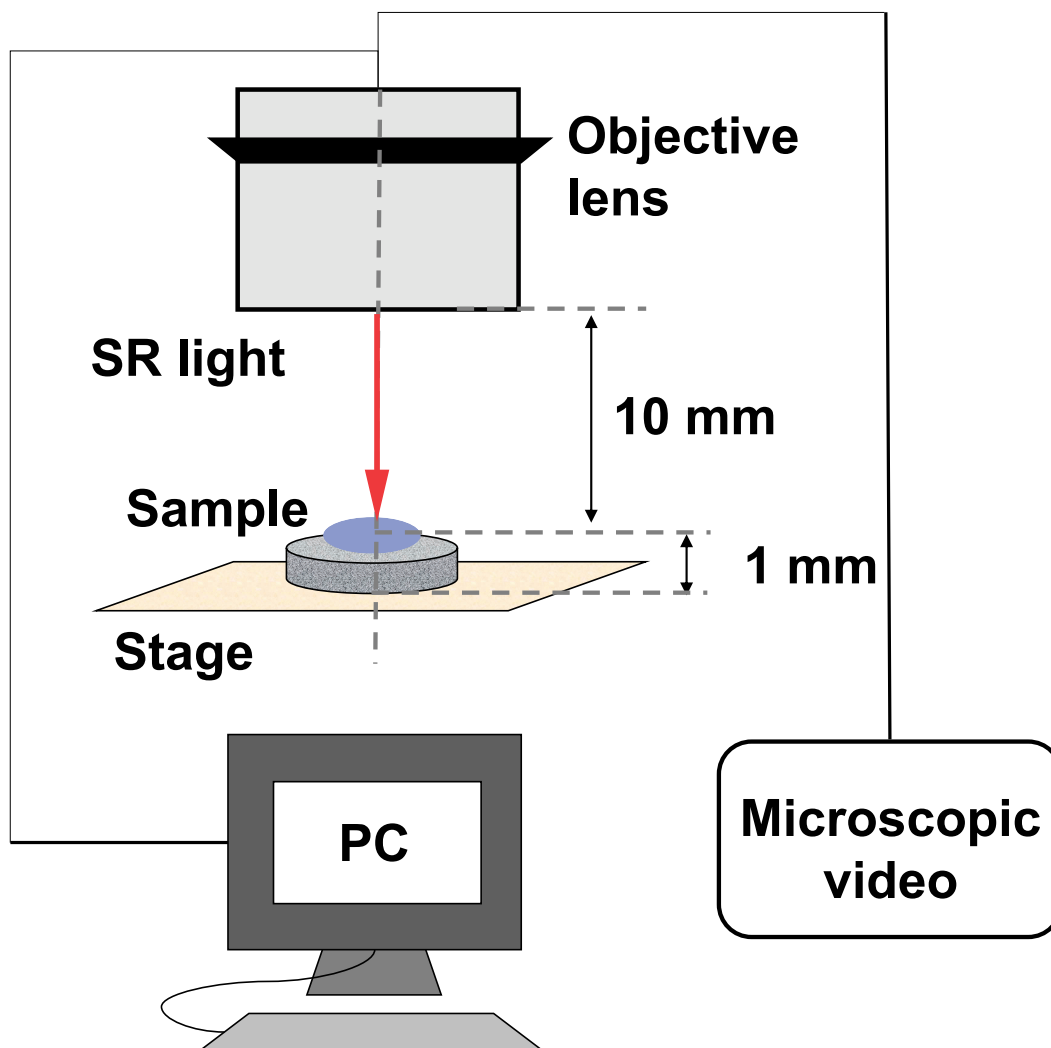
Next, we sought the method to investigate the molecular arrangement and crystal structure inside the individual biogenic guanine crystal, and to investigate the surface of the crystal for analysis of the axes of easy and difficult magnetization.

In this chapter, the vibrations of molecular bonds were measured by using a polarized infrared micro-beam at a synchrotron radiation source. We used the brilliant light radiated by the SPring-8 synchrotron source (Hyōgo Prefecture, Japan), since that powerful source provided us with the greatest research tool to describe and uncover novel features of soft micro-materials. We have an interest in microscopic Fourier transform infrared (FTIR) spectroscopy. The microscopic FTIR spectroscopy facility available at SPring-8 was suited to precisely analyze materials of micro-size, such as our biogenic guanine crystals. In addition, this synchrotron radiation facility can produce synchrotron orbital radiation (SR) beam and we used this beam in this experiment. This SR micro-beam has the ability to measure soft micro-scale biological samples while producing only limited damage. So, we investigated the optical anisotropy of molecular vibration in a biogenic guanine crystal using microscopic synchrotron FTIR.

2.2.2 Methods and Materials

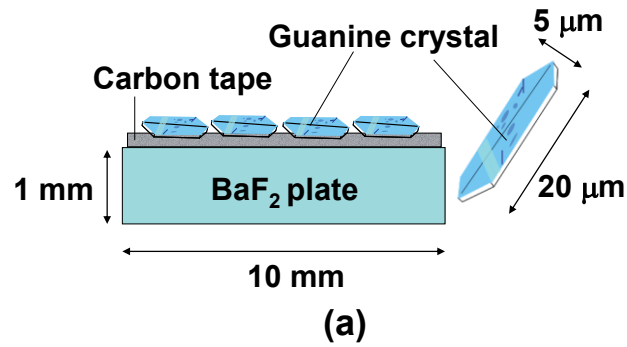
Microscopic synchrotron FTIR at SPring-8 enables measurements on micro-materials using an SR beam irradiating a range of 5–10 μm . This system is combined with microscopic FTIR, which enables irradiation of the soft micro-scale samples to proceed alongside observation in real-time. We performed microscopic synchrotron FTIR measurements at SPring-8, on beam-line 43IR (BL43IR). Figure 2.2.1 shows the experimental configuration for investigating the reflectance and absorbance spectrum of one biogenic guanine crystal platelet via microscopic synchrotron FTIR.

In addition, the central region of a single guanine crystal was irradiated by the SR beam in two polarization directions (parallel and perpendicular to the long axis). Microscopic synchrotron FTIR was performed with a wavenumber resolution of 4 cm^{-1} , over a total of 320 scans. The measurement samples were a biogenic guanine crystals isolated from chromatophore cells, fixed on carbon tape adhering to a BaF_2 plate (approximately 10 mm in diameter; Figure 2.2.2(a)). In the case of reflectance analysis, the samples we used were biogenic guanine crystals that had dried naturally on a BaF_2 plate. (Figure 2.2.2(b)). In the case of absorbance analysis, the guanine crystals on the BaF_2 plate without carbon tape had also been allowed to dry naturally. Also, the (102) plane of the single crystal platelet in the air was measured by fixing on the capillary edge without any substrates (Figure 2.2.2(c)).



Copyright © 2014 IEEE

Figure 2.2.1. Experimental configuration for analyzing the reflectance and absorbance of a single guanine crystal using microscopic synchrotron FTIR. (Y. Mizukawa, Y. Ikemoto, T. Moriwaki, T. Kinoshita, F. Kimura, T. Kimura, and M. Iwasaka, "Synchrotron Microscopic Fourier Transform Infrared Spectroscopy Analyses of Biogenic Guanine Crystals Along Axes of Easy Magnetization," *IEEE Trans. Magn.*, vol. 50, Art. no. 5001804, 2014.) followed by the IEEE copyright line © 2014 IEEE.



Copyright © 2014 IEEE

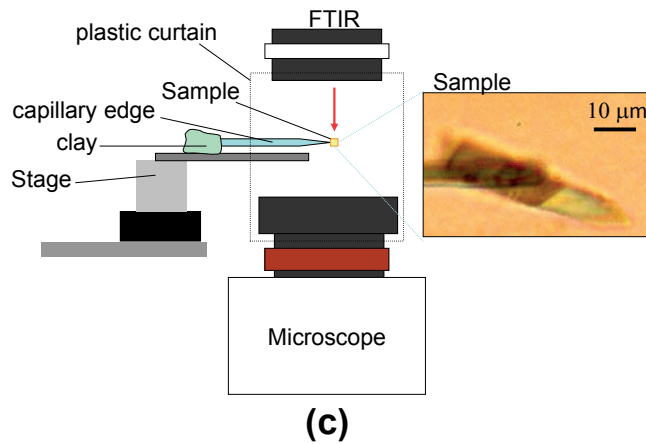
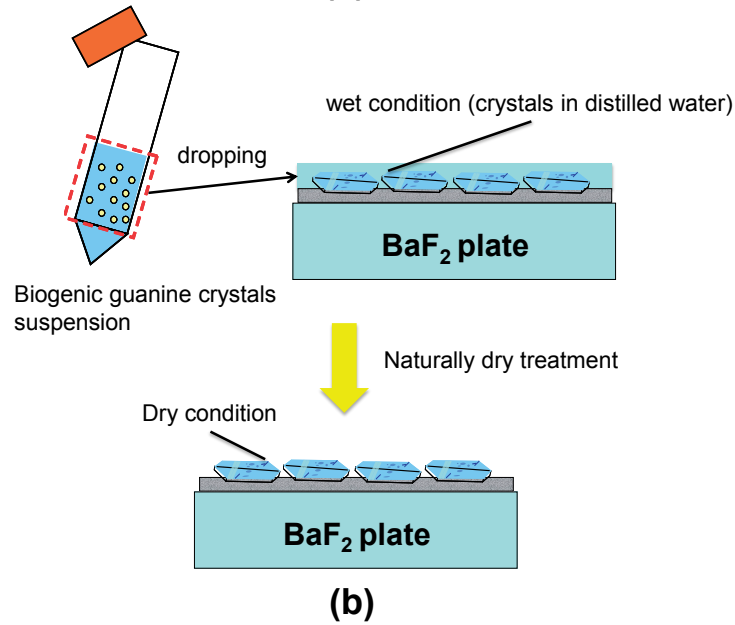


Figure 2.2.2. (a) Illustration of the measurement sample. Biogenic guanine crystals adhered to carbon tape applied to a BaF₂ plate. (Y. Mizukawa, Y. Ikemoto, T. Moriwaki, T. Kinoshita, F. Kimura, T. Kimura, and M. Iwasaka, “Synchrotron Microscopic Fourier Transform Infrared Spectroscopy Analyses of Biogenic Guanine Crystals Along Axes of Easy Magnetization,” *IEEE Trans. Magn.*, vol. 50, Art. no. 5001804, 2014.) followed by the IEEE copyright line © 2014 IEEE. (b) Process of the sample preparation. (c) Experimental setup and sample fixing on the capillary edge in the air.

2.2.3 Results and Discussion

Our analyses of the molecule arrangement, crystal structure and surface structure of biogenic guanine crystals were not resolved by the experiments reported in section 2.1. So, we carried out further experiments measuring the reflectance and absorbance of individual biogenic guanine crystal platelets, exploiting the ability to probe polarization dependent effects by using microscopic synchrotron FTIR.

The central area of an individual guanine crystal platelet was focused on and irradiated with a polarized SR beam of micro-scale spot size. The long axes of individual biogenic guanine crystal platelets were set either parallel or perpendicular to the polarization direction of the SR beam. We obtained data on the light reflectance or absorbance from the crystal maximum surface ((102) plane) using microscopic synchrotron FTIR, as shown in Figure 2.2.3. The reflectance and absorbance spectra indicate that the molecular vibration bands show polarization dependency.

We obtained the peaks during reflectance measurements, at the regions centered around 1150–1160, 1220–1230, 1250–1270, 1360–1380, 1460–1480, 1550–1570, 1680–1700 and 3330–3350 cm^{-1} . When we compared both reflectance spectra in parallel and perpendicular polarization directions relative to the long crystal axis, we focused on the two peaks in the regions around 1680–1700 and 3330–3350 cm^{-1} . Figure 2.2.4 demonstrates clearly that these peaks were suppressed. In particular, the strongest peak around 1680–1700 cm^{-1} was suppressed, between the peaks around 1720–1740 and 1660–1680 cm^{-1} .

Next, we carried out absorbance measurements on individual biogenic guanine crystal platelets using microscopic synchrotron FTIR. Samples were the dried individual guanine crystals on a BaF_2 plate and fixing on the capillary edge in the air.

The polarization direction of the IR radiation was set either parallel or perpendicular to the long axis of guanine crystals.

Figure 2.2.5 shows the absorbance spectra from an individual biogenic guanine crystal analyzed with polarization direction parallel and perpendicular to the long axis of the crystal. The panel (b) in Figure 2.2.5 shows the absorbance of the crystals from the panel (a) over the range of 1000–2000 cm^{-1} . On the other hand, the panel (d) indicates the absorbance of the crystals from the panel (c) over the range of 1000–2000 cm^{-1} . In the panel (a) and (b), the absorbance spectrum shows peaks around approximately 1680–1700 and 3330–3350 cm^{-1} . Yet, as indicated in the panel (c) and (d), these peaks became slightly weaker. In common with the reflectance spectra (Figure 2.2.4), the absorbance spectra also indicated that the differences between the two spectra was related to polarization directions (parallel and perpendicular relative to the long axis of a guanine crystal platelet).

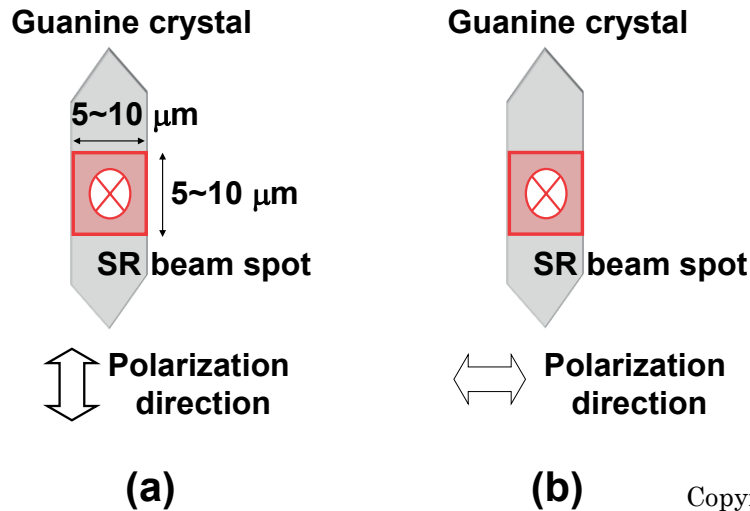
In addition, we measured the individual guanine crystal platelet fixing on the capillary edge to analyze a sample in the air without touching any substrate. Figure 2.2.6 shows the spectra from an individual guanine crystal platelet fixing on the capillary edge with the polarization direction parallel (the angle of about 20 degree) and perpendicular (the angle of about 80 degree) to the long axis of a guanine crystal. When we compared the peaks at around 1680–1700 cm^{-1} and 3330–3350 cm^{-1} in Figure 2.2.6 (a) with that of in Figure 2.2.6 (b), these peaks were slightly suppressed in common with Figure 2.2.5. These results revealed that the crystal (102) plane exhibits anisotropy in molecular orientation.

To summarize the results obtained by synchrotron FTIR, the changes of both the reflectance and absorbance peaks located around 1680–1700 and 3330–3350 cm^{-1}

was clearly associated with the differing polarization directions (perpendicular or parallel to the long axis of a single platelet). Based on these results, we speculate that the two polarization directions of the incident SR beam contributed to C=O and N–H bond vibration within the molecular sheets on the surface of and inside the guanine crystals. In support of this view, the peak at around 1680–1700 cm^{-1} in the spectrum could be assigned to C=O stretching vibration bands, and the peak at about 3330–3350 cm^{-1} could be assigned to N–H stretching vibration bands.

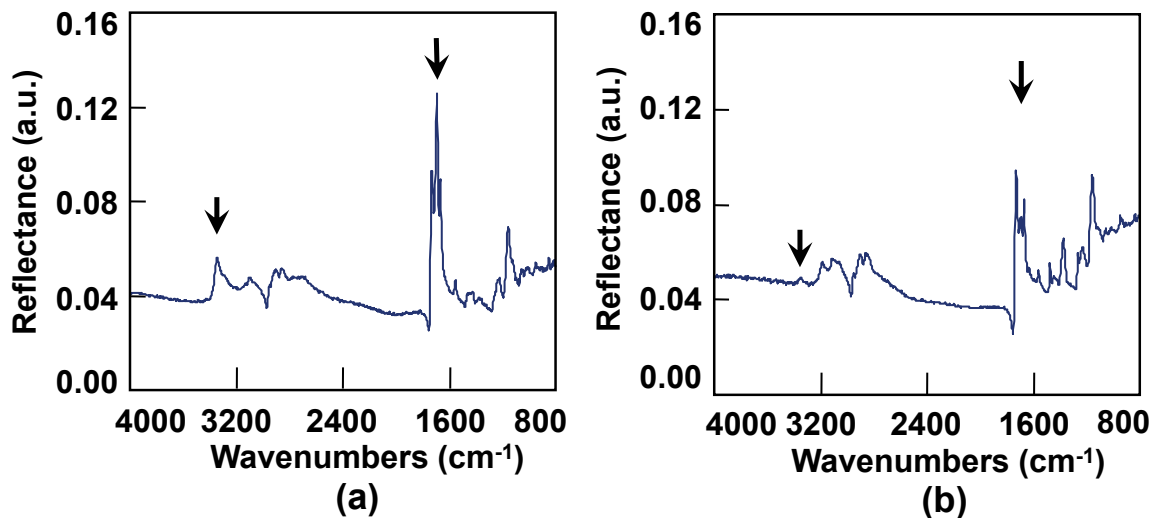
In addition, we compared the molecular arrangement of anhydrous guanine crystals [1] to that of monohydrated guanine crystals [2]. Crystalline architecture was displayed using *Mercury* software. The b-axis of anhydrous crystals aligns parallel to the C=O and N–H bonds. On the other hand, the b-axis of the monohydrated crystal has a molecular structure aligned perpendicular to the C=O and N–H bonds, as shown in Figure 2.2.7. Therefore, based on our modeling, we speculate that individual platelets of biogenic guanine crystals have a molecular arrangement similar to anhydrous crystals.

Moreover, the molecular arrangement of C=O and N–H bonds align with the long axis of a biogenic guanine crystal, as indicated in Figure 2.2.8. Consequently, it is hypothesized that the directional-dependence of the stretching vibrations of the C=O and N–H bonds was caused by the electric field of the incident SR beam, which was polarized parallel to the long axis of the guanine crystal, as shown in Figure 2.2.8.



Copyright © 2014 IEEE

Figure 2.2.3. Schematic diagrams of an individual biogenic guanine crystal platelet irradiated with an SR micro-beam. (a) In this case, the long axis of the guanine crystal is parallel to the polarization direction. (b) In this case, the long axis is perpendicular to the polarization direction. (Y. Mizukawa, Y. Ikemoto, T. Moriwaki, T. Kinoshita, F. Kimura, T. Kimura, and M. Iwasaka, “Synchrotron Microscopic Fourier Transform Infrared Spectroscopy Analyses of Biogenic Guanine Crystals Along Axes of Easy Magnetization,” *IEEE Trans. Magn.*, vol. 50, Art. no. 5001804, 2014.) followed by the IEEE copyright line © 2014 IEEE.



Copyright © 2014 IEEE

Figure 2.2.4. Reflectance spectra from an individual biogenic guanine crystal analyzed by microscopic synchrotron FTIR. (a) Polarization direction parallel to the long axis of the crystal. (b) Polarization direction perpendicular to the long axis. (Y. Mizukawa, Y. Ikemoto, T. Moriwaki, T. Kinoshita, F. Kimura, T. Kimura, and M. Iwasaka, “Synchrotron Microscopic Fourier Transform Infrared Spectroscopy Analyses of Biogenic Guanine Crystals Along Axes of Easy Magnetization,” *IEEE Trans. Magn.*, vol. 50, Art. no. 5001804, 2014.) followed by the IEEE copyright line © 2014 IEEE.

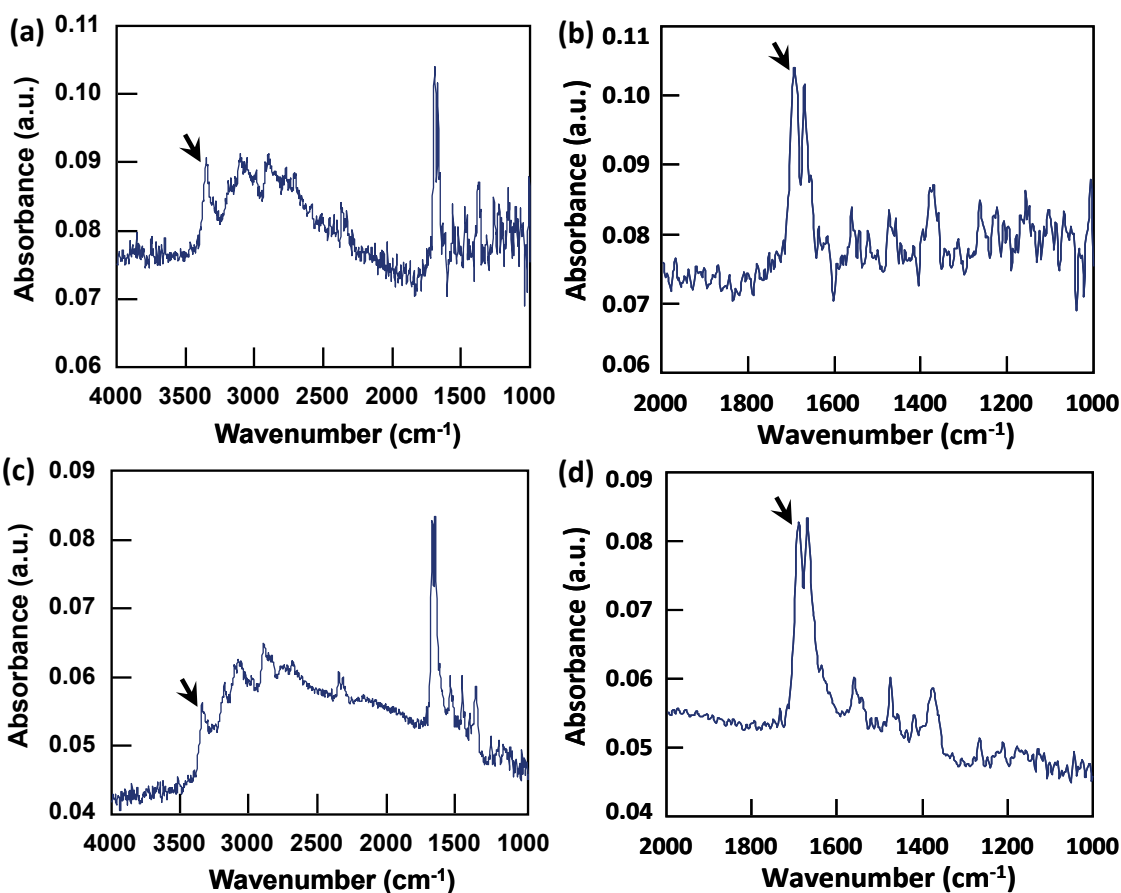


Figure 2.2.5. Absorbance spectra from an individual biogenic guanine crystal analyzed by microscopic synchrotron FTIR. Panels (a) and (b) show spectra obtained when the polarization of the incident SR radiation was parallel to the long axis of the crystal. Panels (c) and (d) show the spectra obtained when the polarization was perpendicular to the long axis.

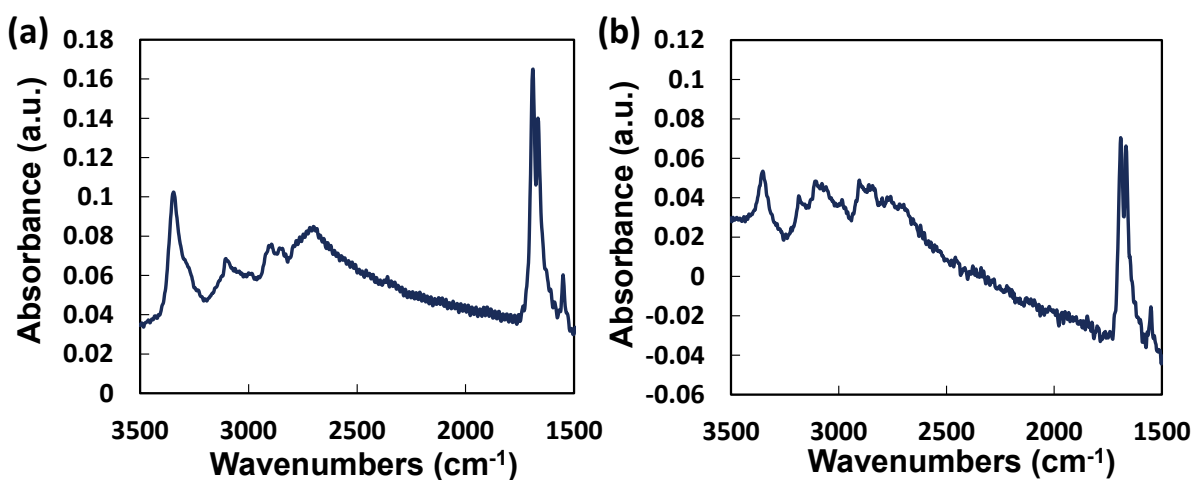


Figure 2.2.6. Absorbance spectra from a single biogenic guanine crystal fixing on the capillary edge. Spectrum analyzed by microscopic synchrotron FTIR (a) parallel and (b) perpendicular to long axis of a crystal.

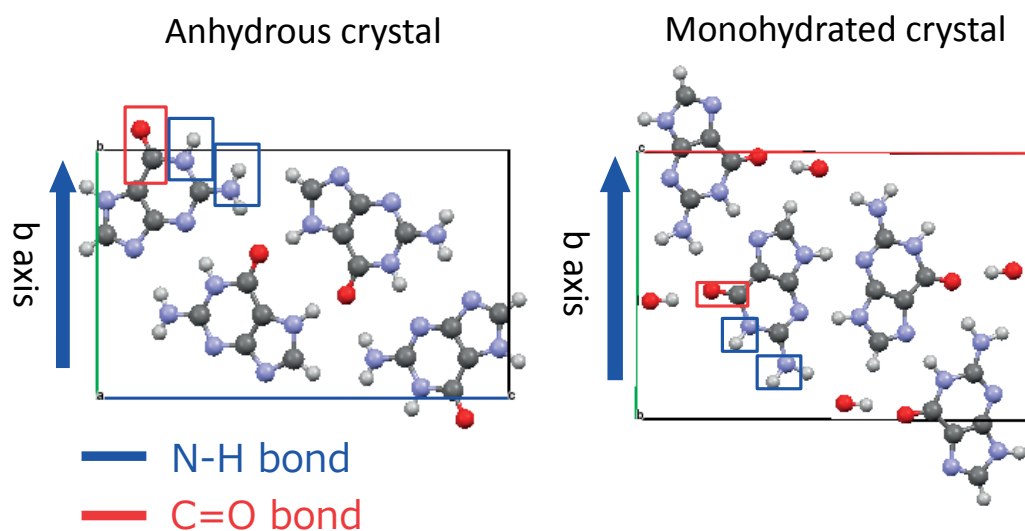


Figure 2.2.7. Arrangement of guanine molecules found in the anhydrous or monohydrated crystal forms. The b-axis is shown in the vertical direction. (Left image; anhydrous crystal. Right image; monohydrated crystal).

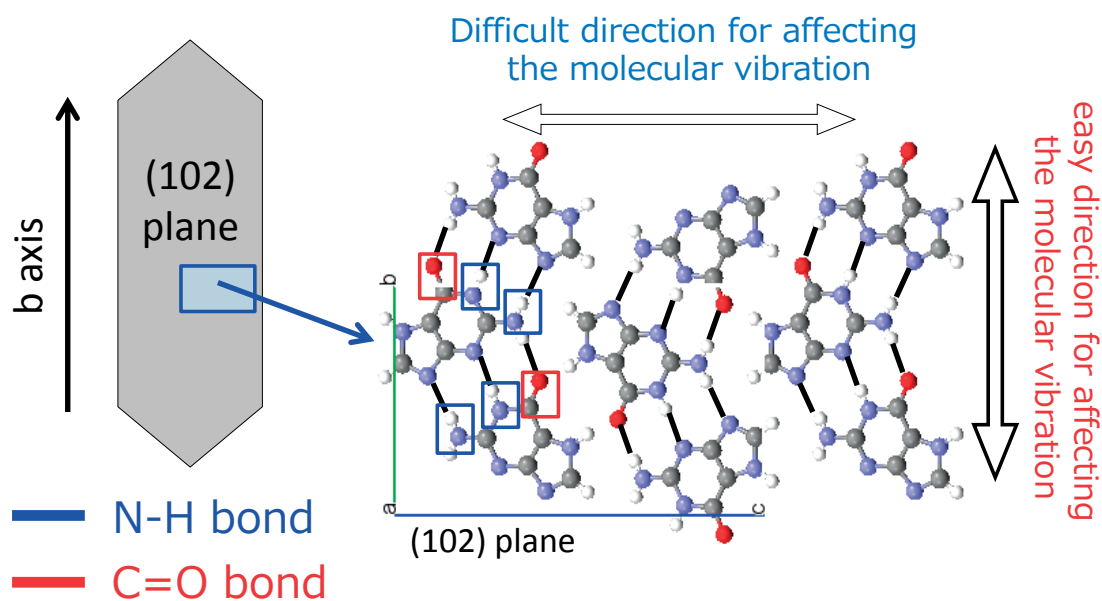


Figure 2.2.8. Schematics of the (102) plane in an anhydrous guanine crystal, depicting the guanine molecules with hydrogen bonding aligned along the b-axis. Hydrogen bonds are shown as black lines.

2.2.4 Summary

The spectra obtained from individual biogenic guanine crystal platelets were compared under differing polarizations of the incident SR radiation, either parallel or perpendicular to the morphological long axis of the crystals. The results for the microscopic synchrotron FTIR measurements demonstrated the suppression of the IR reflectance and absorbance peaks around $1680\text{--}1700\text{ cm}^{-1}$ and $3330\text{--}3350\text{ cm}^{-1}$.

In addition, it was revealed that the biogenic guanine crystal platelets, with an elongated hexagonal morphology, had molecular features consistent with anhydrous guanine crystal form.

2.2.5 References

- [1] K. Guille, and W. Clegg, “Anhydrous guanine: a synchrotron study,” *Acta Crystallogr., Sect. C*, vol. 62, pp. O515–517, 2006.
- [2] U. Thewalt, C. E. Bugg, and R. E. Marsh, “The crystal structure of guanine monohydrate,” *Acta Crystallogr., Sect. B*, vol. B27, pp. 2358–2363, 1971.

3. Magnetic Non-Contact Switching of Light Scattering from Floating Guanine Crystals

3.1 Introduction

As described in chapter 2, physical analyses (SEM, X-ray diffraction and FTIR spectroscopy) were carried out on biogenic guanine crystal platelets, and we revealed the physical properties required to investigate the axes of magnetization. In previous studies [1], [2], magnetic fields suppressed light scattering from the guanine crystals inside chromatophore cells on the goldfish scales. The magnetic behavior of floating and individual biogenic guanine crystals had not been characterized. The aim of this chapter is to exhibit the results of our experiments that clarified the magnetic behavior of floating guanine crystals isolated from chromatophore cells.

We observed biogenic guanine crystal platelets floating in distilled water under applied magnetic fields. Moreover, we tried to switch the light scattering from the floating guanine crystal platelets by manipulating their response to magnetic fields, while altering the incident light and observation direction.

3.2 Methods and Materials

- Observation of the macroscopic behavior of floating guanine crystals

We observed the magnetic behavior of biogenic guanine crystals floating in distilled water through a low-power CCD camera (ELMO Co. Ltd., CC421). The method used to prepare crystal suspensions was described in chapter 2. The experiment setup shown in Figure 3.1(a) was consisted of a low-power CCD camera, an electromagnet, an external optical fiber, and a sample cell containing guanine crystal suspensions. The

applied magnetic field was parallel to the incident light direction, as shown in Figure 3.1(a). Also, the observation direction was perpendicular to the incident light and magnetic field directions. The electromagnet could generate a maximum field of 500 mT. In addition, the measurement sample was set on top of the CCD microscope lens inside the bore of the magnet, as shown in Figure 3.1(a).

As shown in Figure 3.1(b), we used a cylindrical glass tube to enclose the guanine crystals floating in distilled water with the CCD camera. In this experiment, we used a superconducting magnet (5Tr90, Oxford Ltd.), which could generate maximum fields of 5 T and magnetic field direction parallel to Earth's gravity. The rate of the applied magnetic fields was 1 T/min. The temperature inside the magnetic bore was kept at 23 °C. We placed a water-circulation system into the bore of the magnet. The applied magnetic field, the incident light and the observation directions was directed orthogonally.

- Magnetic non-contact switching and spectroscopic measurements of floating guanine crystals

Figure 3.2 illustrates the experimental methods used to observe rapid magnetically controlled light scattering from floating biogenic guanine crystals. The used guanine crystal suspension had a slight silver color and produced random swirling patterns, as shown in Figure 3.2(a). The guanine crystals floating in the distilled water provided cause of these sparkling, swirling patterns. The preparation of this suspension was described in chapter 2.

Figure 3.2(b) schematically illustrates the optical quartz cell filled with floating biogenic guanine crystals. The three blue arrows represent the direction of the applied

magnetic fields. This experimental setup, using an optical cell allowed us to observe and detect remarkable light intensity changes which are dependent on magnetic fields. The experimental configurations consisted of an electromagnet (Hayama Co. Ltd.) generating a maximum of 500 mT, an optical quartz cell filled with a suspension of guanine crystals, CCD microscope (ELMO Ltd.) and the target image covering on the back of the cell. The experiments were configured in three ways, as shown in MODE I–III of Figure 3.2(c). In the basic setup for observing light scattering from the guanine crystals, a combination of magnetic fields direction and optical cell imaging via optical fibers was used to detect light scattering intensity as a function of incident light. The suspension had a density of 0.1×10^6 to 1×10^6 plates/ml. The optical path length was 3 mm. In MODE I setup, the incident light and magnetic field were parallel to each other and the observation direction was perpendicular to both vectors. In the case of MODE II setup, the incident light and magnetic field were orthogonal to each other and the observation direction was parallel to the magnetic field direction. The three vectors were directed orthogonally in MODE III.

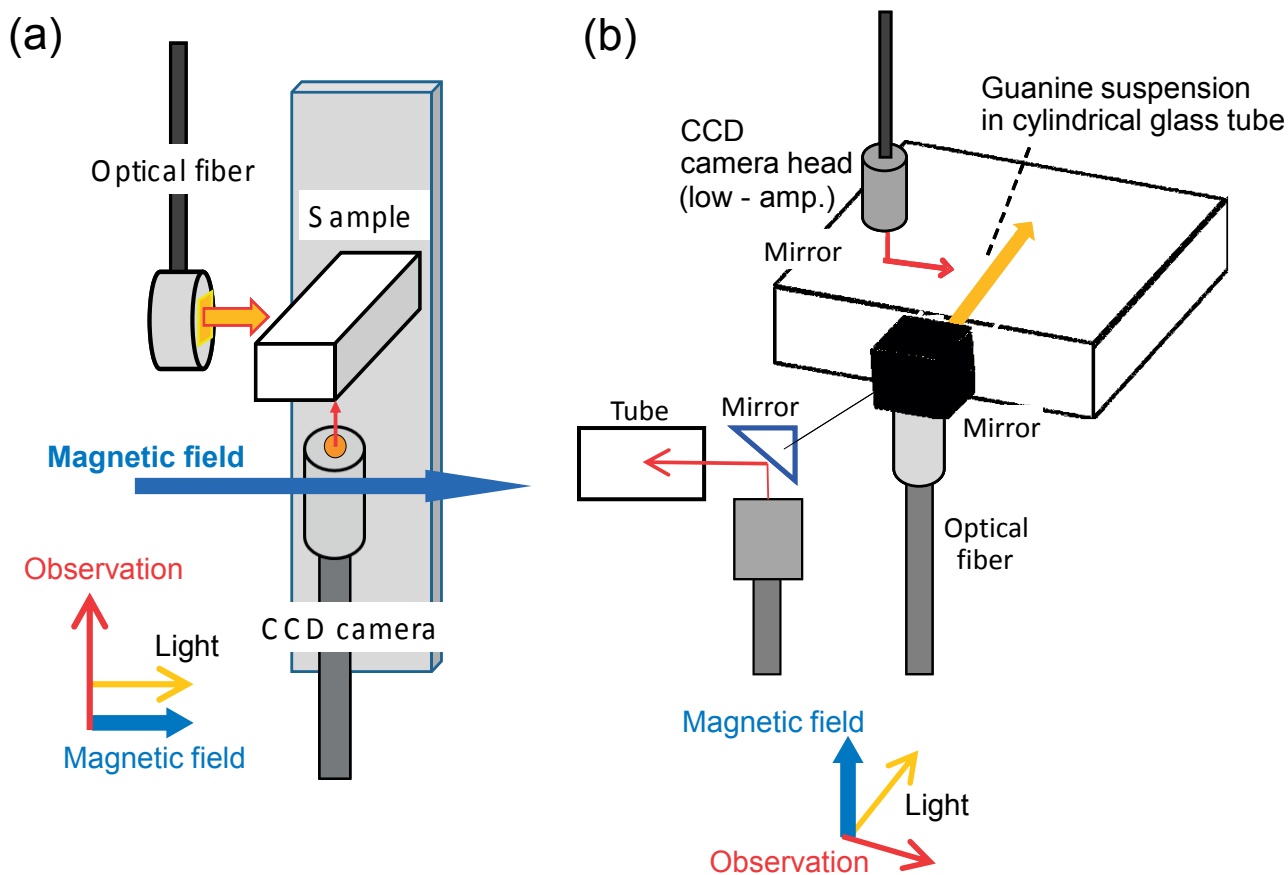


Figure 3.1. (a) Optical macro-observation system, consisted of a low-amplification CCD camera, external optical fiber and a quartz cell filled with floating guanine crystals. Magnetic fields were applied parallel to the incident light direction. (b) Measurement system for low-resolution CCD camera observation of floating guanine crystals when all three vectors, (magnetic fields, incident light and observation), were perpendicular to each other. (Reprinted (adapted) with permission from (M. Iwasaka, and Y. Mizukawa, “Light Reflection Control in Biogenic Micro-Mirror by Diamagnetic Orientation,” *Langmuir*, vol. 29, pp.4328–4334, 2013.). Copyright (2013) American Chemical Society.)

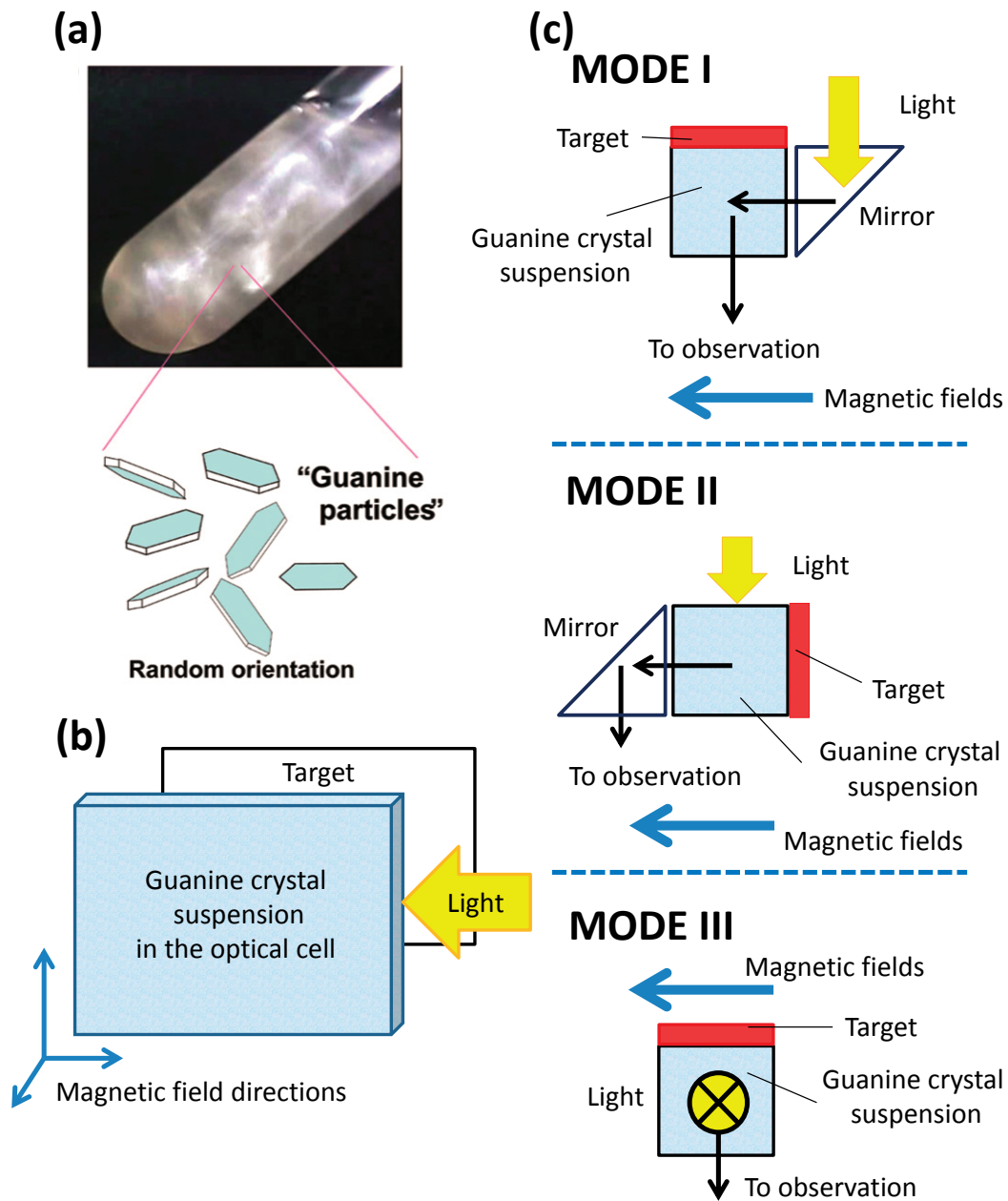


Figure 3.2. Experimental methods for observing rapid magnetic manipulation of light scattering from biogenic guanine crystals. (a) Photograph of a guanine crystal suspension. (b) Schematic image of the optical cell filled with biogenic guanine crystals on the back covering with the target. The blue arrows represent the direction of magnetic fields. (c) Three experimental configurations (MODE I–III) for observing light scattering from the floating guanine crystals under magnetic fields. (Reproduced from [M. Iwasaka, Y. Mizukawa, and Y. Miyashita, *Appl. Phys. Lett.*, vol. 104, Page 024108, (2014).], with the permission of AIP Publishing.)

3.3 Results and Discussion

- Observation of the macroscopic behavior of floating guanine crystals

We investigate the behavior of a suspension of guanine crystals floating in distilled water under magnetic fields. We used two conditions. In the first condition, the magnetic field was parallel to the direction of an incident light. In the second condition, the three vectors, (an incident light, a magnetic field, and an observation direction), were directed orthogonally.

Initially, light scattering was monitored from floating guanine crystals, with and without applied magnetic fields, when the direction of incident light was parallel to the magnetic field. The upper image in Figure 3.3(a) shows the light scattering particles under ambient fields. These particles were guanine crystals. However, light scattering was quenched when magnetic fields of 500 mT were applied.

Next, we observed the magnetic behavior of the floating guanine crystals when the three vectors were orthogonally directed, as shown in Figure 3.3(b). The resulting light reflection from the crystals was enhanced in the presence of magnetic fields of 330 mT, as shown in Figure 3.3(b). Compared to light scattering change in Figure 3.3(a), that in Figure 3.3(b) produced a remarkable light enhancement from floating guanine crystals. The enhancement of light scattering from guanine crystals occurred when magnetic fields of several hundred mT were applied. Suppression of light scattering also occurred under magnetic fields at the same level.

In the previous studies, it was reported that the guanine crystals derived from fish exhibit the refractive anisotropy [3]–[6]. Therefore, the light incident to the maximum surface of a crystal (the (102) plane in anhydrous guanine crystals) is refracted more strongly than the light that is incident normal to the plane. In this study,

it appeared that the enhancement of light scattering under magnetic fields came from refractive anisotropy in the guanine crystals. The number of guanine crystals which directed their (102) planes parallel to the applied magnetic field was increased by the magnetic orientation. Therefore, the light reflection from guanine crystals reached the observation direction easily. Magnetic orientation enabled free rotation around the long axis (b-axis) of the guanine crystals. This rotation enhanced the scattered light sparkling flickeringly from guanine crystals.

Also, the guanine crystals underwent a structural color change under the magnetic field, because there was an increase in a chance the oriented guanine crystals obtained for aligning the (102) planes in the parallel direction. In our previous study, a structural color change was observed in guanine crystal arrays, under strong magnetic fields of 10 T [2]. Figure 3.3(b) shows the strong structural color from floating guanine crystals under magnetic fields of 330 mT. This structural color change was caused by increased optical interference and scattered light enhancement.

It is concluded that these methods allow us to control floating guanine crystals, which behave as diamagnetic micro-mirrors that scatter visible light, by utilizing magnetic fields on the order of millitesla.

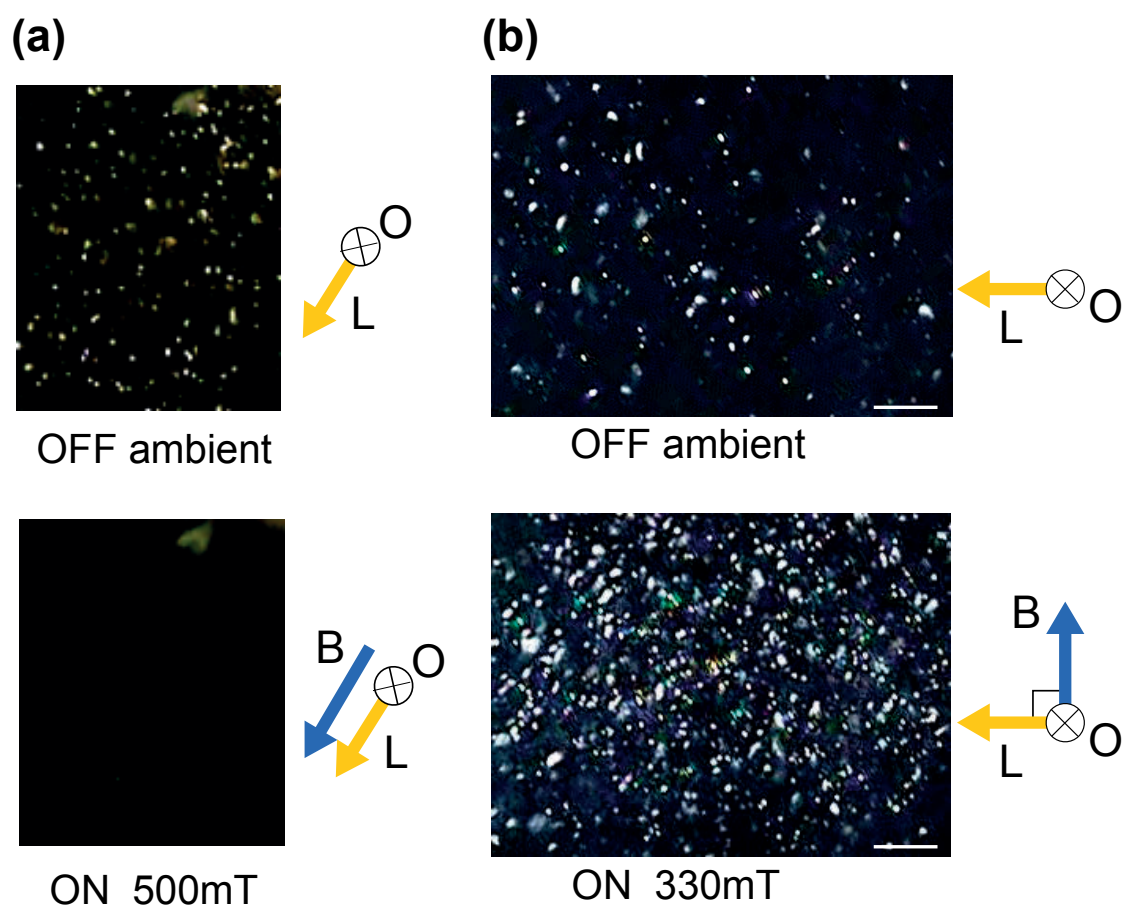


Figure 3.3. Changes in light scattering from guanine crystals floating in the distilled water, in the presence or absence of magnetic fields. The incident light was either parallel or perpendicular to magnetic field. The \otimes mark represents the observation direction. B and L represent magnetic field and light incidence vectors. (a, top image) Light reflection under ambient fields (the geomagnetic field), and (a, bottom image) suppression of light reflection in the presence of an applied 500 mT magnetic field. (b, top image) Light reflection under the ambient fields. (b, bottom image) Light reflection enhancement in the presence of an applied 330 mT magnetic field. (Bar, 1 mm.) (Reprinted (adapted) with permission from (M. Iwasaka, and Y. Mizukawa, “Light Reflection Control in Biogenic Micro-Mirror by Diamagnetic Orientation,” *Langmuir*, vol. 29, pp.4328–4334, 2013.). Copyright (2013) American Chemical Society.)

- Magnetic non-contact switching and spectroscopic measurements of floating guanine crystals

In this section, we demonstrate the non-contact optical switching of light scattering from floating guanine crystals by changing the combination of three vector's directions (magnetic field, incident light, and observation direction).

Figure 3.4(a) and (d) shows photographs of the paper on which word were written at the back of the optical cell filled with guanine crystal suspension, with or without magnetic fields. In MODE I, the floating guanine crystals shone randomly due to side light, hiding the words at the back of the cell (Figure 3.4(a), top image). However, when magnetic field exposures of 500 mT were applied, the light scattering from floating guanine crystals was inhibited, and we could clearly see the words on the paper at the back of the cell. The magnetic field was reached at maximum value (500 mT) for about 83 ms.

Following this, time course changes in light scattering intensity were monitored spectroscopically in MODE I, as shown in Figure 3.4(b) and (c). Figure 3.4(c) is a magnified portion of Figure 3.4(b), showing the moments when the magnetic field exposure was turned on and off. In MODE I, the time course plot shows that the time required to insert the sample and suppress light scattering from the guanine crystals was greater than 1.2 s. Once the electromagnetic switch was turned off, it took approximately 16 s to recover from the quenched state of light scattering.

Magnetically induced inhibition of light scattering occurred in MODE II, as shown in Figure 3.4(d). Magnetic control of light scattering from the floating guanine crystals was achieved by aligning the directions of the incident light and magnetic field, as shown in Figure 3.4(e). The time scale in Figure 3.4(f) was same as that in Figure

3.4(c). When comparison was made of the rate at which light scattering was suppressed in MODE II with that in MODE I, it became clear that the rate was same in both configurations. The suppression of the light scattering from the guanine crystals recovered moderately in the post-exposure to magnetic fields, and the words on the paper became hidden. Diamagnetic orientation of guanine crystals (size = $\sim 5 \mu\text{m} \times 20 \mu\text{m}$), inhibited light scattering in MODE I. In MODE II, the reflectivity from the surface of the guanine crystals was likely influenced by the direction of magnetic field, which was directed parallel to the direction of incident light.

In the next experiment, we carried out measurements in which all three vectors (incident light, magnetic field, and observation direction) were combined orthogonally. We conducted the observation and spectroscopic measurement of light scattering changes in MODE III, which configured the directions of incident light, magnetic fields, and observation (detection) orthogonally. Measurements were carried out in MODE III in the presence or absence of applied magnetic fields (Figure 3.5), using a low concentration of the guanine crystal suspension. We could see the characters on the target under ambient fields, prior to magnetic field exposures. We speculated that the glare from the light scattering of guanine crystals in the cell was occurred and could hide the target rapidly. Light scattering from floating guanine crystals was brighter under magnetic fields than under ambient fields. Furthermore, light scattering from guanine crystals was enhanced by magnetic fields, which caused the words on the target screen in the cell to become disrupted, as shown in Figure 3.5(a). The time scale of the response in MODE III was similar to that seen in MODE I. It seems that combining the directions of magnetic fields and incident light have a role of the mechanism of magnetic orientation for light scattering changes.

These results demonstrated that the light scattering from floating guanine crystals can be controlled, acting as a micro-mirrors that can be switched on/off non-invasively by combining three vectors (incident light, magnetic field, and observation direction). In addition, this optical switching can be performed under more than several hundred millitesla. Optical switching of floating guanine crystals occurred rapidly when the magnetic field was switched on. These methods allow us to control light scattering remotely, rapidly and reversibly, using magnetic fields. The recovery velocity for light scattering is slower after discontinuation of the magnetic field, than that after switching on magnetic fields. However, recovery rate might be expedited by rotating the magnetic field or the incident light direction through 90° .

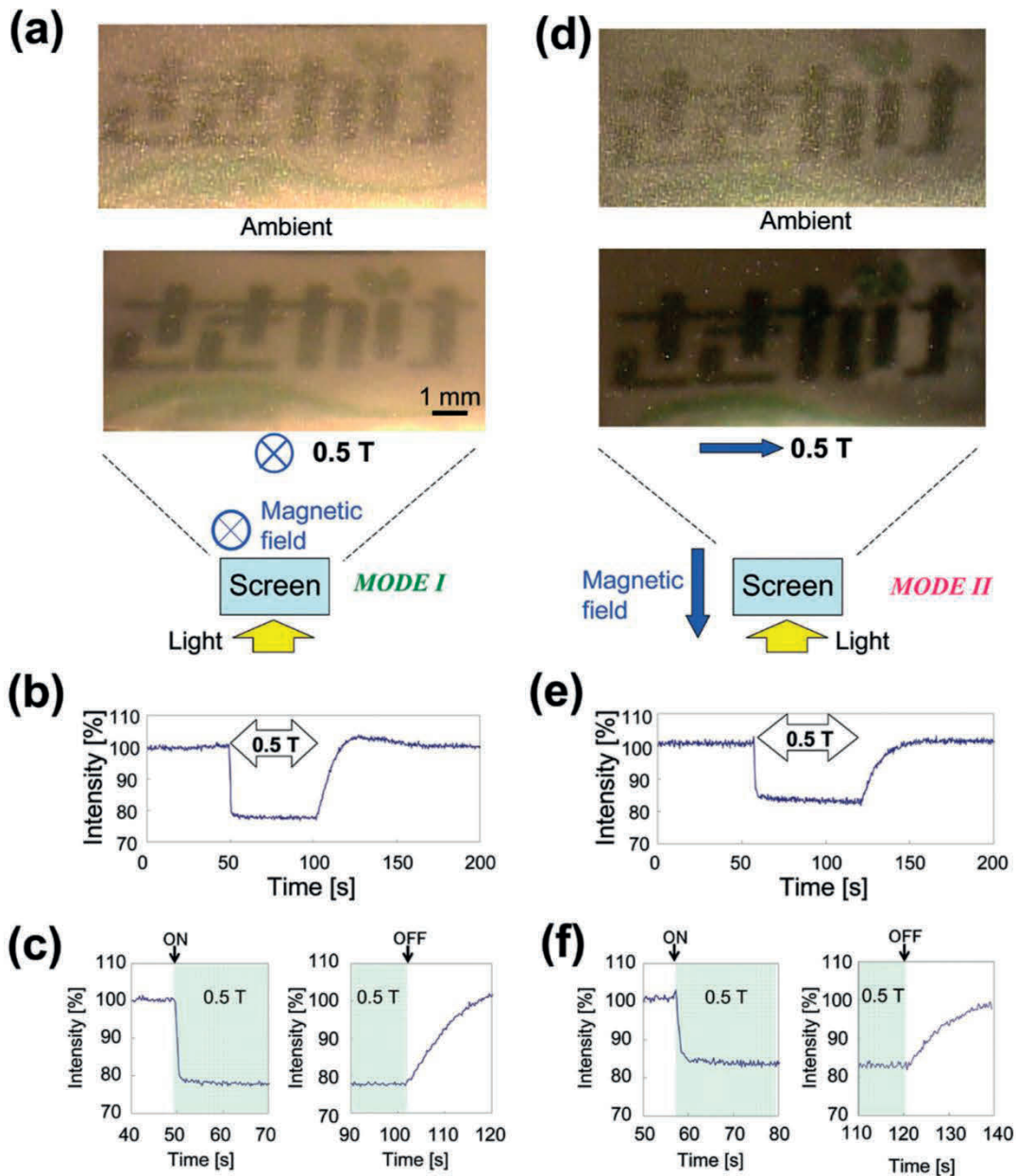


Figure 3.4. Suppression of light scattering from guanine crystals under magnetic fields. (a) Observation of light scattering from floating guanine crystals in an optical cell in front of the target image in MODE-I, under ambient fields and 500 mT, respectively. Bar, 1 mm. (b) Time course changes in light scattering intensity in MODE-I. (d) Images of light scattering in MODE-II, under ambient fields and 500 mT. (e) Time courses of changing light scattering in MODE-II. Panels (c) and (f) are detailed close-ups on the time-courses in panels (b) and (e) at the moments the magnetic field was switched on and off, respectively. (Reproduced from [M. Iwasaka, Y. Mizukawa, and Y. Miyashita, *Appl. Phys. Lett.*, vol. 104, Page 024108, (2014).], with the permission of AIP Publishing.)

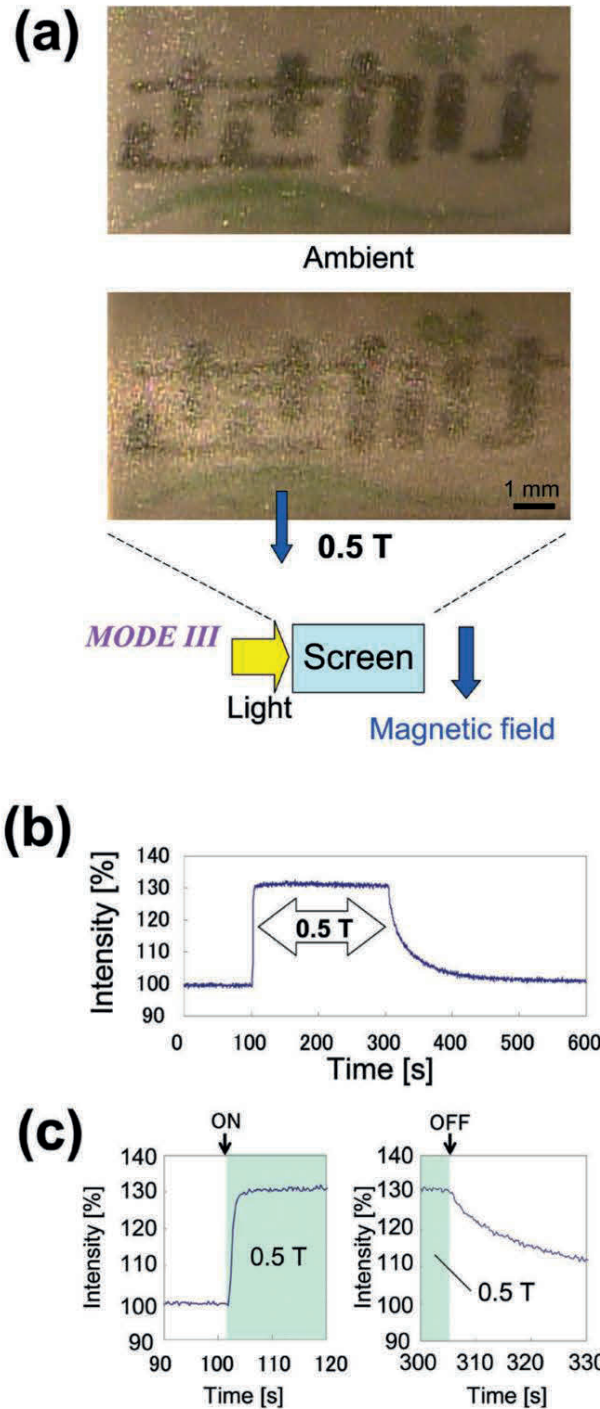


Figure 3.5. Magnetically induced enhancement of light scattering from guanine crystals in MODE-III. (a) Optical images of the scattered light changes from floating guanine crystals, in the presence or absence of applied magnetic fields. (b) Time course changes in light scattering intensity from floating guanine crystals in the optical cell. Panel (c) is a detailed close-up on the time course in panel (b) at the moments the magnetic field was switched on and off. (Reproduced from [M. Iwasaka, Y. Mizukawa, and Y. Miyashita, *Appl. Phys. Lett.*, vol. 104, Page 024108, (2014).], with the permission of AIP Publishing.)

3.4 Summary

In conclusion, the suppression of light scattering from guanine crystals floating in distilled water is caused by exposure to applied magnetic fields when the direction of the magnetic field is parallel to the direction of the incident light. In addition, enhancement of light scattering from the guanine crystal suspension occurred when the directions of the applied magnetic field, incident light, and observation were orthogonal. These results suggest that guanine crystals have potential to be developed as non-contact and remotely controlled micro-mirrors, for a range of applications.

Furthermore, we demonstrated methods for non-invasively controlling magnetically induced changes of light scattering (quenching or enhancement) from the floating guanine crystals. It is speculated that diamagnetic orientation of the floating guanine crystal platelets, in millitesla fields, may be the basis for these optical switching phenomena. It seems clear to us that non-contact, high-speed optical switches could be obtained from guanine crystals, since changes in light scattering occur rapidly in response to applied magnetic fields.

3.5 References

- [1] M. Iwasaka, “Effects of static magnetic fields on light scattering in red chromatophore of goldfish scale,” *J. Appl. Phys.*, vol. 107, Art. no. 09B314, 2010.
- [2] M. Iwasaka, Y. Miyashita, M. Kudo, S. Kurita, and N. Owada, “Effect of 10-T magnetic fields on structural colors in guanine crystals of fish scales,” *J. Appl. Phys.*, vol. 111, Art. no. 07B316, 2012.
- [3] E. J. Denton, “Review Lecture: On the organization of reflecting surfaces in some marine animals,” *Philos. Trans. R. Soc. London, Ser. B*, vol. 258, pp. 285–313, 1970.
- [4] A. Levy-Lior, E. Shimoni, O. Schwartz, E. Gavish-Regev, D. Oron, G. Oxford, S. Weiner, and L. Addadi, “Guanine-Based Biogenic Photonic-Crystal Arrays in Fish and Spiders,” *Adv. Funct. Mater.*, vol. 20, pp. 320–329, 2010.
- [5] T. M. Jordan, J. C. Partridge, and N. W. Roberts, “Non-polarizing broadband multilayer reflectors in fish,” *Nat. Photonics*, vol. 260, pp. 759–763, 2012.
- [6] D. Gur, Y. Politi, B. Sivan, P. Fratzl, S. Weiner, and L. Addadi, “Guanine-based photonic crystals in fish scales form from an amorphous precursor,” *Angew. Chem., Int. Ed.*, vol. 52, pp. 388–391, 2013.

4. Light Reflection Changes Caused by Magnetic Orientation

4.1 Optical Behavior of Guanine Crystals on a Substrate under Magnetic Fields

4.1.1 Introduction

In chapter 3, we established that light scattering from guanine crystals floating in the distilled water could be controlled, and switched by combining the magnetic field, incident light, and observation. In particular, we determined a new method to control of light scattering from isolated guanine crystals. In spite of this, we had not yet revealed the reason for the suppression/enhancement of light scattering. A previous study [1] also investigated the suppression of light scattering from the biogenic guanine crystals found inside chromatophore cells on goldfish scales, and similarly did not report the basis of this effect.

In this chapter, we sought to clarify the reason light scattering changes occur in guanine crystal suspensions and in stacked guanine crystals within chromatophore cells. Therefore, we observed the behavior of isolated biogenic guanine crystals enclosed in a chamber (on a substrate) under dark-field and bright-field illumination, in the presence and absence of magnetic fields. Also, we carried out measurements for revealing the axes of magnetization in individual guanine crystals by the observation in the micro region. The present chapter provides evidence that the isolated guanine crystals from goldfish show light scattering changes on a substrate, when oriented by magnetic fields, due to diamagnetic anisotropy.

4.1.2 Methods and Materials

- Optical behavior of biogenic guanine crystals on a substrate

The sample used for magnetic field experiments was a guanine crystal suspension. We obtained this suspension from the chromatophore cells of a goldfish, *Carassius auratus*, following the method described in chapter 2. We performed the experiments when the guanine crystal suspension was fresh and had a low bacterial concentration. Undesired substances, such as the residual cellular debris from chromatophores and lipid membranes, were removed from the guanine crystal suspension by centrifugation. The freshly prepared guanine crystal suspension was enclosed in a glass chamber, consisting of two coverslips (18 mm \times 18 mm) and a frame seal chamber (9 mm \times 9 mm \times about 300 μ m; 25 μ L capacity, BIO-RAD SLF-0201).

Figure 4.1.1 shows the experimental setup used to observe and measure the isolated guanine crystals inside the glass chamber, in the presence and absence of magnetic fields. The setup consisted of the sample chamber, a high-resolution CCD camera, an external light source and optical fiber, and an electromagnet. The suspension enclosed in a chamber observed using a high-resolution CCD microscope. The sample was arranged statically and horizontal to the bottom before viewing with an optical microscope (500 \times –2000 \times magnification) under vertical magnetic fields, as shown in Figure 4.1.1(a). We performed observations using two CCD microscopes (Keyence VH-5000 and VHX2000). A halogen lamp was used as an external light source providing constant illumination for the bright-field illumination.

In this chapter, a superconducting magnet (Oxford Ltd., 5Tr90) was used, which could generate maximum fields of 5 T and magnetic field direction parallel to Earth's gravity. For keeping the temperature stable at 23 $^{\circ}$ C, we set up a

water-circulation tube inside the bore of the magnet. The measurement sample was placed on top of the lens of the CCD microscope, inside the bore of the magnet, as shown in Figure 4.1.1(a). The magnetic field in the superconducting magnet changed at the rate of 1 T/min.

Figure 4.1.1(b) depicts the spectroscopic measurement setup for light scattering from guanine crystals, in the same measurement system as Figure 4.1.1(a). This fiber-optic measurement system consisted of an optical fiber for measurements, an external light fiber, an optical mirror, and the measurement cell containing the floating guanine crystal suspensions. We carried out these spectroscopic measurements using a superconducting magnet with a horizontal bore (Oxford Ltd., 14Tr70).

- Optical behavior of recrystallized guanine crystals on a substrate

We utilized an artificial guanine powder (code: 079-01091/WAKO Ltd.) to recrystallize guanine crystals. The dispersed liquid, consisting of guanine powder in distilled water, was refluxed and filtered. Next, we allowed the filtrate in the glass container to cool to room temperature, obtaining microcrystals that were enclosed in a chamber, consisting of two glass coverslips (18 mm × 18 mm) and a rubber spacer (9 mm × 9 mm × about 300 μm; 25 μL capacity, BIO-RAD SLF-0201).

Figure 4.1.2 shows the experimental configurations used to observe the recrystallized guanine crystals. We observed the sample using a CCD camera (VH-5000/Keyence Ltd.) at 1000× magnification, under external lighting from an optical fiber. This camera was placed in the interior space between two electromagnet poles (WS15-40-5K-MS /Hayama Ltd.). We could observe the recrystallized guanine crystals in real time, under magnetic fields with this approach. The direction of the magnetic

field was parallel to the surface of the glass chamber. Observations were performed under dark-field illumination, utilizing an external optical fiber (diameter: 10 mm) as a light source.

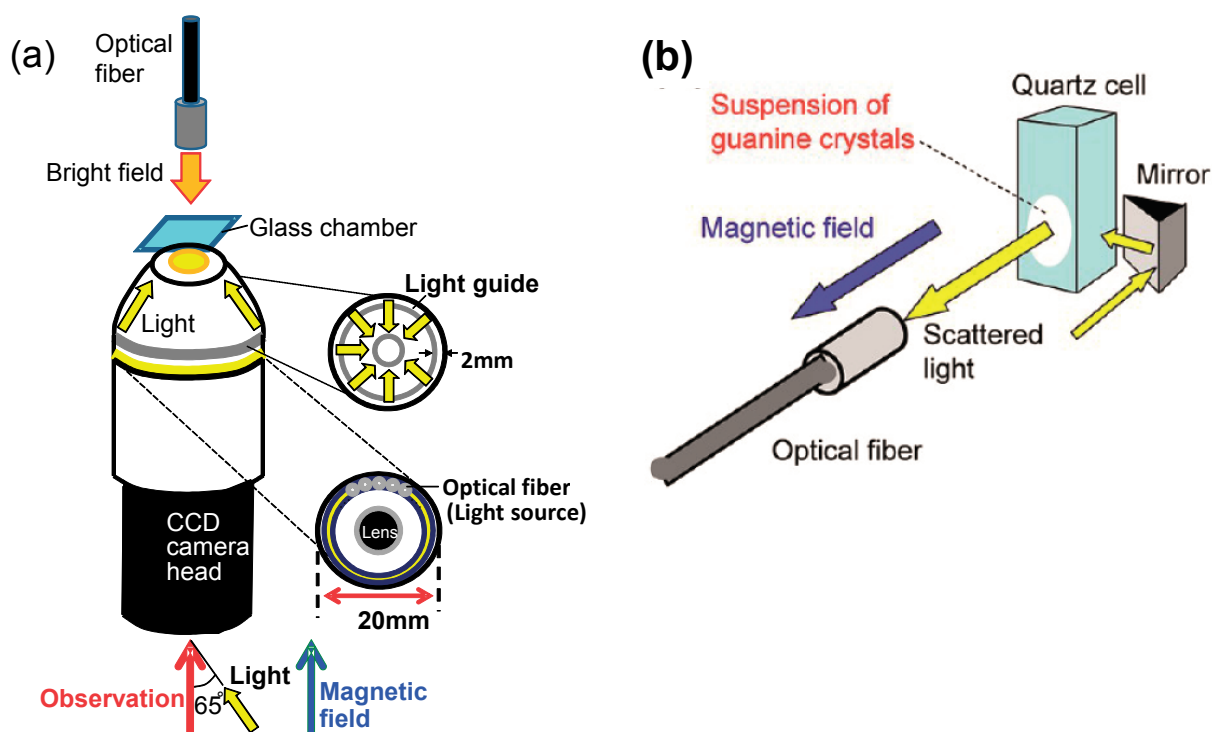
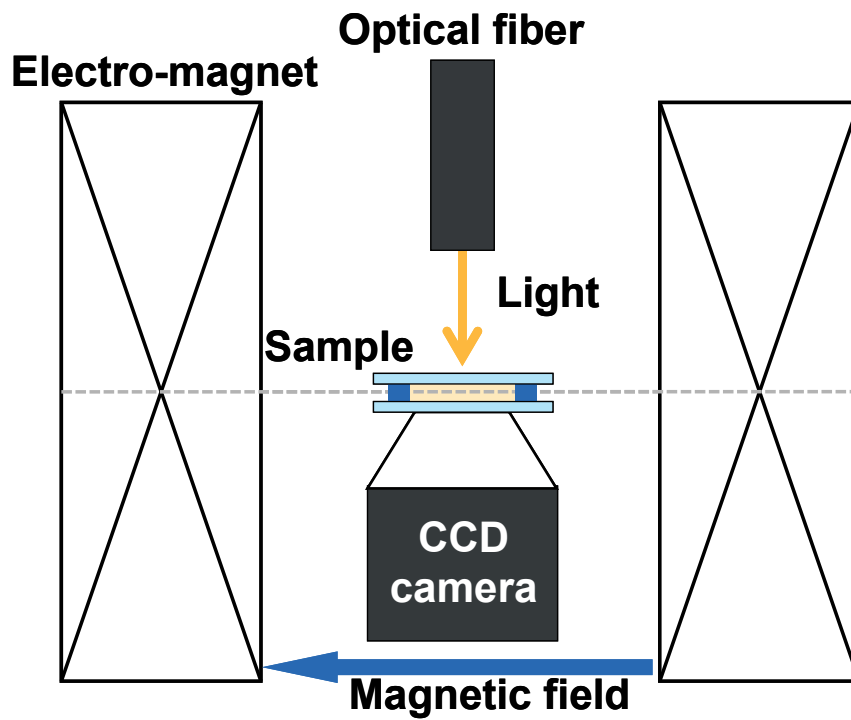


Figure 4.1.1. Experimental setup for observations, consisting of the prepared sample, a CCD or low-amplification camera, an external light source, and orientable magnetic field, incident light, and detection vectors. (a) Measurement system for micro-scale observation using a cylindrical high-resolution CCD camera (Keyence, VH-5000 with VHS501 lens/500× magnification). (b) Spectroscopic measurement system for light scattering from guanine crystals, using the same measurement system shown in panel (a). (Reprinted (adapted) with permission from (M. Iwasaka, and Y. Mizukawa, “Light Reflection Control in Biogenic Micro-Mirror by Diamagnetic Orientation,” *Langmuir*, vol. 29, pp.4328–4334, 2013.). Copyright (2013) American Chemical Society.)



Copyright © 2014 IEEE.

Figure 4.1.2. Experimental configuration for measurements of the magnetic properties of recrystallized guanine crystals, under ambient field and magnetic fields. (Y. Mizukawa, K. Suzuki, S. Yamamura, Y. Sugawara, T. Sugawara, and M. Iwasaka, “Magnetic Manipulation of Nucleic Acid Base Microcrystals for DNA Sensing,” *IEEE Trans. Magn.*, vol. 50, Art. no. 5001904, 2014.) followed by the IEEE copyright line © 2014 IEEE.

4.1.3 Results and Discussion

- Optical behavior of biogenic guanine crystals on a substrate

When the direction of the magnetic field was parallel to the observation direction with incident light coming from the side, we observed the sample under dark-field or bright-field illumination, as shown in Figure 4.1.3.

Under dark-field illumination, the isolated guanine crystal platelets sparkled randomly due to Brownian motion under ambient fields. However, light scattering from these platelets was suppressed by magnetic fields above 100 mT (Figure 4.1.3(a)). Following 10 sec exposures to a 200 mT magnetic field, we could observe quenching of light scattering for most of the guanine crystals.

Next, we observed the guanine crystal platelets under bright-field illumination in the absence and presence of magnetic fields.

Figure 4.1.3(b) shows the optical and magnetic behavior of the individual guanine crystal platelets, both in ambient fields and in a magnetic field of 200 mT, under bright-field illumination. The Results demonstrated that the suppression of light scattering arose from the magnetic orientation of the isolated guanine crystals. We revealed the relationship between magnetic orientation and light reflection of guanine crystal platelets.

Moreover, we could observe the behavior of guanine crystals in real time, in the presence and absence of magnetic fields, by utilizing a high amplification CCD microscope, as shown in Figures 4.1.3(c) and 4.1.4(a). The light scattering was likely suppressed by magnetic orientation of the guanine crystals, due to an induced diamagnetic moment in the crystals [2]. As a result, the morphological short axes of the guanine crystal platelets (the (102) planes of guanine crystal platelets) aligned parallel

to the applied magnetic fields (Figure 4.1.3(c)). These photographs show that the suppression of light reflection and the changes in orientation of a guanine crystal platelet (the white regions in the photos) were observed in magnetic fields ranging from 400–501 mT.

Figure 4.1.4(a) indicates that the orientation of the (102) planes of guanine crystal platelets aligned with the magnetic field applied in the vertical direction, which was parallel to gravitational direction, decreasing the white regions in images. The red line, which represents the average data, indicates that the minimum magnetic field intensity required for magnetic orientation of guanine crystals was between 200 mT–300 mT. These results were consistent with previous research reporting the threshold magnetic field intensity (260 mT) needed to suppress light reflection from golfish-derived guanine crystal arrays [1]. A novel finding of the present study is the response in a long period to the magnetic field. We could observe magnetic orientation of the biogenic guanine crystal platelets when the magnetic fields were kept steady at 100 mT, the minimum threshold for detecting magnetic orientation. Figure 4.1.4(b) shows that the light scattering from guanine crystal platelets was inhibited within 10 sec by magnetic fields ranging from 50 mT–200 mT. This finding was revealed by detecting the light scattered from floating guanine crystal platelets in aqueous solution, as shown in Figure 4.1.4(c). The configuration of the magnetic field, incident light, and observation direction was the same as in Figure 4.1.4(b). Light reflective intensities were sequentially measured from the observation direction. Figure 4.1.4(c) indicates the quenching of light scattering detected in a magnetic field of 100 mT. However, significant changes did not occur in the range from 0–50 mT.

We explain the mechanism of magnetic orientation in biogenic guanine crystal

platelets, as follows. It is speculated that the maximum diamagnetic moment, which is normal to the (102) plane of the guanine crystal, is induced by the applied magnetic field. The results show that (102) planes orient directly parallel to the applied magnetic field, minimizing the diamagnetic moment. Figure 4.1.5(a) schematically represents the magnetic orientation of guanine crystal platelets derived from goldfish scales. The maximum diamagnetic moment comes from the aromatic six-membered ring structures of the guanine molecules. According to previous studies investigating the molecular assembly structures of guanine, it is reported that a specific guanine tetraplex structure is formed by the hydrogen bonding between the guanine molecules [2]–[4].

Diamagnetic energy for orienting the (102) plane parallel to the applied external magnetic field was obtained by hydrogen bonded guanine molecules. The guanine crystals were randomly orientation in the absence of an applied magnetic field. In addition, the refractive index of biogenic guanine crystal was around ~ 1.83 and comparatively large. Therefore, the surface of a biogenic guanine crystal can scatter light strongly [2], [5]–[11]. These results revealed that guanine crystal have a high refractive index, and the strong light scattering can be oriented by magnetic fields.

- **Optical behavior of recrystallized guanine crystals on a substrate**

In the prior section, biogenic guanine crystal platelets were oriented immediately by magnetic fields, due to their diamagnetic anisotropy, with a concomitant change in light reflection. Next, the optical and magnetic behavior of recrystallized guanine crystals was investigated and compared with that of biogenic guanine crystal platelets.

The magnetic behavior of recrystallized guanine crystals, both in the ambient

field and in a magnetic field at 500 mT, was observed using a CCD microscope. Figure 4.1.6 shows the behavior of the recrystallized guanine crystals in the presence and absence of magnetic fields. The light scattering from the recrystallized crystal was weak. The morphological long axis of the recrystallized crystal was directed perpendicular to the direction of the applied magnetic field. Diamagnetic orientation of this recrystallized crystal recovered for 30 seconds in the post-exposure. We have established that orientation of recrystallized guanine crystals in response to applied magnetic fields arises from diamagnetic anisotropy, in common with biogenic guanine crystals. But, the light scattering changes of the recrystallized crystal was not occurred under magnetic fields.

These results clarified that the morphological long axis of recrystallized crystals align perpendicular to the direction of applied magnetic fields, due to diamagnetic susceptibility [12]–[15] arising from eddy currents generated in six-membered aromatic rings. Therefore, it is speculated that the difference between recrystallized and biogenic crystals was caused by stacking patterns of the guanine molecules along the morphological long axis. Also, it is difficult to control the light reflection from the recrystallized guanine crystal selectively.

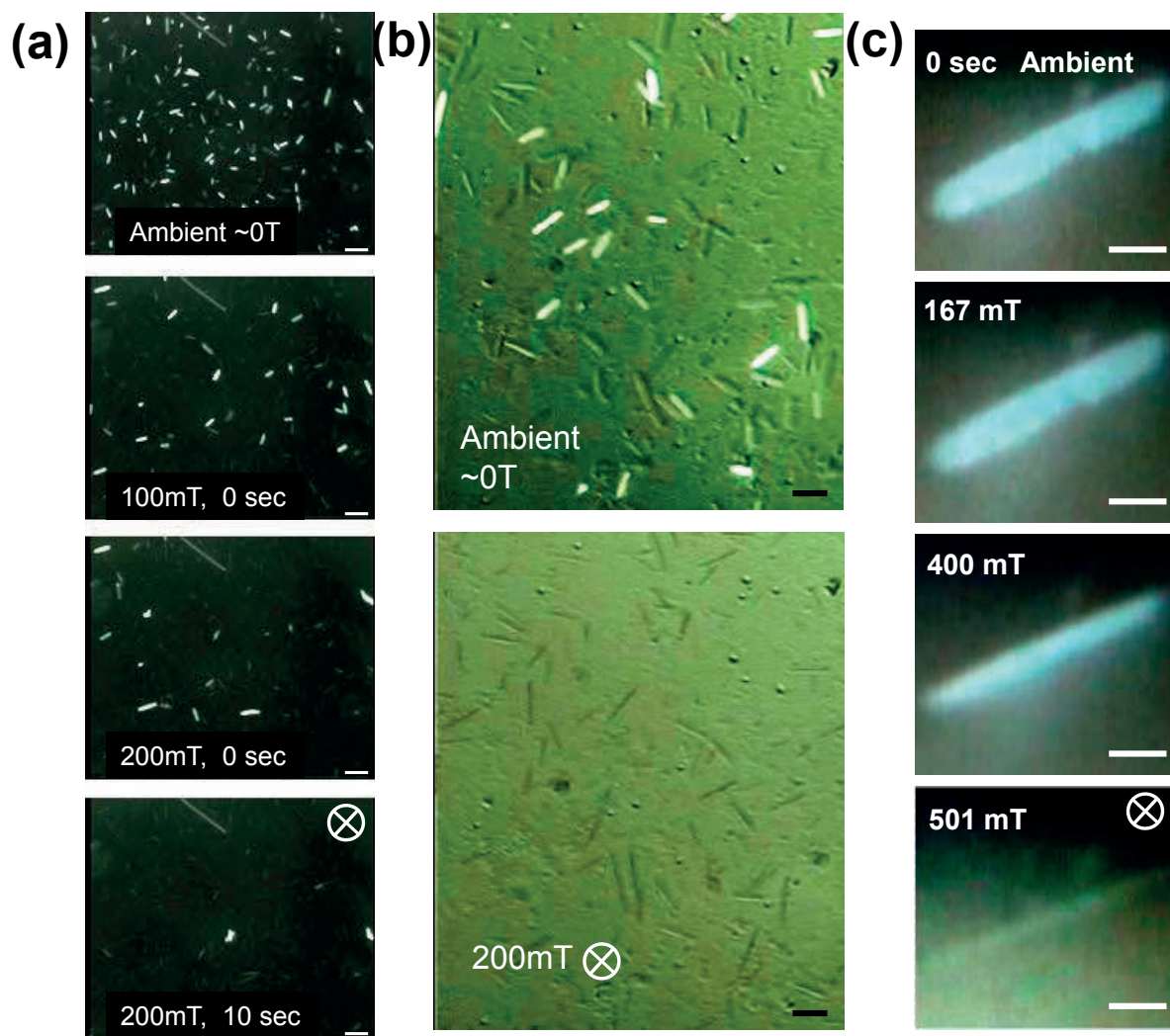


Figure 4.1.3. Magnetic effects suppress light reflection from guanine crystals. (a) Time course changes in suppressed light reflection from guanine crystals, with a magnetic field sweeping from 0–200 mT, under dark-field illumination. (Bar (white), 20 μm). The \otimes mark symbolizes the direction of the applied magnetic field. (b) Optical images of guanine crystals in the ambient field or in a magnetic field of 200 mT under bright-field illumination. (Bar (black), 20 μm). Two incident light sources were directed from the top and from the side of the sample. The elongated white rod is the light scattering from the guanine crystals illuminated from the side. (c) Magnetic rotation of a guanine crystal platelet around the length direction of the (102) plane due to diamagnetic anisotropy. (Bar (white), 5 μm). (Reprinted (adapted) with permission from (M. Iwasaka, and Y. Mizukawa, “Light Reflection Control in Biogenic Micro-Mirror by Diamagnetic Orientation,” *Langmuir*, vol. 29, pp.4328–4334, 2013.). Copyright (2013) American Chemical Society.)

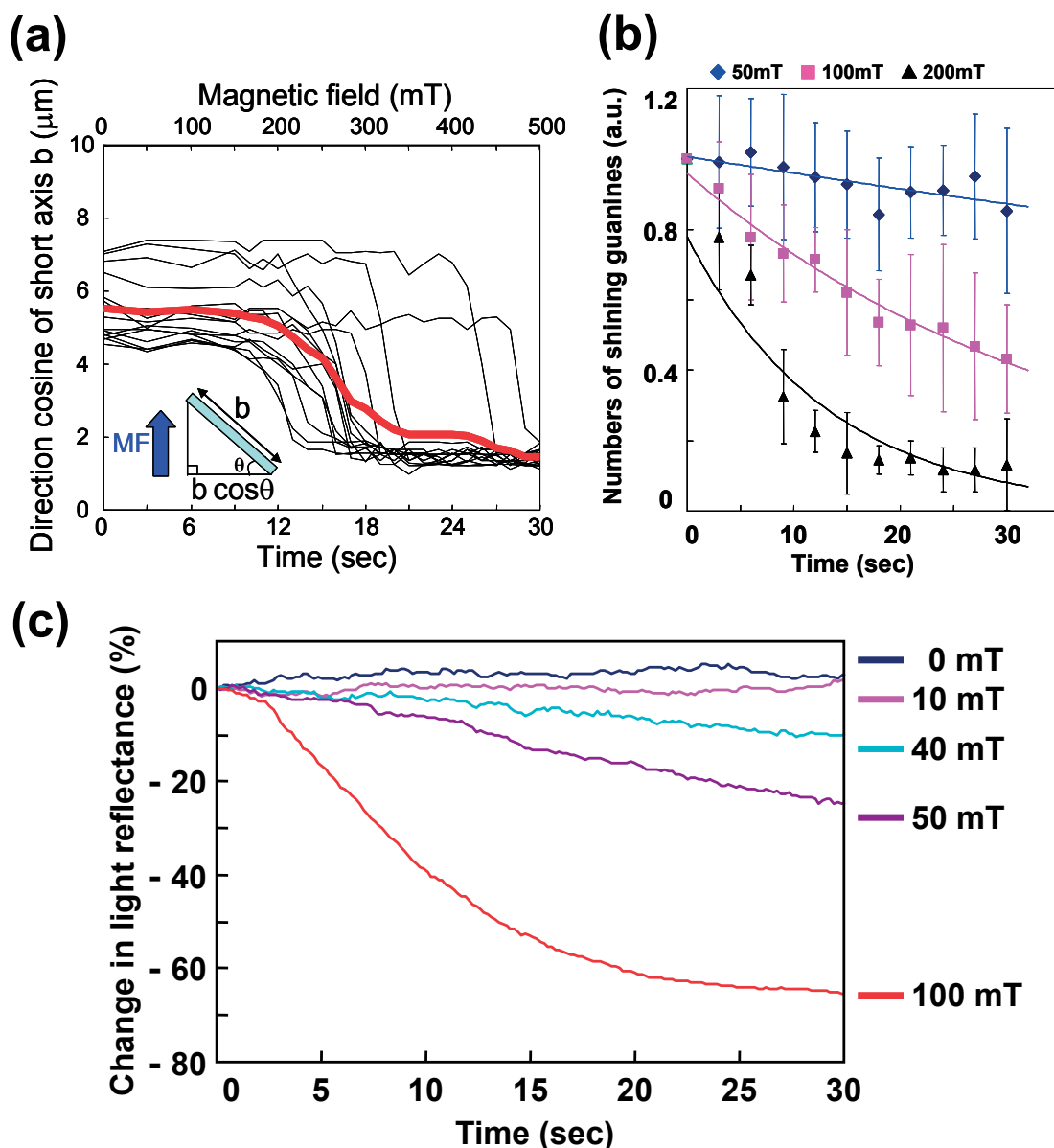


Figure 4.1.4. (a) Time course changes in the orientation of width direction of the (102) plane when the magnetic field swept up from 0–500 mT ($n = 14$). The magnetic field was changed at a rate of 1000 mT per minute. Black lines represent changes in orientation of width direction from individual guanine crystals. The heavy red line represents the mean result. The b -line (inset hypotenuse) on a pale blue bar represents the orientation of width direction of the (102) plane. The angle θ refers to the angle between the horizontal axis and the b -line. (MF; magnetic field). The orientation of width direction of the (102) plane, given by $b \times \cos \theta$, was calculated and plotted. (b) Suppression of light scattering from guanine crystals during continuous application of magnetic fields of 50, 100 and 200 mT ($n = 8$ per group). The graph shows the number of shining guanine crystal platelets having a length greater than 10 μm . Crystals were counted every 3 sec in the observation region (610 $\mu\text{m} \times 460 \mu\text{m}$), and mean

counts \pm standard deviations are shown. (c) Changes in light scattering intensity (%) from a suspension containing guanine crystals. The direction of both of the magnetic field and spectroscopic detection was perpendicular to the incident light. The relative change in the normalized the light intensity, immediately after magnetic fields were applied, is shown on the vertical axis of this graph. When we defined the intensity at the moment the magnetic field was applied as 100 %, and used this as a basis for calculating relative changes. When no magnetic fields were applied, the graph was obtained by randomly sampling. (Reprinted (adapted) with permission from (M. Iwasaka, and Y. Mizukawa, "Light Reflection Control in Biogenic Micro-Mirror by Diamagnetic Orientation," *Langmuir*, vol. 29, pp.4328–4334, 2013.). Copyright (2013) American Chemical Society.)

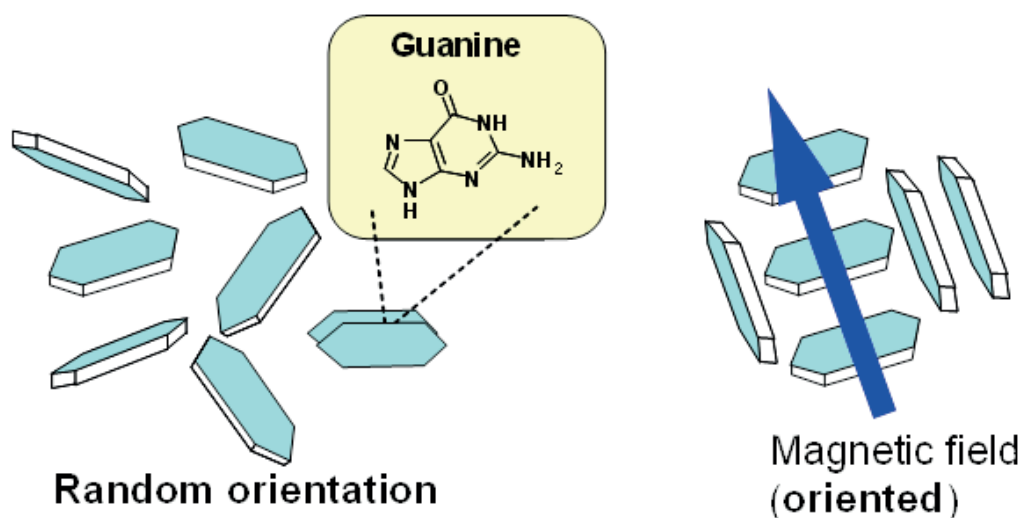
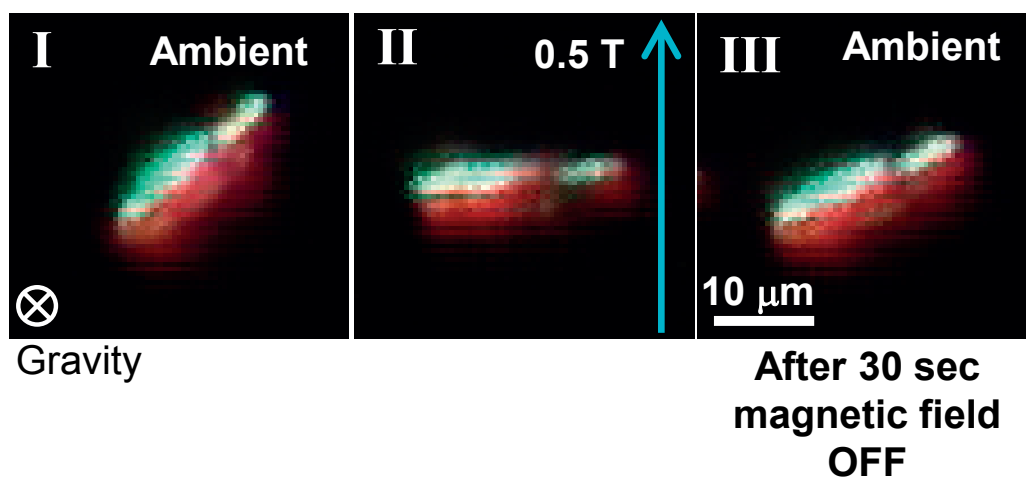


Figure 4.1.5. Schematic illustrations of diamagnetic orientation by guanine crystals derived from goldfish. (Reprinted (adapted) with permission from (M. Iwasaka, and Y. Mizukawa, "Light Reflection Control in Biogenic Micro-Mirror by Diamagnetic Orientation," *Langmuir*, vol. 29, pp.4328–4334, 2013.). Copyright (2013) American Chemical Society.)



Copyright © 2014 IEEE.

Figure 4.1.6. Observation of a recrystallized guanine crystal by optical microscopy (pre-exposure, during exposure to 500 mT, and post-exposure). White bar: 10 μm . (Y. Mizukawa, K. Suzuki, S. Yamamura, Y. Sugawara, T. Sugawara, and M. Iwasaka, “Magnetic Manipulation of Nucleic Acid Base Microcrystals for DNA Sensing,” *IEEE Trans. Magn.*, vol. 50, Art. no. 5001904, 2014.) followed by the IEEE copyright line © 2014 IEEE.

4.1.4 Summary

In conclusion, in this chapter we revealed that biogenic guanine crystals, which are very thin and have high refractive index, behave like a micro-scale mirror and that their light scattering can be changed by a diamagnetic rotation. In addition, it was demonstrated that light scattering from biogenic guanine crystals on a substrate can be inhibited by a noncontact, remote control method, exploiting diamagnetic orientation.

The reflection of light which we obtained from the side is inhibited by diamagnetic orientation of the isolated guanine crystals, when the magnetic field is directed parallel to the direction of observation and the gravitational field. Therefore, it was demonstrated that the suppression of light scattering from biogenic guanine crystals fixed in chromatophore cells [1], and the change in light scattering from floating biogenic guanine crystals described in chapter 3, could occur by diamagnetic

orientation.

In addition, we revealed that recrystallized guanine crystals can be oriented by magnetic fields on the order of millitesla. Further, it was revealed that the orientation of the morphological long axis of a recrystallized guanine crystal perpendicular to magnetic fields occurred and their ability of light scatter was less capable than that of biogenic crystals. We demonstrated that biogenic guanine crystals exhibit superior performance compared to recrystallized guanine crystals, when considering that their ability to reflect light and their light scattering is controlled magnetically.

4.1.5 References

- [1] M. Iwasaka, “Effects of static magnetic fields on light scattering in red chromatophore of goldfish scale,” *J. Appl. Phys.*, vol. 107, Art. no. 09B314, 2010.
- [2] A. Levy-Lior, B. Pokroy, B. Levavi-Sivan, L. Leiserowitz, S. Weiner, and L. Addadi, “Biogenic Guanine Crystals from the Skin of Fish May Be Designed to Enhance Light Reflectance,” *Cryst. Growth Des.*, vol. 8, pp. 507–511, 2008.
- [3] G. Laughlan, A. I. H. Murchie, D. G. Norman, M. H. Moore, P. C. E. Moody, D. M. J. Lilley, and B. Luisi, “The high-resolution crystal structure of a parallel-stranded guanine tetraplex,” *Science*, vol. 265, pp. 520–524, 1994.
- [4] K. Phillips, Z. Dauter, A. I. H. Murchie, D. M. J. Lilley, and B. Luisi, “The crystal structure of a parallel-stranded guanine tetraplex at 0.95Å resolution,” *J. Mol. Biol.*, vol. 273, pp. 171–182, 1997.
- [5] S. Yoshioka, B. Matsuhana, S. Tanaka, Y. Inouye, N. Oshima, and S. Kinoshita, “Mechanism of variable structural color in the neon tetra: quantitative evaluation of the Venetian blind model,” *J. R. Soc. Interface*, vol. 8, pp. 56–66, 2011.

- [6] H. Nagaishi, N. Oshima, and R. Fujii, "Light-reflecting properties of the iridophores of the neon tetra *Paracheirodon innesi*," *Comp. Biochem. Physiol.*, vol. 95A, pp. 337–341, 1990.
- [7] P. J. Herring, "Reflective systems in aquatic animals," *Comp. Biochem. Physiol.*, vol. 109A, pp. 513–546, 1994.
- [8] J. N. Lyngsum, and J. Shand, "Changes in spectral reflexions from the iridophores of the Neon tetra," *J. Physiol.*, vol. 325, pp. 23–34, 1982.
- [9] E. J. Denton, "Review Lecture: On the organization of reflecting surfaces in some marine animals," *Philos. Trans. R. Soc. London, Ser. B*, vol. 258, pp. 285–313, 1970.
- [10] A. Levy-Lior, E. Shimoni, O. Schwartz, E. Gavish-Regev, D. Oron, G. Oxford, S. Weiner, and L. Addadi, "Guanine-Based Biogenic Photonic-Crystal Arrays in Fish and Spiders," *Adv. Funct. Mater.*, vol. 20, pp. 320–329, 2010.
- [11] T. M. Jordan, J. C. Partridge, and N. W. Roberts, "Non-polarizing broadband multilayer reflectors in fish," *Nat. Photonics*, vol. 260, pp. 759–763, 2012.
- [12] L. Pauling, "The Diamagnetic Anisotropy of Aromatic Molecules," *J. Chem. Phys.*, vol. 4, pp. 673–677, 1936.
- [13] M. Fujiwara, M. Fukui, and Y. Tanimoto, "Magnetic Orientation of Benzophenone Crystals in Fields up to 80.0 KOe," *J. Phys. Chem. B*, vol. 103, pp. 2627–2630, 1999.
- [14] M. Fujiwara, E. Oki, M. Hamada, and Y. Tanimoto, "Magnetic Orientation and Magnetic Properties of a Single Carbon Nanotube," *J. Phys. Chem. A*, vol. 105, pp. 4383–4386, 2001.
- [15] M. Fujiwara, T. Chidiwa, and Y. Tanimoto, "Magnetic Orientation under Gravity: Biphenyl and Naphthalene Crystals," *J. Phys. Chem. B*, vol. 104, pp. 8075–8079, 2000.

4.2 Two Magnetic Orientations of Biogenic Guanine Crystals

4.2.1 Introduction

As described in chapter 3 and section 4.1, isolated biogenic guanine crystals in distilled water can be oriented by magnetic fields, and light reflection from the crystals changes due to this orientation.

The aim of this chapter is to reveal the detailed mechanism of magnetic orientation of isolated biogenic guanine crystals on a substrate, by observing them under an optical microscope in the presence of applied magnetic fields. In particular, the experiments in reported this section focused on the easy and difficult magnetization axes of isolated biogenic guanine crystal platelets by using either vertical or horizontal magnetic fields. Biaxial alignment of the biogenic guanine crystals was demonstrated, due to two diamagnetic anisotropies.

4.2.2 Methods and Materials

- **Calculating diamagnetic anisotropic energy**

Diamagnetic anisotropic energy is calculated by using the equation (4.2.1) as follows:

$$E_{d\Delta} = - \frac{\Delta\chi B^2}{2\mu_0} \quad \dots \dots \dots (4.2.1)$$

This equation is based on the cgs (centimeter-gram-second) system of units. $\Delta\chi$ is the difference in a magnetic susceptibility of the two magnetization axes. B is the magnetic field intensity. μ_0 is the space permeability constant. When the diamagnetic anisotropic energy exceeds the thermal energy kT (k = Boltzmann's coefficient $\approx 1.38 \times 10^{-23}$ (J/K), T = temperature in degrees kelvin), we can observe magnetic orientation due to diamagnetic anisotropy.

- Calculating the inertial moment and rotation energy

The inertial moment of a guanine crystal can be calculated by using the following equations:

$$I_L = \frac{M}{3}(7b^2 + c^2) \quad \dots \dots \dots (4.2.2)$$

$$I_W = \frac{M}{3}(7a^2 + c^2) \quad \dots \dots \dots (4.2.3)$$

I_L and I_W represent the inertial moment in the length direction and the inertial moment in the width direction, respectively. M represents the mass of the crystal. $2a$, $2b$ and $2c$ are the width, length and thickness of the crystal, respectively.

- Materials

Guanine crystal suspensions were prepared from the chromatophore cells of goldfish scales, as described in chapter 2. The goldfish scales were placed in distilled water, poked with a plastic stick and the suspension was centrifuged (approximately 30 xG/ 1500~2000 rpm) for 5–10 seconds to obtain pure samples and we obtained the isolated guanine crystal suspension which is high pure.

- Methods

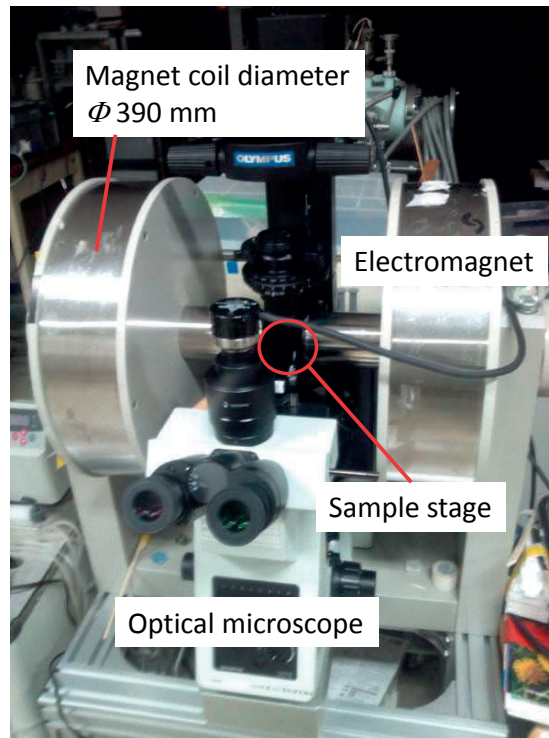
We carried out observations of the magnetic behavior of guanine crystal platelets in a chamber under magnetic fields, using a high-resolution microscope. This microscope enables viewing between two poles of an electromagnet, while applying horizontal magnetic fields.

The experimental environment for investigating biaxial magnetic alignment of isolated biogenic guanine plates in distilled water consisted of a resistive electromagnet

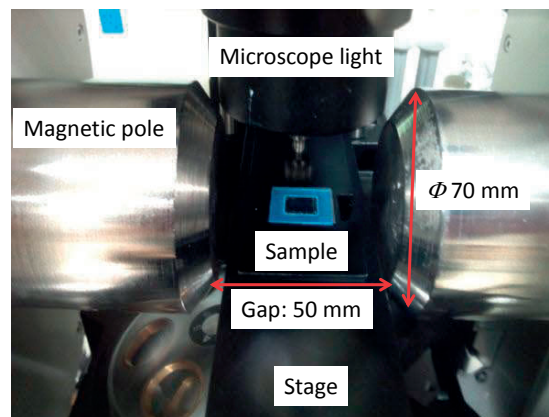
and an optical high-resolution microscope, as shown in Figure 4.2.1. The electromagnet is able to generate horizontal magnetic fields up to a maximum magnetic intensity of 500 mT in the area between both magnetic poles. Figure 4.2.2(a) also shows how we applied a vertical magnetic field to the sample, by using a permanent magnet, which produced vertical magnetic fields of 340 mT. Since we needed to rapidly observe the magnetic behavior of biogenic guanine crystals in the presence and absence of magnetic fields, the permanent magnet was set on the measurement sample and moved as quickly as possible.

The gap between the surface of permanent magnet and the measurement sample was 3 mm. The measurement sample containing guanine crystal suspensions consisted of two coverslips (18 mm × 18 mm, 0.12–0.17 mm in thickness) fixed completely by a frame seal (9 mm × 9 mm × about 300 μm, Bio-Rad SLF0201). We enclosed the fresh biogenic guanine crystal suspension in this chamber (25 μL capacity). This chamber was placed on the stage of an optical microscope (Olympus IX73).

The stage of the optical microscope was set in the central area between both poles of the electromagnet. When the horizontal magnetic field was applied, the electromagnet generated a 500 mT magnetic field parallel to the measurement sample, on the stage of the optical microscope.

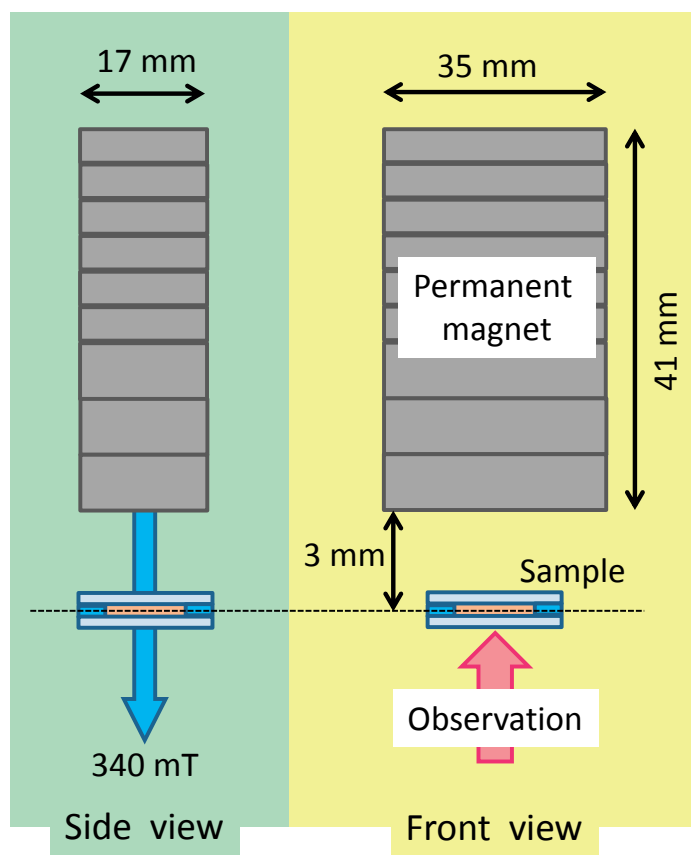


(a)

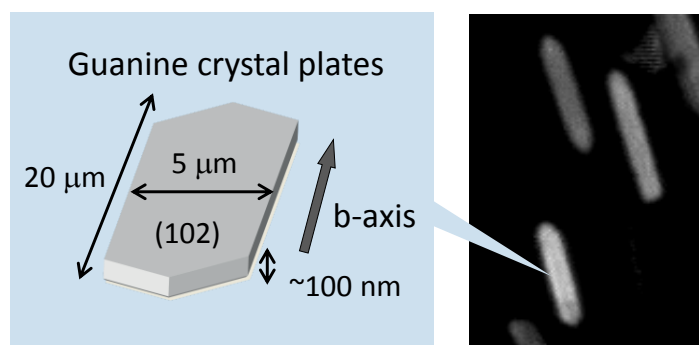


(b)

Figure 4.2.1. Measuring diamagnetic orientation of guanine crystals under magnetic fields. The experimental configuration is shown, consisting of an electromagnet, an optical microscope and a chamber containing the crystal sample. (a) Observations of guanine crystals were recorded by using an inverted optical microscope while applying a horizontal magnetic field. The electromagnet coil diameter Φ was 390 mm. (b) Sample stage of an optical microscope. Magnetic pole gap, 50 mm; magnetic pole diameter, Φ 70 mm.



(a)



(b)

Figure 4.2.2. (a) Experimental setup for observing diamagnetic orientation of guanine crystals on an inverted optical microscope, immediately after applying vertical magnetic fields to the sample using permanent magnet at 340 mT. (b, Left) Schematic representation of a guanine crystal platelet, which shows the b-axis, the (102) plane and crystal size, and (b, Right) a photo showing guanine crystals in dark-field under the optical microscope.

4.2.3 Results and Discussion

Figure 4.2.2(b) shows that a biogenic guanine crystal has a very thin structure, with (102) plane on the surface of an elongated hexagonal platelet. In chapter 2, X-ray powder diffraction analysis and FTIR spectroscopy was carried out. The results in chapter 2 established that the crystalline structure of individual biogenic guanine crystals derived from goldfish, had similar properties as anhydrous crystals [1]–[2]. The maximum area of a guanine crystal is found on the hexagonal (102) plane. The platelets have a long axis parallel to the b-axis, in agreement with a previous study [2]. The length and the width of the isolated guanine crystals were about 10–20 μm and 4–8 μm , respectively. The maximum area of a biogenic guanine crystal showed high light scattering, owing to the significant difference in the refraction index between guanine crystals and the surrounding distilled water.

First, we demonstrated that biogenic guanine crystal platelets could be observed *in situ*, in the presence or absence of a horizontal magnetic field, by combining an optical microscope and a electromagnet. As shown in Figure 4.2.3(a)–(e), the longitudinal axis (b-axis) of the isolated guanine crystal platelets aligned along the applied horizontal magnetic field direction. The guanine crystal platelets were oriented randomly under ambient fields (Figure 4.2.3(a)). However, the guanine crystal platelets aligned along the direction of the magnetic field gradually, and the diamagnetic rotation could be observed under horizontal magnetic fields (Figure 4.2.3(b)–(c)). Most of the guanine crystal orientations were completed within five minutes (Figure 4.2.3(d)).

The angular distribution of the guanine crystal platelets under ambient and applied magnetic fields was analyzed (Figure 4.2.4(a)). The measured angle, θ , was formed between the b-axis of guanine crystals and the horizontal direction (magnetic

field direction). The number of platelets that divided into the angle θ was counted. It became apparent that the long axis direction gradually became parallel to the horizontal magnetic fields at 500 mT. In order to describe this phenomenon, we show the diamagnetic energy regarding the diamagnetic susceptibility (χ_l and χ_w) of the long axis and the short axis in the (102) plane of a guanine crystal platelet in Figure 4.2.4(b).

The χ_l and χ_w have a negative value in a diamagnetic material, and χ_w is smaller than χ_l . Therefore, the values of the diamagnetic energy of the length direction being subtracted to that of the depth direction ($-\chi_d B^2/2\mu_0$) are different from that of the width direction. This result indicates that the diamagnetic energy of the width direction is larger than that of the length direction. From this information, the energy level estimations can be calculated for the diamagnetic orientation behaviors. It was hypothesized that the observed diamagnetic orientation of biogenic guanine crystals could be explained by the same physical mechanism as that reported for lecithin crystals in a previous study [3]. The lecithin crystals had a similar size as the goldfish guanine crystals. Furthermore, this previous study reported the diamagnetic orientation of lecithin crystals in magnetic fields between 160–900 mT. It is speculated that the diamagnetic orientation is caused by the magnetic fields of mT order when the crystals have sufficient diamagnetic anisotropy to enable the generation of high diamagnetic energies, overcoming thermal energy kT , as indicated in the introduction.

To demonstrate this hypothesis, the diamagnetic energy of biogenic guanine crystals derived from goldfish was estimated using the equation (4.2.1) shown in the method section, based on the cgs-gauss system of units. The diamagnetic susceptibility of biogenic guanine crystals with a goldfish scale was measured by a DC-SQUID (direct current-superconducting quantum interference device). Measurements showed that the

diamagnetic susceptibility was 4.52×10^{-7} emu/g. We speculated that the maximum $|\Delta\chi|$ of a biogenic guanine crystal was approximately 1×10^{-7} emu/g. It was revealed that the thickness of a biogenic guanine crystal was approximately $0.1 \mu\text{m}$ by performing atomic force microscopy (AFM) analysis. Also, we estimated that the size of an average biogenic guanine crystal is $20 \times 5 \times 0.1 \mu\text{m}^3$, giving a volume of 10^{-11}cm^3 , calculated based on a density $\approx 1 \text{g/cm}^3$. In addition, we conjecture that the $|\Delta\chi|$ of a biogenic guanine crystal is 1×10^{-18} emu/g. Therefore, the evaluated diamagnetic energy (E) is 8×10^{-12} erg in magnetic fields of 400mT. On the other hand, the thermal energy kT at 300 K (a room temperature) is 4.14×10^{-14} erg. Consequently, the calculated diamagnetic energy is 100 times greater than the thermal energy, kT . This hypothesis was supported quantitatively, since diamagnetic orientation of the biogenic guanine crystals was achieved using magnetic fields of 400 mT, as expected by these estimations.

In the next experiment, we observed diamagnetic orientation of the biogenic guanine crystal platelets under vertical magnetic fields, which were applied perpendicular to their (102) planes. Figure 4.2.5 (a) shows that the (102) plane of a guanine crystal platelet stood up on the glass substrate, when the gravitational and magnetic field directions were directed parallel to the depth direction of the crystal (102) plane. So, the long thin (001) plane [2] of a guanine crystal platelet became parallel to the plane of the glass substrate. Immediately after switching the vertical magnetic fields off by using permanent magnet, the long thin (001) plane became visible under the optical microscope. In Figure 4.2.5 (a), very thin lines can be seen. These are the (001) planes of the guanine crystals. Figure 4.2.5 (b) shows the guanine crystal platelets on the glass substrate after exposure to the magnetic field has ended for 20 seconds. As a result, a few guanine crystal platelets were inclined. After 60 seconds had

elapsed, most of guanine crystal platelets no longer stood up and the crystal (102) planes became parallel to the glass substrate surface, as shown in Figure 4.2.5(c). These results revealed that the guanine crystal platelets standing up in response to vertical magnetic fields, gradually laid back down under gravity as time elapsed. We carried out a statistical analysis, in which we measured the width of the inclining guanine crystal platelets, as shown in Figure 4.2.6(a). This analysis quantitatively demonstrated that the guanine crystal platelets gradually inclined over time. The process by which the (102) planes of guanine crystal platelets returned, from standing up in response to vertical magnetic fields to lying back down due to gravity, is represented schematically in Figure 4.2.6(b).

In order to explain the mechanism by which these orientations occur, Figure 4.2.6(c) compares the inertial moments between the length direction (I_L) and width direction (I_W) of crystals. We estimate that the size of an average guanine crystal is $20 \times 5 \times 0.1 \mu\text{m}$, and we estimate that the mass is 10^{-11} g (density $\approx 1 \text{ g/cm}^3$). Based on our results, we calculate that I_L ($\approx 233.33 \times 10^{-19} \text{ [g}\cdot\text{cm}^2]$) is larger than I_W ($\approx 14.58 \times 10^{-19} \text{ [g}\cdot\text{cm}^2]$) by using the equation (4.2.2) and (4.2.3).

Therefore, it is easy for a lying guanine crystal platelet to align along the width direction of the (102) plane under magnetic fields. However, it is more difficult for a platelet to stand up in the length direction. When the absolute value of the diamagnetic energy for the length direction is smaller than the rotational energy for the length rotation, it is conjectured that magnetic rotation aligns along the width direction is easy, provided the rotational energy for the width direction is small enough. Therefore, these calculations based on our measurements suggest that the magnetic rotation of biogenic guanine crystal platelets occurs rapidly due to diamagnetic torque

forces around the length direction (b-axis). On the other hand, magnetic orientation around depth direction requires several minutes.

Similar to lecithin crystals [3], biogenic guanine crystals exhibit rapid orientation around the length direction of the platelets in response to diamagnetic anisotropy. On the other hand, rotation around the depth direction of guanine crystal platelets occurred at a moderate rate in horizontal magnetic fields. These results demonstrated that the biogenic guanine crystal undergo biaxial orientation in response to magnetic fields of two directions. From these results, we clarified the easy and difficult magnetization axes of the biogenic guanine crystal platelet.

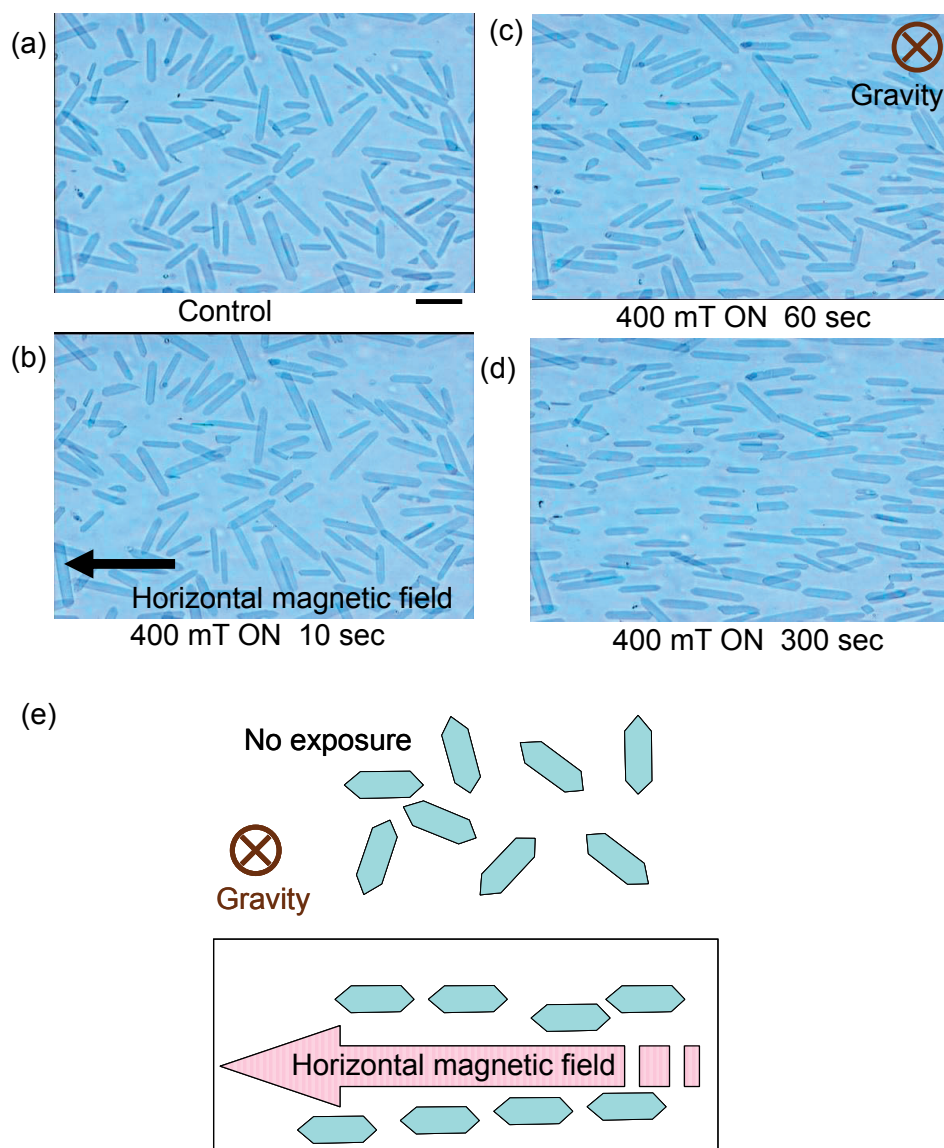
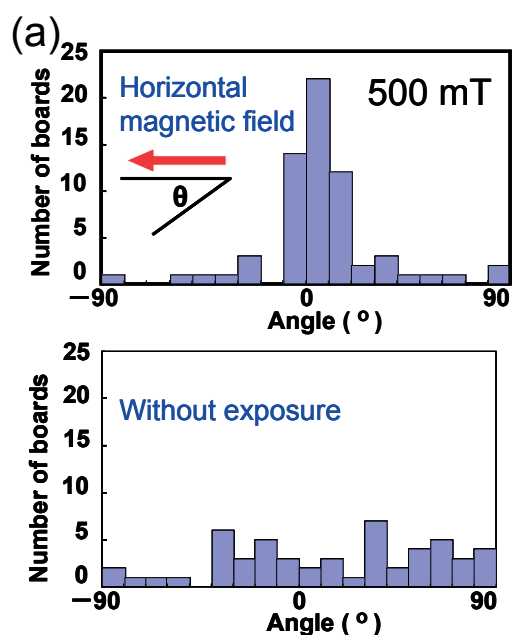
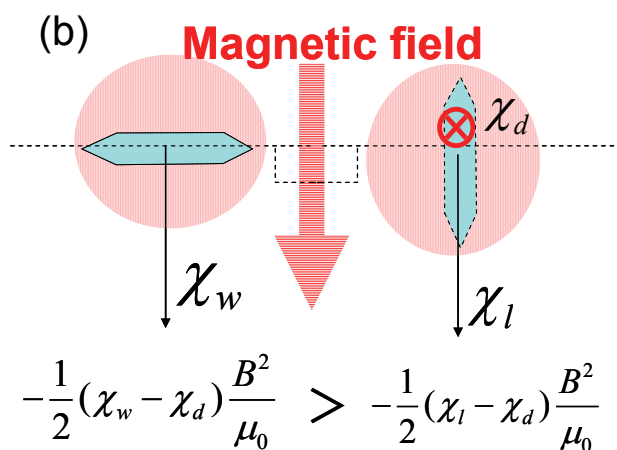


Figure 4.2.3. Diamagnetic orientation of guanine crystal platelets gradually aligning to the length direction of the (102) plane (b-axis direction) under horizontal applied magnetic fields. (Magnetic rotation around the depth direction of the (102) plane of the guanine crystal platelet.) (a) Guanine crystal platelets oriented randomly under ambient fields. The direction of the gravitational field is perpendicular the horizontal plane in these images. Bar, 20 μm . (b)–(d) Changes of the diamagnetic orientation of guanine crystal platelets in 400mT horizontal magnetic fields as time advances. (e) Schematic illustration rationalizing the diamagnetic orientation of guanine crystal platelets aligning their long axes (b-axis) parallel to the horizontal magnetic field. ([M. Iwasaka, Y. Miyashita, Y. Mizukawa, K. Suzuki, T. Toyota, and T. Sugawara, “Biaxial Alignment Control of Guanine Crystals by Diamagnetic Orientation,” *Appl. Phys. Express*, vol. 6, Art. no. 037002, 2013.] Copyright (2013) The Japan Society of Applied Physics.)



Oriental angle distributions



Diamagnetic anisotropic energies

Figure 4.2.4. (a) Statistical analysis of the distribution of the angle θ , which is defined for guanine crystal platelets aligning their long axis (b-axis) to the horizontal direction, either in ambient fields or a horizontal magnetic field of 500 mT. (b) A model comparing the diamagnetic anisotropic energy of guanine crystal platelets, depending on whether they align their length or width in direction of the magnetic field. ([M. Iwasaka, Y. Miyashita, Y. Mizukawa, K. Suzuki, T. Toyota, and T. Sugawara, “Biaxial Alignment Control of Guanine Crystals by Diamagnetic Orientation,” *Appl. Phys. Express*, vol. 6, Art. no. 037002, 2013.] Copyright (2013) The Japan Society of Applied Physics.)

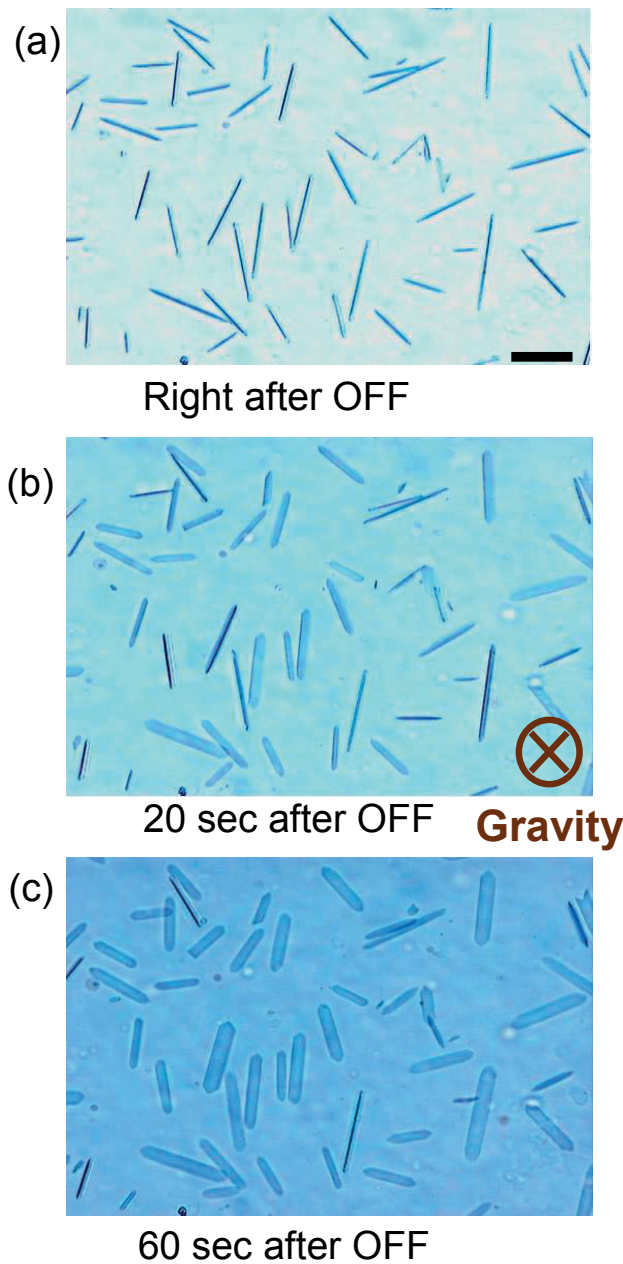


Figure 4.2.5. Diamagnetic rotation of guanine crystal platelets oriented along the width direction of the (102) plane parallel to the vertical magnetic fields and gravity direction. (Magnetic rotation around the length direction of the (102) plane of the guanine crystal platelet.) (a) Immediately after the 340 mT permanent magnet was removed. The platelets are standing up on the glass substrate due to vertical magnetic fields. Bar, 20 μm . (b and c) Guanine crystal platelets begin to lie down gradually on the glass substrate, under gravity. ([M. Iwasaka, Y. Miyashita, Y. Mizukawa, K. Suzuki, T. Toyota, and T. Sugawara, “Biaxial Alignment Control of Guanine Crystals by Diamagnetic Orientation,” *Appl. Phys. Express*, vol. 6, Art. no. 037002, 2013.] Copyright (2013) The Japan Society of Applied Physics.)

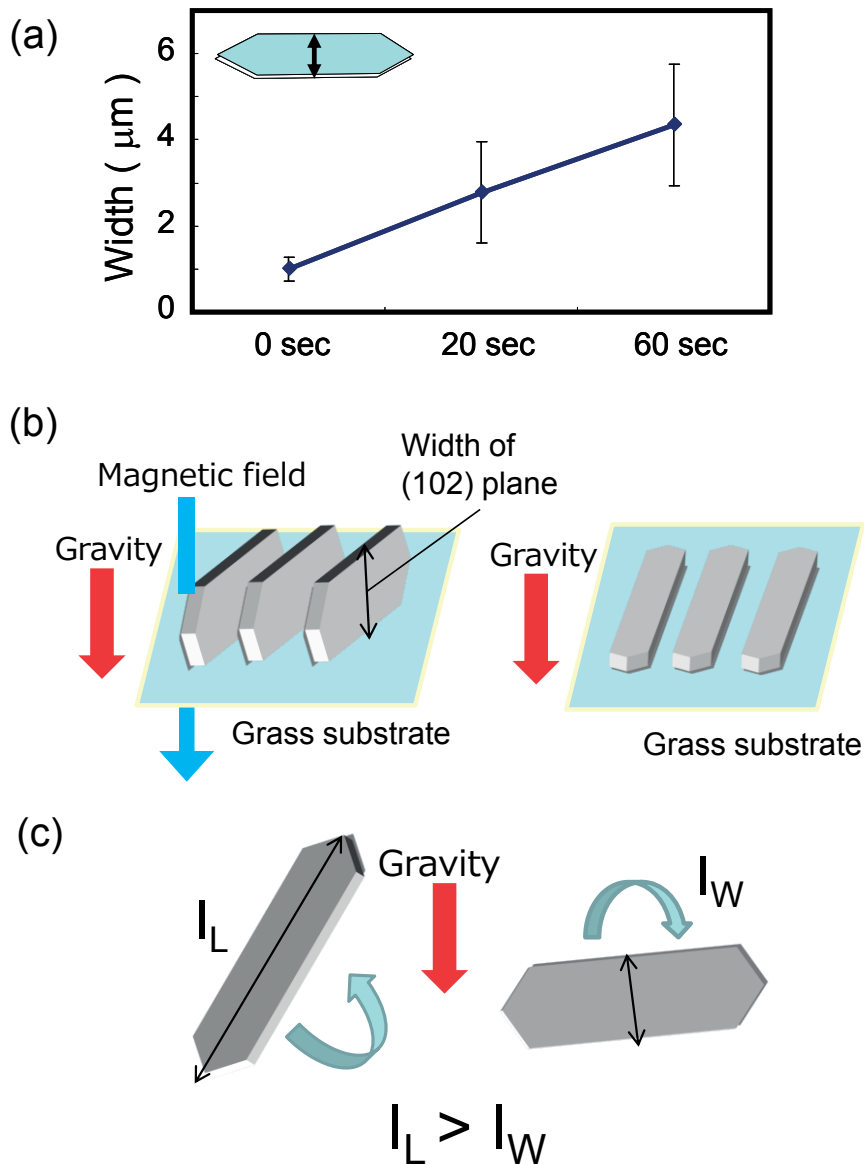


Figure 4.2.6. (a) Time course of apparent width changes in guanine crystal platelets. Mean \pm SD (n = 44). (b) Schematic rationalization of magnetic rotation of guanine crystal platelets, aligning the width direction of the (102) plane parallel to both the magnetic field and gravity direction. (c) Comparing the inertial moment in the length direction with that in the width direction when a lying crystal platelet rotates about its length or width to stand up. ([M. Iwasaka, Y. Miyashita, Y. Mizukawa, K. Suzuki, T. Toyota, and T. Sugawara, “Biaxial Alignment Control of Guanine Crystals by Diamagnetic Orientation,” *Appl. Phys. Express*, vol. 6, Art. no. 037002, 2013.] Copyright (2013) The Japan Society of Applied Physics.)

4.2.4 Summary

In this study, we applied vertical and horizontal magnetic fields to the biogenic guanine crystal platelets while observing them with an optical microscope.

When vertical magnetic fields of 340 mT were applied, the crystal platelets stood up on the glass substrate for several tens of seconds, and the width directions of their (102) planes was aligned parallel to both of the gravitational field and the applied magnetic field. When horizontal magnetic fields of 400 mT were applied, the long-axes (b-axes) of the lying guanine crystal plates gradually rotated on the glass substrate, requiring several minutes. From these results, we succeeded in clarifying the first easy magnetization axis (b-axis), the second easy magnetization axis (parallel to the width direction of the (102) plane of a guanine crystal platelet) and a difficult magnetization axis (perpendicular to the (102) plane of a guanine crystal platelet) and two kinds of diamagnetic rotations due to two diamagnetic anisotropies.

4.2.5 References

- [1] K. Guille, and W. Clegg, “Anhydrous guanine: a synchrotron study,” *Acta Crystallogr., Sect. C*, vol. 62, pp. O515–517, 2006.
- [2] A. Levy-Lior, B. Pokroy, B. Levavi-Sivan, L. Leiserowitz, S. Weiner, and L. Addadi, “Biogenic Guanine Crystals from the Skin of Fish May Be Designed to Enhance Light Reflectance,” *Cryst. Growth Des.*, vol. 8, pp. 507–511, 2008.
- [3] I. Sakurai, Y. Kawamura, A. Ikegami, and S. Iwayanagi, “Magneto-orientation of lecithin crystals,” *Proc. Natl. Acad. Sci. U.S.A.*, vol. 77, pp. 7232–7236, 1980.

5. Reflection Angle Specificity of Biogenic Guanine Crystals

5.1 Introduction

The experiments described in chapters 2–4, demonstrated that biogenic guanine crystals may play a role as biogenic optical micro-mirrors, and exhibit two sorts of rapid orientation responses to applied magnetic fields. Also, we revealed two kinds of diamagnetic orientation around length and width direction of (102) plane due to the two diamagnetic anisotropies. We established that light reflection from floating guanine crystals could be suppressed or enhanced and switched on/off by combining magnetic fields and incident lighting, under suitable observation conditions.

In this chapter, as a preliminary experiment, we tried to reconstruct and manipulate a micro-mirror system, similar to the optical system of a fish, using guanine crystals and DNA. A guanine crystal “mirror” was adhered on to a glass substrate using vertical magnetic fields with DNA present. We could control the angle of individual guanine crystals fixed on the glass substrate by applying horizontal magnetic fields. Additionally, more complex and effective 3-dimensional diamagnetic manipulation of biogenic guanine crystals was achieved by biaxial orientation, combining vertical and horizontal magnetic fields. Also, we tried to analyze the optical property and angular region for light reflection of the individual guanine crystal platelet with the established 3-dimensional diamagnetic manipulation.

5.2 Methods and Materials

- Fabrication and magnetic manipulation of biogenic guanine micro-mirrors

Figure 5.1(a) shows the experimental configuration for observing guanine crystals with DNA. This system consisted of an electromagnet (WS15-40-5 K-MS; Hayama), an optical microscope (IX-73; Olympus), and the prepared sample. The electromagnet generated a maximum horizontal magnetic field of 500 mT. The diameter of this pole was about 70 mm. The permanent magnet generated a vertical magnetic field of about 480 mT.

A suspension of biogenic guanine crystals was freshly prepared from goldfish scales. In addition, DNA powder derived from salmon sperm (047-17322; Wako) was added to boiling distilled water at 90–100 °C. The hot DNA solution and the biogenic guanine crystal suspension were mixed, in equal volumes. The measurement chamber was made of two glass coverslips (18 mm × 18 mm), and a flame-sealed chamber (9 mm × 9 mm, 25 μL capacity; Bio-Rad) containing the mixed solution. After enclosing the prepared solution in a chamber, this chamber was rapidly placed in the vertical magnetic field generated by the permanent magnet, and held there for more than 15 minutes.

The (001) planes of biogenic guanine crystal platelets adhered to the glass substrate, in the presence of DNA, which played a role as an adhesive material. The DNA between the guanine crystals and the glass substrate may facilitate the motion of adherent crystals. The behavior of the guanine crystals fixed on the glass substrate with the present of DNA, was observed in horizontal magnetic fields using an optical microscope. In addition, the absorbance of the micro-mirror consisting of the guanine

crystal and DNA on a quartz plate was measured by transmission spectroscopy. From these absorbance measurements, we investigated whether DNA can serve as an adhesive material for fixing guanine crystals to the glass substrate.

- Three axes of magnetic orientation and optical specificity of biogenic guanine crystals

The sample is a biogenic guanine crystal suspension enclosed in a glass chamber (9 mm × 9 mm, 25 μL capacity; Bio-Rad). When we measured and analyzed the twisting magnetic orientation and the angular velocity of that by using two kinds of diamagnetic rotation of a guanine crystal, the experimental setup described in section 4.2 was used.

Also, we setup the experimental method for the analysis of the optical property and angular region for light reflection of the individual guanine crystal platelet with the established 3-dimensional diamagnetic manipulation. This setup consisted of an electromagnet (WS15-40-5 K-MS; Hayama), an optical microscope (VH-5000; Keyence) and an external optical fiber (light source).

When investigating the selectivity of light reflection of individual guanine crystal platelets, the experimental setup was consisted of an electromagnet (WS15-40-5 K-MS; Hayama), an optical microscope (IX-73; Olympus) and an external optical fiber (light source). The angle between the external optical fiber and the sample was 25°.

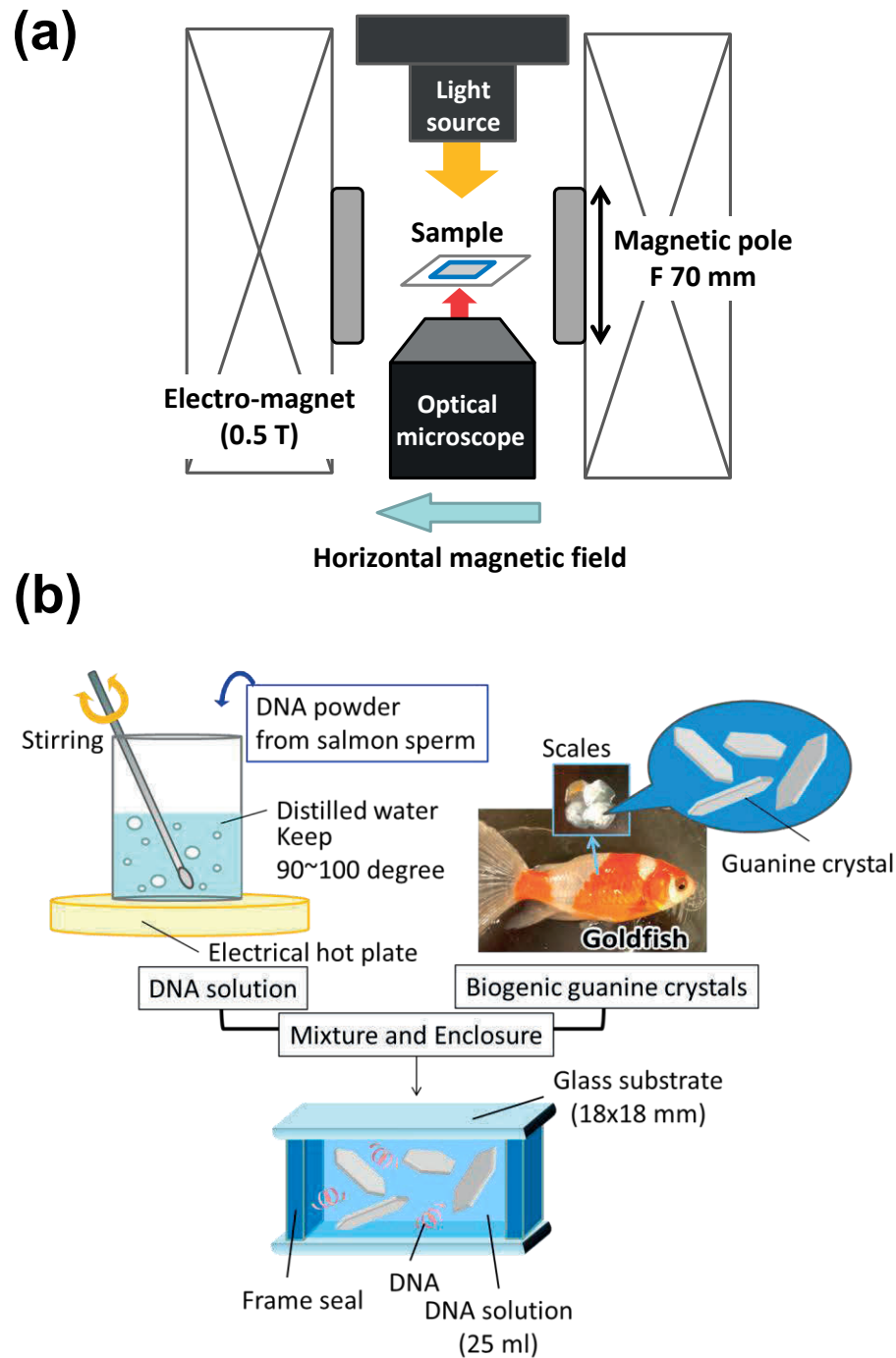


Figure 5.1. (a) Experimental setup consisting of an electromagnet and an optical microscope for observing the behavior of guanine crystals with DNA. (b) Preparation of micro-mirrors made from guanine crystals and DNA. (Reproduced from [Y. Mizukawa, and M. Iwasaka, *J. Appl. Phys.*, vol. 117, Page 17B730, (2015).], with the permission of AIP Publishing.)

5.3 Results and Discussion

- Fabrication and magnetic manipulation of biogenic guanine micro-mirrors

We reconstructed the light reflection system in the chromatophore cells on fish scales, similar to micro-mirrors, by combing biogenic guanine crystals, a DNA solution, and vertical magnetic fields. The reconstructed mirror system could be controlled under horizontal magnetic fields of 450 mT. Prior to magnetic exposure (in ambient fields), the micro-mirror containing DNA did not move (the upper left image of Figure 5.2(a)). However, the optical microscope images of Figure 5.2(a) show that the reconstructed micro-mirror moved during exposures to horizontal magnetic fields. This phenomenon, which is a change in the angle of the (102) plane of the reconstructed micro-mirror under a horizontal magnetic field, resulted from diamagnetic orientation of the guanine crystal platelets due to their diamagnetic anisotropy. Comparing the width of guanine crystals before and during exposure, the angular change was obvious. The width during magnetic field exposure was larger slightly than that seen once the horizontal magnetic field was turned off. The width of the reconstructed micro-mirror recovered to pre-exposure conditions for 570 sec after the magnetic field was removed.

A similar experiment was performed in which distilled water was used as a substitute for the DNA solution. Guanine crystals in the absence of DNA stood in vertical magnetic fields of 480 mT, and the behavior of these standing crystals was also observed under horizontal magnetic fields of 450 mT. When we compared the width of the guanine crystals prior to exposure with that during exposure, the width change was larger in distilled water than that of the reconstructed micro-mirror. The width did not change post-exposure and the angle of the guanine crystal did not recover that attained

during exposure. These results revealed that the presence of DNA in samples enables the movement of the reconstructed micro-mirror under applied horizontal magnetic fields.

We needed to reveal whether DNA played a role of as an adhesive material between the guanine crystal and the glass substrate. Therefore, we carried out absorbance analyses on the reconstructed micro-mirror system.

Figure 5.3 shows the absorbance for the reconstructed micro-mirror with DNA on dried quartz substrate surfaces, after washing with a three kinds of solutions. The b-line (blue dotted line) in Figure 5.3 is the absorbance spectrum of the dried plate surface in the open air-space after washing with phosphate-buffered saline (PBS). The a-line (green line) and the c-line (red line) in Figure 5.3 show the absorbance spectra for the dried plate, after the plate was washed with either Tris-EDTA buffer and distilled water, respectively. A peak in the 250–280 nm range was related to the absorbance peak of DNA. The absorbance of the a-, b- and c-lines peak over the 250–280 nm range. On the other hand, the d-line (gray line) shows the absorbance for a control sample, without DNA, and this line did not contain a peak in the 250–280 nm range. These results suggest that DNA potentially played a role as an adhesive material between the plate and the biogenic guanine crystals.

Figure 5.4 shows a schematic representation of the reconstruction micro-mirrors made from guanine crystals and DNA, and their motions under vertical and horizontal magnetic fields. The upper left image in Figure 5.4 shows the guanine crystal platelet and DNA in the solution without magnetic fields (under ambient fields). The (102) plane (the maximum area of a guanine crystal) of the floating guanine crystal was oriented in vertical magnetic fields due to the diamagnetic anisotropy, as shown in

the upper right image in Figure 5.4. In addition, the side surface of the guanine crystal platelet was fixed to the substrate with DNA and by gravity. Therefore, we conclude that we have successfully reconstructed a micro-mirror. The inclination angle of the reconstructed micro-mirror was controlled using horizontal magnetic fields, as shown in the bottom left image of Figure 5.4. The bottom right image shows that the angle of inclination of the micro-mirror recovered once the horizontal magnetic field was removed. This micro-mirror containing a flexible adhesive material (DNA) could be fabricated and controlled by using both vertical and horizontal magnetic fields.

- Three axes of magnetic orientation and optical specificity of biogenic guanine crystals

In spite of our promising initial results, these reconstructed micro-mirrors enabled only 2-dimensional rotations and the degree of freedom of light reflection is low. Therefore, this method was not suitable as an analysis for the optical property of biogenic guanine crystals when we considered the 3-dimensional motion of fish.

So, we sought to achieve more complex 3-dimensional rotations by introducing weaker bonding to the glass chamber. As a more effective method for investigating the light reflection properties of guanine crystal platelets, the 3-dimensional diamagnetic manipulation, enabling rapid rotation about the long axis of the platelets and a more complex rotation, was established by the method combining the two kinds of magnetic rotation around z-axis and y-axis. This manipulation is suitable for the optical analysis of an individual guanine crystal platelet.

In the next experiment, we observed the 3-dimensional controls by manipulating vertical and horizontal magnetic fields *in situ*. The time course changes in the rotation of guanine crystals under bidirectional magnetic fields was analyzed, as shown in Figure 5.5. Figure 5.5(a) shows an optical image of the guanine crystal platelets directing their width direction on the (102) plane parallel to the vertical magnetic fields applied by a permanent magnet. Immediately after the permanent magnet was removed from the sample chamber, while the guanine crystal platelets were still standing up due to vertical magnetic fields, horizontal magnetic fields were applied to the sample chamber using an electromagnet. We observed the twisting orientation of guanine crystal platelets under the horizontal magnetic fields and the quick orientation of the (102) plane, aligning the long axis of the guanine crystal platelets to the horizontal direction, as shown in Figure 5.5(b). The long axes of a few standing guanine crystal platelets oriented twistedly parallel to the horizontal direction. Also, some of the (102) planes of crystal platelets were lying down horizontally.

From these results, we succeeded in demonstrating rapid rotation in horizontal direction by combining the method which consisted of the orientation of crystals standing up in vertical magnetic fields and the rotation around the depth direction on the (102) plane caused by horizontal magnetic fields. Also, Figure 5.6 indicates that the distribution of the angle θ between the horizontal direction and the length direction on guanine crystal (102) planes. This analysis was performed when 400 mT horizontal magnetic fields were applied after immediately removing the 340mT permanent magnet, and after 3 seconds had passed since the guanine crystal platelets had been made to stand up in vertical magnetic fields. This result statistically indicates that most of guanine crystals were completely oriented. In addition, we compared the angular

velocity of single axis rotation with that of twisting magnetic orientation, as shown in Figure 5.7. The analyzed number is 8, respectively. An angular velocity of 0.0057 (rad/s) about a single axis of magnetic rotation was calculated. The angular velocity was about 0.063 (rad/s), with twisting magnetic orientation. Therefore, the angular velocity of twisting magnetic orientation is about 0.057 (rad/s) faster than single-axis magnetic rotation.

In Figure 5.8, this image indicates that the time course changes of schematic illustrations and optical images of an individual guanine crystal platelet during the twisting magnetic orientation due to two kinds of diamagnetic orientation, which is the rotation around the depth direction and the length direction on the (102) plane of a guanine crystal platelet. From this result, when 1.6 sec had elapsed since the twisting magnetic orientation of the guanine crystals had occurred, an individual guanine crystal platelet achieved maximum brightness and reflected light strongly.

Next, we analyzed the angle changes of a long axis and a crystal (102) plane of a guanine crystal during the twisting magnetic orientation. In Figure 5.9(a), the schematic images in the top and side view define an angle θ and ϕ . The angle θ is an angle between the x axis and the long axis of a guanine crystal and the angle ϕ is an angle between the x-y plane and the (102) plane of a guanine crystal. Figure 5.9(b) indicates that the time course changes of brightness, angle θ and angle ϕ of a guanine crystal during the twisting magnetic orientation. From this table, it is revealed that the strong light reflection from the isolated guanine crystal platelet during the twisting magnetic orientation occurred in the narrow angular range within 0.3 sec. We found a possible relationship between light reflection and the crystal axes of a guanine crystal. Therefore, our next experiment investigated the light reflection selectivity of an

individual guanine crystal platelet, directing parallel or perpendicular to incident light.

Figure 5.10 shows our optical observations on a single guanine crystal platelet illuminated by incident light at an angle of 0° (perpendicular), 45° , or 90° (parallel) to the long axis (b-axis) of the guanine crystal. When the angle was 0° , bright light reflection occurred. However, no reflection could be seen from a guanine crystal at 45° or 90° . Figure 5.11 provides optical images and a distribution graph of the number of bright guanine crystal platelets as a function of the angle φ . In Figure 5.11(a), there are two optical images of bright guanine crystals. The left image (pattern 1) shows that the incident light direction is parallel to the horizontal axis. The right image (pattern 2) shows that the incident light direction is parallel to the vertical axis. We analyzed these patterns and the number in pattern 1 is 111 and that in pattern 2 is 98. The distribution graph (Figure 5.11(b)) represents the number of the bright guanine crystal platelets *versus* the angle φ between the long axis of a crystal platelet and the vertical axis in both photographs. From this graph, we revealed that many guanine crystal platelets tended to be bright when the long axis of platelets directed perpendicular to the incident light in the x-y plane. These results clarified that the guanine crystal platelets have light reflection selectivity. This permits the light switching depending on the direction of the incident light. It is conjectured that the mechanism for these phenomena is relates to rotation around the long axis and the depth axis of guanine crystal platelets. This is because there are some guanine crystals which have no change in light reflection due to adherence to a glass substrate.

Also, we tried to analyze the feasible region of light reflection from an individual biogenic guanine crystal platelet from the results of these optical experiments. In Figure 5.12, two kinds of the schematic illustrations exhibits and

defines the region and the coordinate system of the rotation around z-axis and the rotation around y-axis for analyzing the available region of a light reflection from an individual guanine crystal platelet by using the twisting magnetic rotation. A and B points represent an edge of a guanine crystal as the reference point for an analyzing the angle θ and angle ϕ , respectively. Also, Figure 5.13 shows that the feasible region, which is orange region, of light reflection from a guanine crystal platelet analyzed by using the twisting magnetic orientation. From these optical experimental results, we could revealed the feasible region of light reflection from an individual biogenic guanine crystal platelet is [angle θ , angle ϕ]=[0~46°,10~22°]. In addition, from the graph of Figure 5.9(b), it was revealed that the reflection switching region which can cause the strong light reflection within the feasible region of light reflection was [angle θ , angle ϕ]=[2°,12°]. From this result, the biogenic guanine crystal platelet can show the strong light reflection and light switching in the narrow region because the individual biogenic guanine crystal platelet possesses the very narrow angular range about 2° for the light reflection switching.

In chapter 3, we demonstrated that the light scattering from guanine crystals floating in distilled water could be controlled, through a combination of magnetic fields and incident light direction. The results in this chapter allow us to clarify the mechanism of controllable light switching in the floating guanine crystals.

Figure 5.14 provides a schematic explanation of the mechanism for changing light scattering as a function of magnetic fields and the direction of incident light. When magnetic field directions were parallel to incident light directions, the guanine crystal platelets scattered light randomly due to the Brownian motion under ambient fields. However, when guanine crystal platelets were oriented by magnetic fields, light

scattering was suppressed. That is because the incident light was direction parallel to the long axis of the guanine crystal platelets, as shown in Figure 5.14(a). On the other hand, Figure 5.14(b) shows the behavior of the guanine crystal platelet when the magnetic field direction was perpendicular to the incident light direction. Again, under ambient fields, random reflection resulted from thermal Brownian motion. Enhanced light scattering from guanine crystal platelets was observed under magnetic fields, because the long axes of guanine crystal platelets aligned perpendicularly to the incident light upon magnetic orientation. Therefore, we can explain the mechanism of switchable light reflection in floating guanine crystals.

The magnetic exposures combining “vertical and horizontal” application, demonstrated that the rapid twisting diamagnetic manipulation of guanine crystal platelets can be effected. The procedure involves orienting the crystal width direction so that the platelets stand up parallel to the direction of the gravitational field, followed by the rotation about their length direction parallel to the horizontal magnetic field. We were able to achieve the twisting magnetic orientation by combining two kinds of magnetic rotation around z-axis and y-axis, because of reducing the friction between the (102) plane and a glass substrate.

In this chapter, we demonstrated reconstruction of micro-mirrors consisting of biogenic guanine crystals in a DNA solution. These micro-mirrors constitute a microstructural diamagnetic reflective material, which we were able to control remotely. These results suggest that the reconstructed micro-mirrors may have possible applications as underwater micro-actuators, or in micro-scale optical devices, such as microfluidic systems. Also, we established a new technique for the 3-dimensional diamagnetic manipulation of biogenic guanine crystals by exploiting the biaxial

orientation under vertical and horizontal magnetic fields. The guanine crystal platelets act like micro-mirrors because of their high light scattering in distilled water. Light reflection from biogenic guanine crystals can be controlled noninvasively by the diamagnetic manipulation on the micro-scale. This novel method enabled the 3-dimensional diamagnetic manipulation (twisting magnetic orientation), which combining two kinds of diamagnetic rotation around z-axis and y-axis by using vertical and horizontal magnetic fields. Moreover, we could clarified that the narrow angular range ($[\text{angle } \theta, \text{angle } \phi]=[2^\circ, 12^\circ]$) for the strong light reflection and light switching with the established 3-dimensional diamagnetic manipulation.

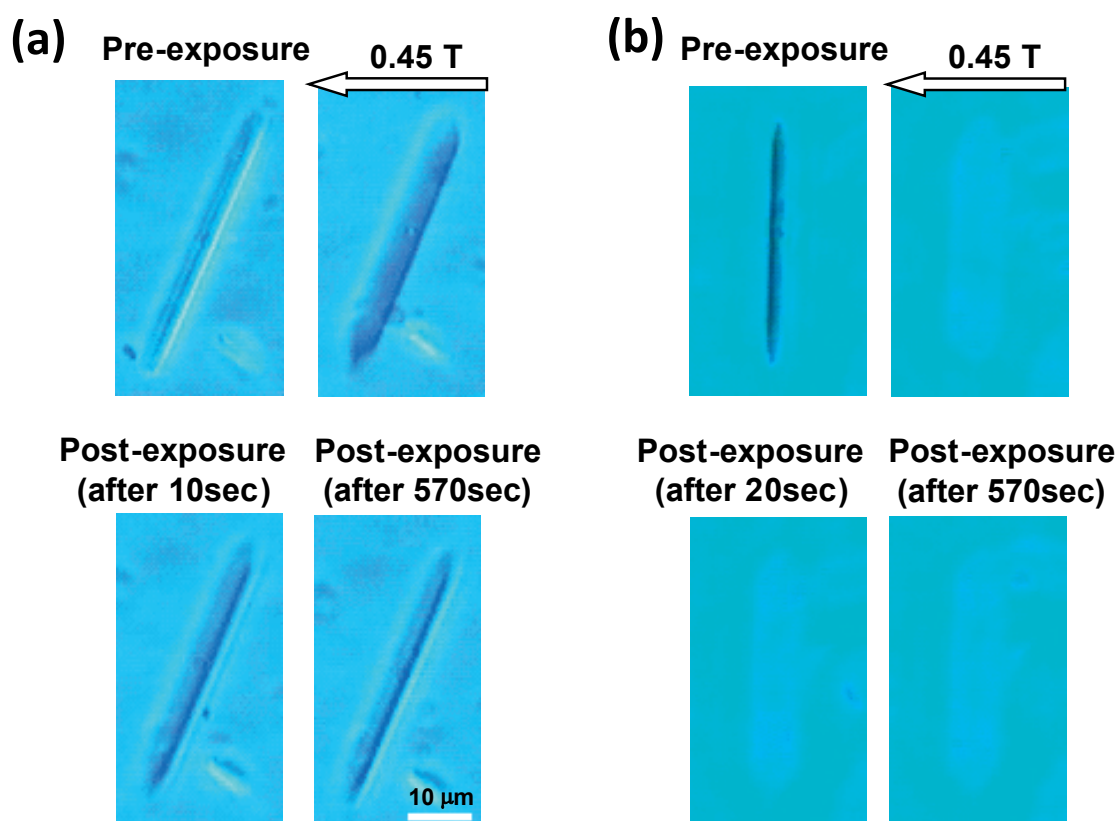


Figure 5.2. (a) Behavior of a guanine crystal with DNA in pre-exposure, during exposure to 450 mT, and in post-exposure. (b) Immediately after applying a vertical magnetic field of 480 mT, the behavior of a guanine crystal without DNA was recorded in pre-exposure, during exposure to 450 mT, and in post-exposure. (Reproduced from [Y. Mizukawa, and M. Iwasaka, *J. Appl. Phys.*, vol. 117, Page 17B730, (2015).], with the permission of AIP Publishing.)

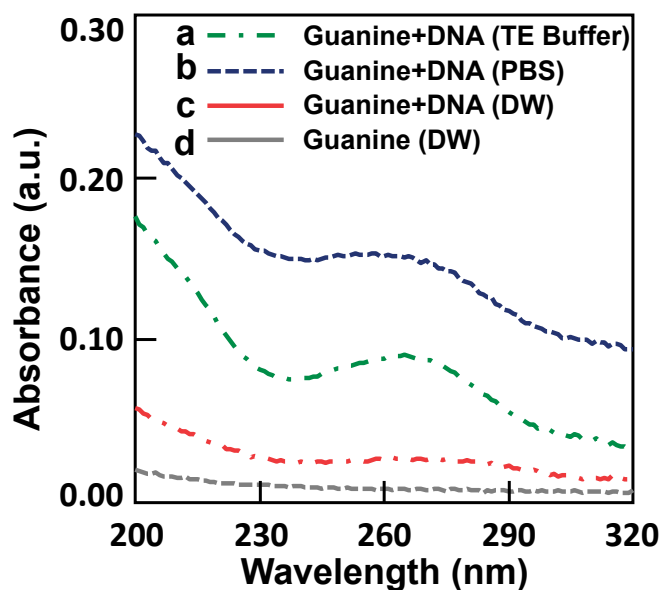


Figure 5.3. Absorbance spectra from guanine micro-mirrors in DNA solution on substrate when drying after washing with the line (a) Tris- EDTA buffer, (b) PBS solution, or (c) distilled water. (d) Guanine crystals and the substrate in the absence of DNA, washed with distilled water (negative control experiment). (Reproduced from [Y. Mizukawa, and M. Iwasaka, *J. Appl. Phys.*, vol. 117, Page 17B730, (2015).], with the permission of AIP Publishing.)

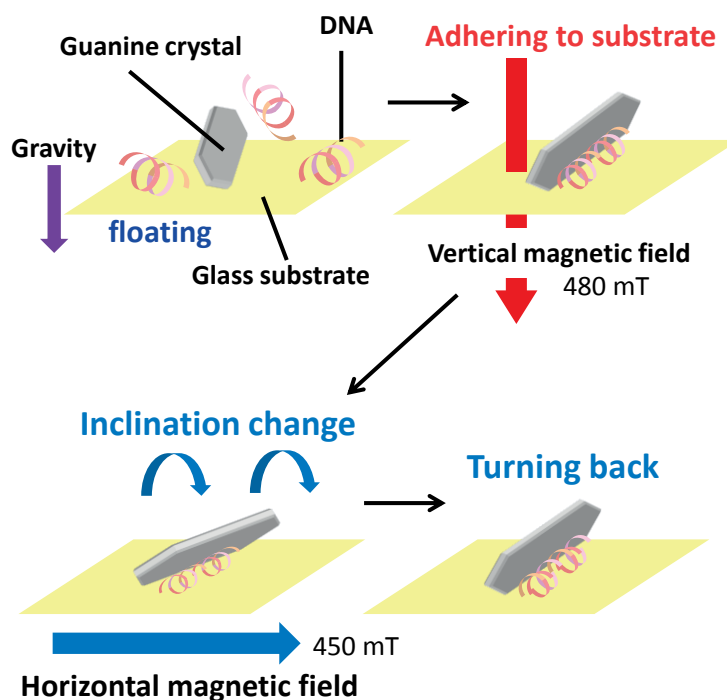


Figure 5.4. Schematic images of the reconstructed biogenic guanine crystal micro-mirrors, and their motions in the presence or absence of magnetic fields. (Reproduced from [Y. Mizukawa, and M. Iwasaka, *J. Appl. Phys.*, vol. 117, Page 17B730, (2015).], with the permission of AIP Publishing.)

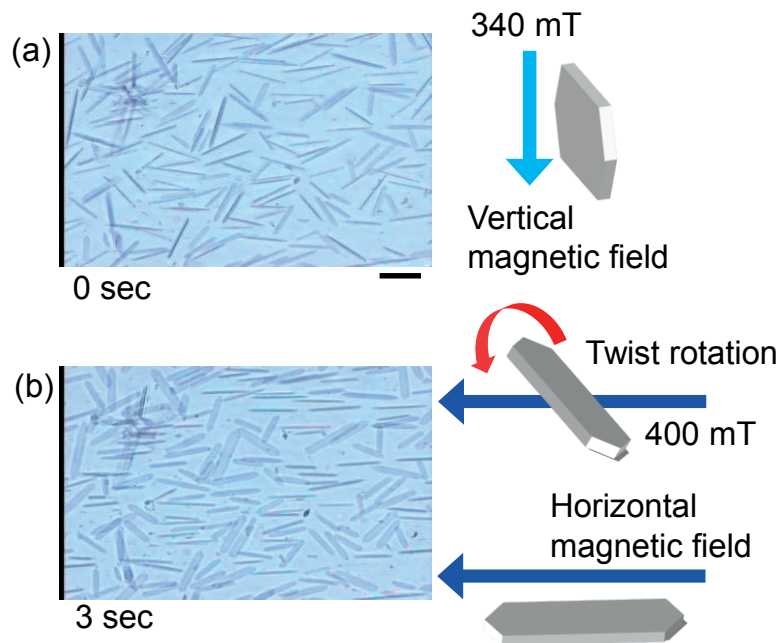


Figure 5.5. Twisting magnetic orientation under horizontal magnetic fields of 400 mT, applied to pre-standing guanine crystal platelets under vertical magnetic fields of 340 mT from a permanent magnet. (a) Optical image taken immediately after the permanent magnet was removed from the chamber. (Zero seconds elapsed). Bar, 20 μm . (b) Image of the guanine crystal plates under horizontal magnetic fields of 400mT. (Elapsed time at 3 seconds after applying horizontal magnetic fields) ([M. Iwasaka, Y. Miyashita, Y. Mizukawa, K. Suzuki, T. Toyota, and T. Sugawara, “Biaxial Alignment Control of Guanine Crystals by Diamagnetic Orientation,” *Appl. Phys. Express*, vol. 6, Art. no. 037002, 2013.] Copyright (2013) The Japan Society of Applied Physics.)

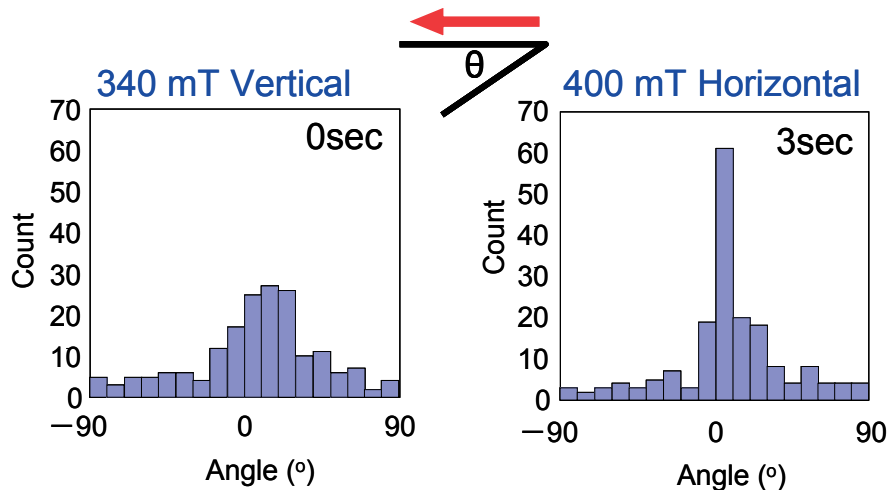


Figure 5.6. Distribution graphs of the angle θ between the long axis of a crystal plate and the horizontal direction, obtained by analyzing the photographs in panels (a) and (b) of Figure 5.5. ([M. Iwasaka, Y. Miyashita, Y. Mizukawa, K. Suzuki, T. Toyota, and T. Sugawara, “Biaxial Alignment Control of Guanine Crystals by Diamagnetic Orientation,” *Appl. Phys. Express*, vol. 6, Art. no. 037002, 2013.] Copyright (2013) The Japan Society of Applied Physics.)

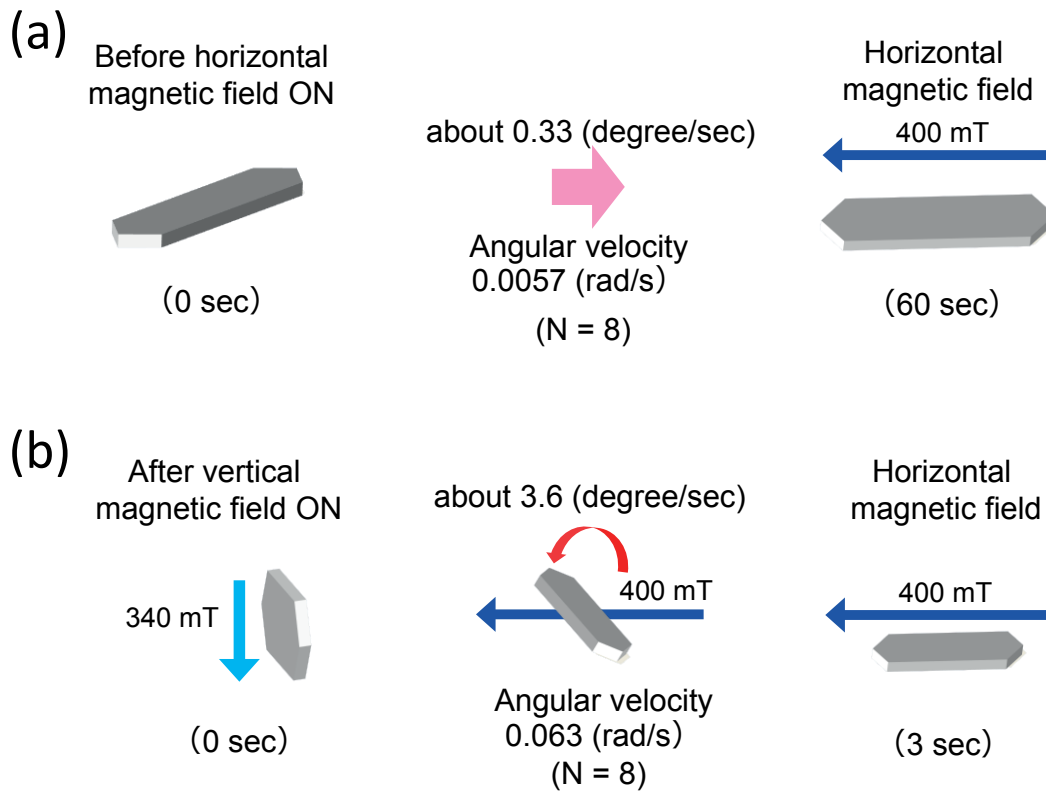


Figure 5.7. Schematic representation of the angular velocities during (a) magnetic rotation around the depth direction of a crystal, and (b) 3-dimensional diamagnetic manipulation.

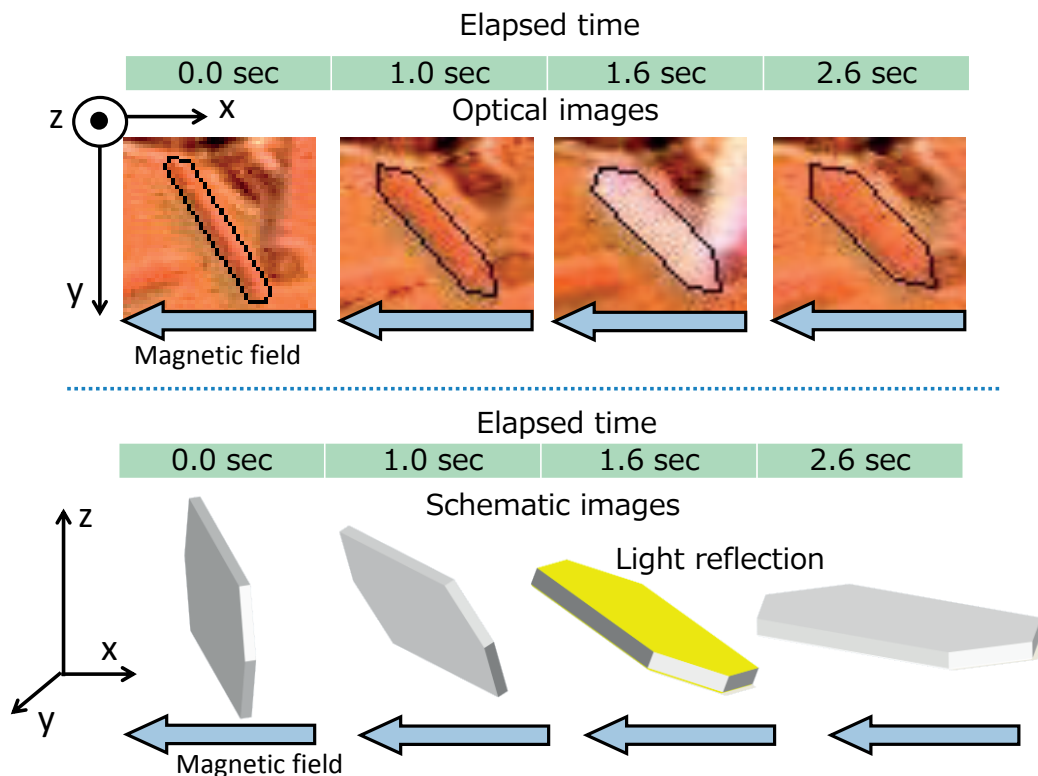


Figure 5.8. Schematic images and optical images of time course changes of a guanine crystal platelet during the twisting magnetic orientation.

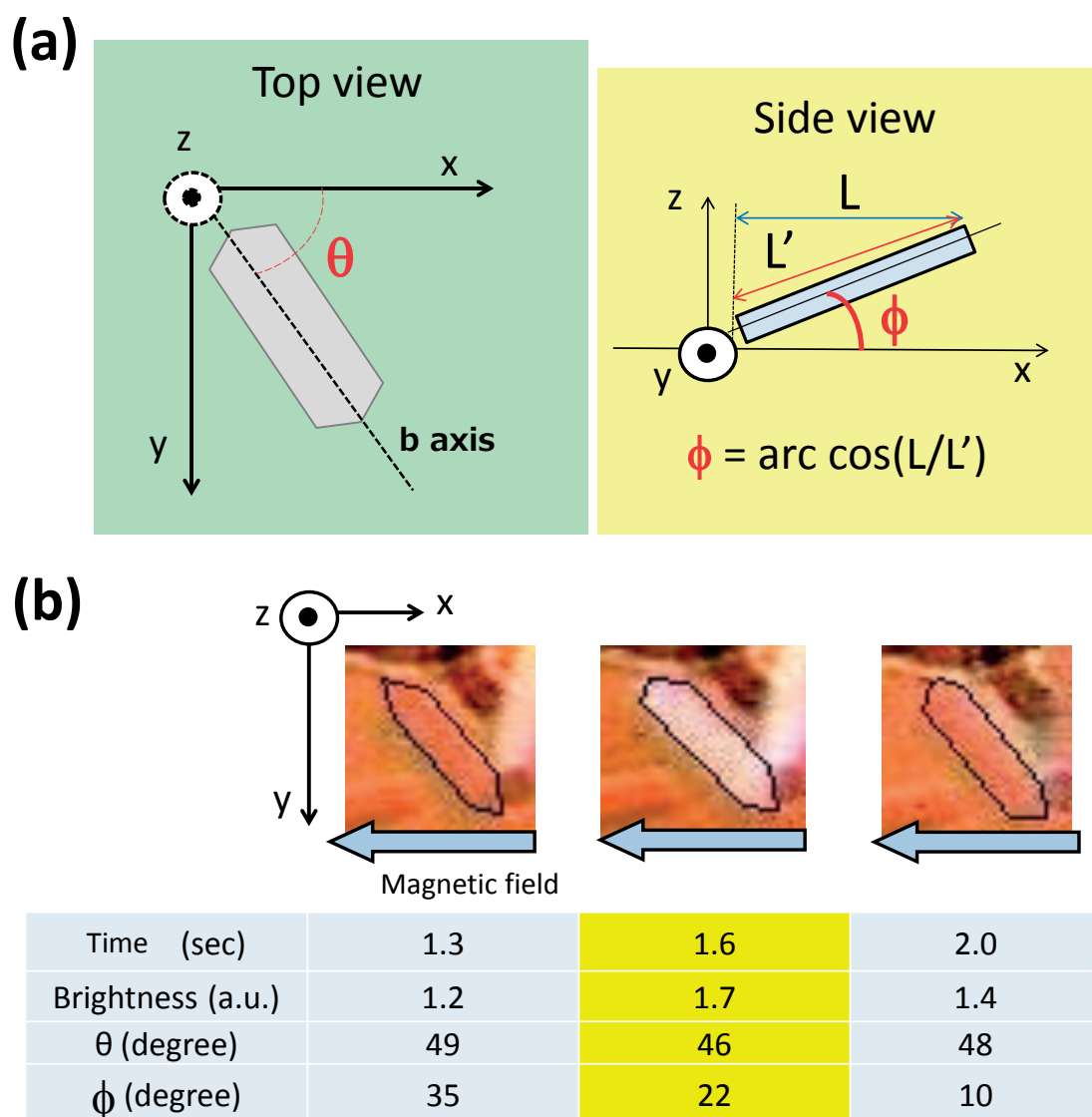


Figure 5.9. (a) Schematic images for analyzing an angle θ between the x-axis and the long axis and ϕ between the x-y plane and the (102) plane of a guanine crystal in the top view and side view. (b) Time course of the changes in brightness, angle θ and angle ϕ during twisting magnetic orientation.

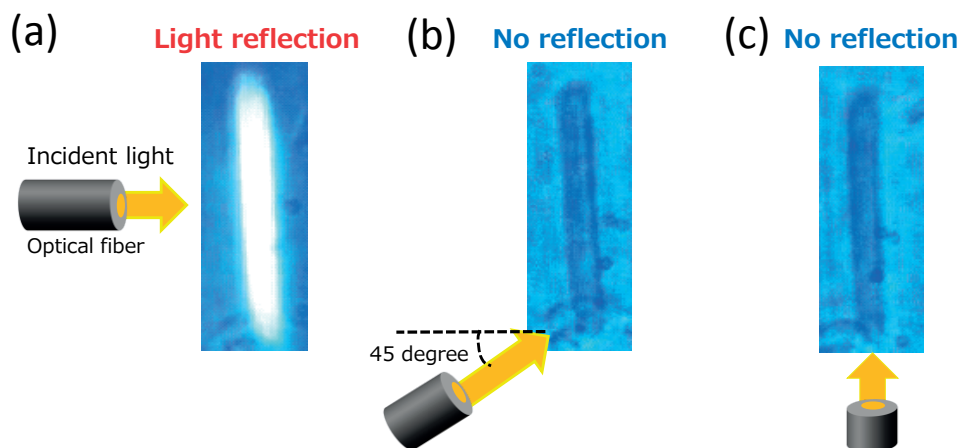


Figure 5.10. Light reflection selectivity when the direction of incident light was perpendicular, parallel, or an angle at 45° to the long axis of an individual guanine crystal platelet. (a) Light reflection from light directing perpendicular to the long axis. (b) Light reflection inclined at an angle of 45°. (c) Light reflection from light directing parallel to the long axis. (Reprinted (adapted) with permission from (M. Iwasaka, Y. Mizukawa, and N. W. Roberts, “Magnetic Control of the Light Reflection Anisotropy in a Biogenic Guanine Microcrystal Platelet,” *Langmuir*, vol. 32, pp.180–187, 2016.). Copyright (2015) American Chemical Society.)

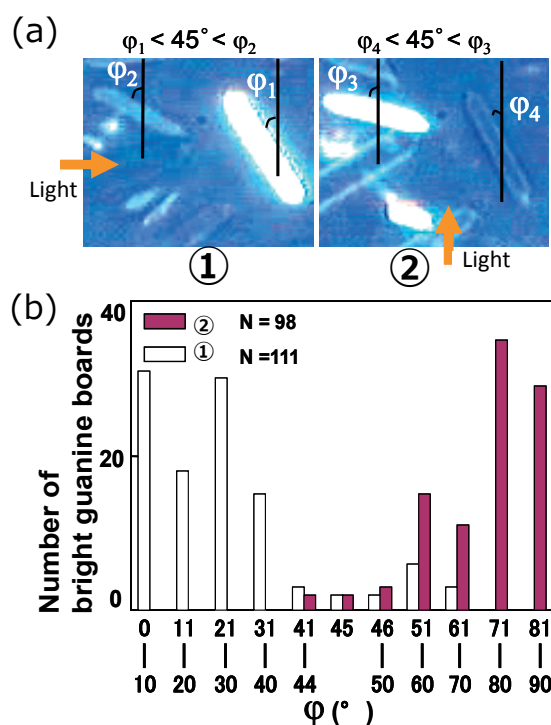


Figure 5.11. (a) Two optical images for investigation of bright guanine crystals. (Left image: The incident light direction is parallel to the horizontal axis. Right image: The incident light is parallel to the vertical axis.) (b) Distribution graph for the angle ϕ between the long axis of a crystal platelet and the vertical axis, produced by analyzing the two photographs in panel (a). (Reprinted (adapted) with permission from (Reprinted (adapted) with permission from (M. Iwasaka, Y. Mizukawa, and N. W. Roberts, “Magnetic Control of the Light Reflection Anisotropy in a Biogenic Guanine Microcrystal Platelet,” *Langmuir*, vol. 32, pp.180–187, 2016.). Copyright (2015) American Chemical Society.)

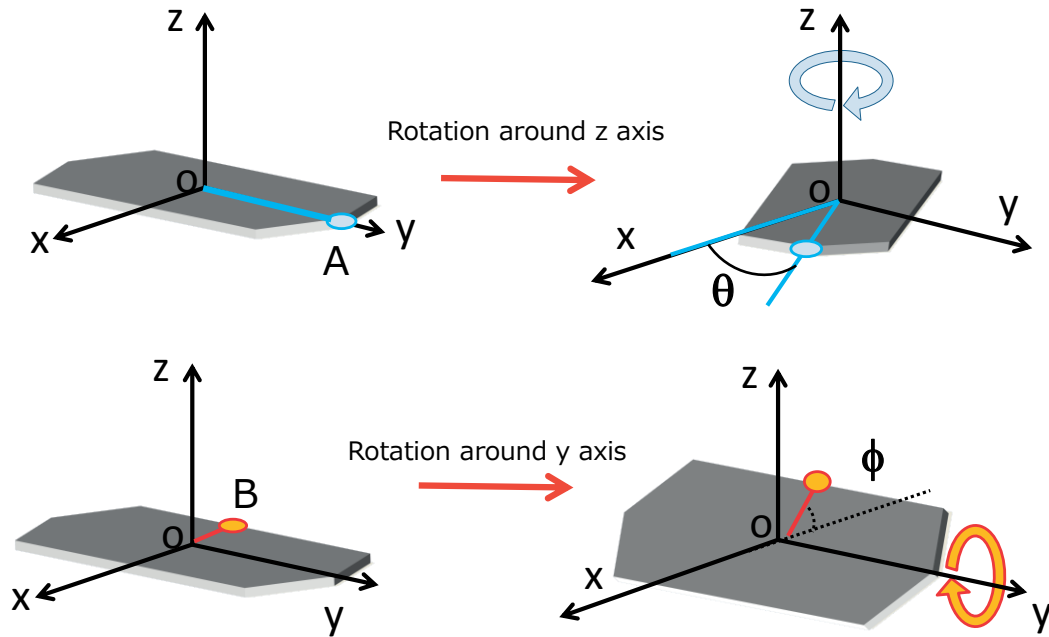


Figure 5.12. Schematic illustration indicating the rotation around z-axis and the rotation around y-axis for analyzing the region of a light reflection from a guanine crystal platelet by using twisting magnetic rotation. A and B represents an edge of a guanine crystal as the reference point for an analyzing the angle θ and angle ϕ .

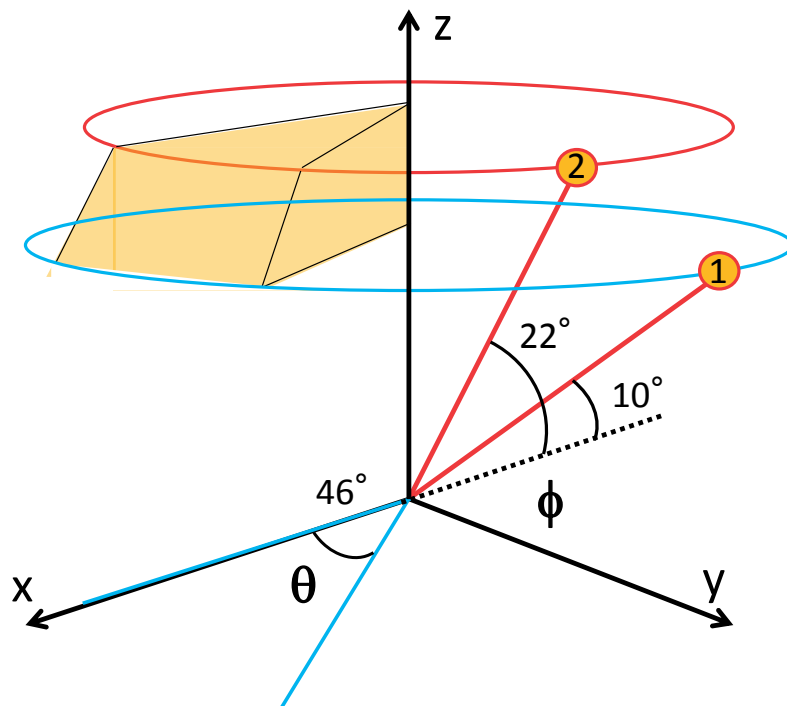


Figure 5.13. Feasible region (orange region) of light reflection from a guanine crystal analyzed by using twisting magnetic orientation. ([angle θ , angle ϕ]=[0~46°,10~22°])

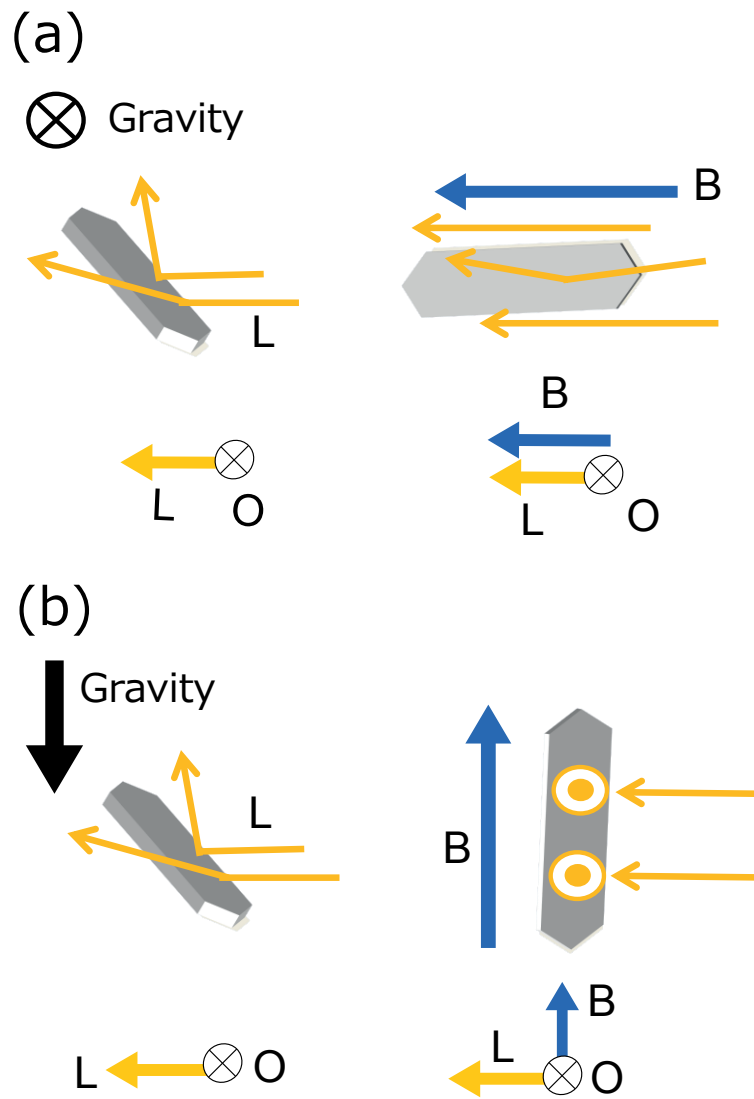


Figure 5.14. Schematic representation of the mechanism of changing light scattering, as a function of the direction of the magnetic field and incident light. (a) In the case of magnetic fields directed parallel to the incident light. (b) In the case of magnetic fields directed perpendicular to the incident light.

5.4 Summary

Micro-mirrors were reconstructed from biogenic guanine crystals and a DNA solution. The fabrication and the angle change of this micro-mirror were controlled by vertical and horizontal magnetic fields. Remote control of the inclination of a micro-mirror made of microstructural diamagnetic materials might enable underwater applications in microfluidic systems.

Moreover, we successfully achieved the complex magnetic manipulation of a biogenic guanine crystal platelet by using “twisting magnetic orientation”, which combined the two kinds of magnetic rotations under magnetic fields. These magnetic rotations are the rotation around z axis (perpendicular to the (102) plane) by applying horizontal magnetic field and the rotation around y axis (parallel to b axis of guanine crystal) by applying vertical magnetic field. Each rotation did not allow us to reveal the specific angular range of light reflection. But, twisting magnetic orientation combining these magnetic rotations could reveal the angular range of specific light reflection from an isolated single guanine crystal platelet. It was revealed that the feasible region of light reflection is [angle θ , angle ϕ]=[0~46°,10~22°]. Furthermore, we could clarified that the narrow angular range ([angle θ , angle ϕ]=[2°,12°]) for the strong light reflection with the twisting magnetic orientation.

In addition, analysis of the light reflection during the twisting magnetic orientation demonstrated light reflection selectivity that depended on the incident light being directed either parallel or perpendicular to the long axis individual guanine crystal platelets. These results clarified the mechanism of controlled light switching by combining directed magnetic fields and incident light. This also clarified the light reflection selectivity and magnetic orientation properties of guanine crystals.

6. Conclusion

6.1 Conclusions

Biogenic guanine crystals have attracted much attention among researchers due to their optical properties, such as their high refractive index and high light scattering ability. In this thesis, we carefully investigated the magnetic and optical properties of isolated biogenic guanine crystal platelets obtained from the chromatophore cells on goldfish scales.

In chapter 2, in order to observe and analyze the nano- and micro-scale structure of biogenic guanine crystals, SEM and X-ray powder diffraction analysis was performed. Additionally, single biogenic guanine crystals were analyzed by microscopic synchrotron FTIR. We revealed that individual biogenic guanine crystals have a very thin structure under SEM. The diffraction pattern indicated that the guanine crystals had properties of both anhydrous and monohydrated guanine crystals. Further, FTIR analysis revealed that individual biogenic guanine crystals have a molecular arrangement similar to that known for anhydrous crystals.

In chapter 3, we experimentally investigated the optical behavior of guanine crystals floating in distilled water, under both ambient and applied magnetic fields. It was established that suppression and enhancement of light scattering occurs from floating guanine crystals under certain directional combinations of the magnetic field, observation point, and incident lighting. In addition, optical switching of the light scattering of floating guanine crystals could be induced magnetically. These results may potentially enable applications using guanine micro-mirrors.

In chapter 4, microscopic observation of isolated guanine crystals on a substrate was recorded under magnetic fields. This identified the suppression of light scattering

from guanine crystals that had been reported regarding the guanine crystals stacked inside chromatophore cells on goldfish scale by a previous study. Our experiments clarified that the suppressed light scattering from guanine crystals was caused by diamagnetic orientation. Guanine crystals showed diamagnetic orientation in two directions, under horizontal and vertical magnetic fields. We revealed that it is challenging to control light scattering from recrystallized guanine crystals.

In the final chapter, we could fabricate a reconstructed micro-mirror. This was reconstructed from the isolated guanine crystals and a DNA solution. DNA functioned as an adhesive material, fixing the micro-mirror to the substrate in vertical magnetic fields. Additionally, we demonstrated the feasibility of fabricating remote controlled micro-mirrors using horizontal magnetic fields, again using guanine crystals and DNA. By combining vertical and horizontal magnetic fields, we successfully achieved twisting magnetic orientation of the isolated guanine crystals about two kinds of diamagnetic rotation for analyzing the light reflection property of an individual guanine crystal platelet. It was clarified that the feasible region of light reflection is [angle θ , angle ϕ]=[0~46°,10~22°]. Moreover, we could revealed the narrow angular range ([angle θ , angle ϕ]=[2°,12°]) for the strong light reflection switching by using the twisting magnetic orientation. We also clarified the light reflecting selectivity of guanine crystals, and the mechanism by which controlled light switching occurs, dependent on the direction of magnetic fields and incident light.

To summarize this study:

- X-ray powder diffraction data from guanine crystals isolated from goldfish were compared with the data for guanine crystals from Japanese koi. We revealed that goldfish guanine crystals have properties of both anhydrous and monohydrated guanine crystals. We also revealed the molecular arrangement and structure of individual biogenic guanine crystals using microscopic synchrotron FTIR analysis. These results suggest that individual goldfish guanine crystals have a predominantly anhydrous structure, and it is speculated that anhydrous crystals lie adjacent to amorphous guanine areas, which includes monohydrated guanine crystals as in a previous study.
- Light scattering from isolated guanine crystals floating in distilled water, could be controlled by changing the configuration of magnetic fields, the incident lighting and the observation direction. In addition, we clarified that magnetic orientation of isolated guanine crystals on substrates occurred due to diamagnetic anisotropy. The crystals were viewed under a microscope in both dark-field and bright-field illumination. The circumstances under which light scattering changes occur from guanine crystals in response to applied under magnetic fields were identified. We have demonstrated that magnetic orientation can be carried out about two kinds of diamagnetic orientation around z axis and y axis of the guanine crystal platelet under vertical and horizontal magnetic fields.

- We demonstrated the feasibility of reconstructing a biomimetic reflective system from biogenic guanine crystals with DNA joints. We were also able to control this system remotely using vertical and horizontal magnetic fields. Also, we succeeded in controlling the twisting magnetic orientation of an individual guanine crystal platelet by using two kinds of diamagnetic orientation around z-axis and y-axis. Moreover, we could clarify that the narrow angular range (angle θ , angle $\phi=[2^\circ, 12^\circ]$) for the strong light reflection with the twisting magnetic orientation. Also, the mechanism of controlled light switching in chapter 3 was revealed by investigating the optical selectivity and magnetic orientation of guanine crystal platelets in directional magnetic fields, and under different incident light directions.

6.2 Future development and applications

In conclusion, it is anticipated that isolated guanine crystal platelets reflect light selectively within the very narrow angular range and can execute the light switching by using applied magnetic fields and the incident light direction change.

In the future, it is hoped that these results and methods may allow us to contribute to the breakthrough clarifying the light reflex function of a fish having a complex motion with twisting swimming-action. This breakthrough may reveal the association with light reflection system of a fish and the camouflage function or the communication between fishes. For example, we can consider that light reflection property of biogenic guanine crystals of fishes have in the narrow angular range enables to use the camouflage function and the strong light reflection switching momentarily when they swim in the sea and twist their body surface.

Also, the development of the methods outlined in this thesis may allow us to construct novel 'micro-mirror systems' or 'micro-actuator systems' and to control these systems noninvasively in the micro region. For example, it is potential that the micro-mirror or micro-actuator systems being able to perform noninvasively in the micro fluidic systems are developed.

Acknowledgments

First of all, I would like to express my profound appreciation and respect to my supervisor, Professor Masakazu Iwasaka in Research Institute for Nanodevice and Bio Systems of Hiroshima University for his precious guidance, invaluable advice and precise suggestions on all of my research and doctoral thesis. I would like to appreciate to three co-supervisors for the examination of my doctoral thesis; Professor Shin Yokoyama, Professor Seiichirou Higashi and Professor Yutaka Nakashimada. I could have their many suggestions and invaluable advice for accomplishing and reviewing this thesis. I would like to be deeply thankful to Professor Tadashi Sugawara (Kanagawa University), Professor Yoko Sugawara (Kitasato University), Shigefumi Yamamura (Kitasato University) and Kentaro Suzuki (Kanagawa University) for their advice and discussion on my work. I would like to express my great gratitude to Tsunehisa Kimura and Fumiko Kimura in Kyoto University, Toyohiko Kinoshita, Yuka Ikemoto and Taro Moriwaki in Japan Synchrotron Radiation Research Institute. They kindly supported my experiment and carried out helpful discussion for my research. I'm grateful to Yuka Takeuchi and Yuito Miyashita in Iwasaka laboratory for their heartfelt help and advice. I couldn't have the accomplishment of this thesis and research without their supports and encouragements. Finally, I thank the members in RNBS and Professor Takamaro Kikkawa. This work was supported in part by SPring-8 in JASRI, Grant 2013A1910, 2013B1655 and 2014B1728, and JSPS KAKENHI Grant 14J06583.

This thesis and research was supported by many professors and colleagues. I fortunately could have their precious support and cheer. I would like to have a renewed appreciation for all the people's help for this thesis and all of my research.

March, 2016 Yuri Mizukawa

公表論文

- (1) Light Reflection Control in Biogenic Micro-Mirror by Diamagnetic Orientation
M. Iwasaka and Y. Mizukawa
Langmuir, **29**, 4328–4334 (2013).
[\[http://dx.doi.org/10.1021/la400046a\]](http://dx.doi.org/10.1021/la400046a)
- (2) Synchrotron Microscopic Fourier Transform Infrared Spectroscopy Analyses of Biogenic Guanine Crystals Along Axes of Easy Magnetization
Y. Mizukawa, Y. Ikemoto, T. Moriwaki, T. Kinoshita, F. Kimura, T. Kimura and M. Iwasaka
IEEE Transactions on Magnetics, **50**, 5001804(1–4) (2014).
[\[https://doi.org/10.1109/TMAG.2014.2329239\]](https://doi.org/10.1109/TMAG.2014.2329239)
- (3) Rapid magnetic wiper featuring biogenic guanine particles: Magnetic non-contact switching of opto-fluidic mirrors featuring biogenic guanine crystals
M. Iwasaka, Y. Mizukawa and Y. Miyashita
Applied Physics Letters, **104**, 024108(1–4) (2014).
[\[http://dx.doi.org/10.1063/1.4862083\]](http://dx.doi.org/10.1063/1.4862083)
- (4) Biaxial Alignment Control of Guanine Crystals by Diamagnetic Orientation
M. Iwasaka, Y. Miyashita, Y. Mizukawa, K. Suzuki, T. Toyota and T. Sugawara
Applied Physics Express, **6**, 037002(1–4) (2013).
[\[http://dx.doi.org/10.7567/APEX.6.037002\]](http://dx.doi.org/10.7567/APEX.6.037002)
- (5) Magnetic Manipulation of Nucleic Acid Base Microcrystals for DNA Sensing
Y. Mizukawa, K. Suzuki, S. Yamamura, Y. Sugawara, T. Sugawara and M. Iwasaka
IEEE Transactions on Magnetics, **50**, 5001904(1–4) (2014).
[\[https://doi.org/10.1109/TMAG.2014.2328633\]](https://doi.org/10.1109/TMAG.2014.2328633)

- (6) Magnetic control of the inclination of biogenic guanine crystals fixed on a substrate
Y. Mizukawa and M. Iwasaka
Journal of Applied Physics, **117**, 17B730(1–4) (2015).
[<http://dx.doi.org/10.1063/1.4917243>]
- (7) Magnetic Control of the Light Reflection Anisotropy in a Biogenic Guanine Microcrystal Platelet
M. Iwasaka, Y. Mizukawa and N. W. Roberts
Langmuir, **32**, 180–187 (2016).
[<http://dx.doi.org/10.1021/acs.langmuir.5b03522>]

参考論文

- (1) Magnetic field effects on mitochondrion-activity-related optical properties in slime mold and bone forming cells
Y. Mizukawa and M. Iwasaka
35th Annual International Conference of the IEEE Engineering in Medicine and Biology Society (EMBC2013), Proceedings of the Annual International Conference of the IEEE Engineering in Medicine and Biology Society 2013, 1442–1445, Osaka, Japan, July 3-7 (2013).
[\[https://doi.org/10.1109/EMBC.2013.6609782\]](https://doi.org/10.1109/EMBC.2013.6609782)
- (2) Magnetic orientational tweezers for cell manipulation
Y. Mizukawa and M. Iwasaka
Transactions of Japanese Society for Medical and Biological Engineering, **51**(Supplement), M-127 (2013).
[\[http://doi.org/10.11239/jsmbe.51.M-127\]](http://doi.org/10.11239/jsmbe.51.M-127)
- (3) Electromagnetic Viability Control of Aquatics by the Combination of Weak Electric Currents and 10 T Magnetic Fields
Y. Mizukawa and M. Iwasaka
IEEE Transactions on Magnetics, **49**, 3480–3483 (2013).
[\[https://doi.org/10.1109/TMAG.2013.2240439\]](https://doi.org/10.1109/TMAG.2013.2240439)
- (4) Novel Magnetic Responses of Uric Acid Crystals under Light Irradiations
Y. Mizukawa and M. Iwasaka
IEEJ Transactions on Fundamentals and Materials, **133**, 383–384 (2013).
[\[http://doi.org/10.1541/ieejfms.133.383\]](http://doi.org/10.1541/ieejfms.133.383)